1971

Stabilities of some rare-earth malonato chelate species in aqueous and methyl alcohol solution

Douglas Kiester Johnson
Iowa State University

Stabilities of some rare-earth malonato chelate species in aqueous and methyl alcohol solution

by

Douglas Kiester Johnson

A Dissertation Submitted to the
Graduate Faculty in Partial Fulfillment of
The Requirements for the Degree of
DOCTOR OF PHILOSOPHY

Major Subject: Inorganic Chemistry

Approved:

Signature was redacted for privacy.

In Charge of Major Work

Signature was redacted for privacy.

Head of Major Department

Signature was redacted for privacy.

Dean of Graduate College

Iowa State University
Of Science and Technology
Ames, Iowa

1971

TABLE OF CONTENTS

INTRODUCTION

At the commencement of this work there were data available regarding lanthanide complexes of several α-substituted malonate ligands. Gelles and Nancollas (1) had reported values for the first formation constants of lanthanum, neodymium, and lutetium malonate species. Powell (2) had reported K_1 and K_2 values for lanthanide complexes of the malonate ligand and several disubstituted malonate derivatives. Adolphson (3) later reported K_1 and K_2 values for several monosubstituted malonate derivatives. No data were available, however, for malonate analogues with cyclic α-substituents, e. g., 1,1-cyclobutanedicarboxylate.

The ligands with the bulkier α-substituents exhibited a notable increase in chelate stability compared to malonate itself. This was accredited to a greater disruption of the hydration sphere about the cation upon coordination, resulting in correspondingly larger entropy changes. One might expect such an effect to be minimal with cyclic substituents due to restricted motion of additional methylene units. Therefore, it would be expected that the OOC-C-COO bond angle variation is the only significant variable related to lanthanide complex stability in malonate analogues having cyclic α-substituents. The 1,1-cyclobutanedicarboxylate (CBDA), 1,1-cyclopentanedicarboxylate

(CPDA) and dimethylmalonate (DMMA) complexes of the lanthanides were investigated subsequently to ascertain the effect of bond angle variation on the stability of the lanthanide complexes. Powell (4) had previously suggested that carboxyl groups possibly bond one oxygen directly to the lanthanide and coordinate the second oxygen via hydrogen bonding to a coordinated water molecule. The possibility of this type of coordination stimulated an interest in studying lanthanide malonate complexes in a nonaqueous solvent. The terbium-CBDA and terbium-α-hydroxyisobutyrate complexes were studied in methyl alcohol with the intent of noting whether K_1/K_2 ratios were affected by changing solvents. The K_1/K_2 ratios are affected by changes in dentate character. Therefore, if the carboxyl group functions bidentately in aqueous media as described above, one should observe a change in the K_1/K_2 ratio with a change in solvent.

There has been some data collected on lanthanide carboxylate complexes in methyl alcohol. Romanenko and Kostromina (5) determined the dependence of log K_1 on the mole fraction of methanol for erbium and neodymium complexes of several carboxylate ligands in methanol-water mixtures. Vobecky and Mastalka (6) separated ^{147}Pm from a mixture of ^{152}Eu and ^{153}Eu with NH_4-α-HIBA eluant on a Dowex X-8 resin bed in the presence of methanol and noted an enhanced separation. Alexa (7) reported the

the log of the formation constants of Eu-α-HIBA in aqueous-methanol mixtures as a function of weight percent methanol.

However, there is a lack of published data concerning formation constants of metal carboxylate species in pure solvents with low dielectric constants. This is doubtless due to the increased complexity of such systems resulting from extensive ion pair formation. The terbium carboxylate complexes were investigated in methanol for the purpose of developing a method for determining formation constants of this type of complex in solvents having low dielectric constants.

PART I. CHELATE SPECIES IN AQUEOUS SOLUTION

CALCULATIONS

Formation Constants

In this study of rare-earth malonate chelate species it was assumed that ion association occurs between the anion of the organic acid and hydrogen and lanthanide ions. It was assumed that the metal does not chelate with the undissociated acid species HA^- and HA. The latter assumption was based on experimental work performed by Sonneson (8). He has shown, in the case of acetic acid, that no appreciable complexation occurs between neodymium ions and HA species. He examined solutions I and II (in table 1) and found no difference between the extinction curves obtained in the wavelength region 3000 and 9000 angstroms. He therefore concluded no complexation had occurred with the undissociated ligand acid.

Table 1. Sample preparation for determination of extent of complexation between neodymium ions and undissociated acetic acid

Acid	Concentration I	Concentration II
$NdClO_4$	50 MM	50 MM
$HClO_4$	100	100
$NaClO_4$	1600	1600
Acetic Acid	0	2500

The method of determining formation constants used in this research required the determination of the free ligand concentration, a, and the average number of ligands bound per lanthanide atom in solution, n. This method was originally introduced by Bjerrum (9). Both a and $\bar{n}$ were determined from a potentiometric measurement of the concentration of free hydrogen ion and predetermined dissociation constants of the acid form of the ligand.

$$H = h + HA + 2H_2A \tag{1}$$

$$a = \frac{H - h}{h/K_{a2} + 2(h)^2/(K_{a1} \cdot K_{a2})} \tag{2}$$

$$\bar{n} = \frac{A - a\,h/K_{a2} + (h)^2/(K_{a1} \cdot K_{a2}) + 1}{B} \tag{3}$$

Material balance equations 4 and 5 can be written to account for the total metal and total ligand concentrations in terms of the various forms in which they appear in solution.

$$B = b + [BA^+] + [BA_3^{-3}] \tag{4}$$

$$A = a + [BA] + 2[BA_2^-] + 3[BA_3^{-3}] + [HA] + [H_2A] \tag{5}$$

In these equations:

B = total metal concentration,

b = free uncomplexed metal concentration,

A = total ligand concentration,

a = free uncomplexed ligand concentration,

H_nA = undissociated acid species concentration,

BA_n = metal chelate species concentration,

and h = free hydrogen ion concentration.

The step formation constants of the metal chelate species are defined as in equation 6 and the overall formation constants, β_n, are products of the individual step formation constants (equation 7).

$$K_n = \frac{[BA_n]}{[BA_{n-1}][a]} \tag{6}$$

$$\beta_n = K_1 \cdot K_2 \cdots K_n \tag{7}$$

The formation constants were determined under constant ionic medium conditions described by Rossotti and Rossotti (10, p. 23), thus, activity coefficients of all species may be assumed to be constant and, therefore, not to enter into the stability constant determination. In the determination of the individual formation constants, a substitution was made for each chelate species represented in the material balance equation in terms of overall formation constants and the free ligand concentration. A similar substitution may be made for the undissociated acid species in terms of the predetermined acid dissociation cosntants and the free ligand concentration. These substitutions yield equations 8 and 9.

$$B = b\left[1 + \beta_1[a] + \beta_2[a]^2 + \beta_3[a]^3\right] \tag{8}$$

$$A - a = b\left[\beta_1[a] + 2\beta_2[a]^2 + 3\beta_3[a]^3\right] + \frac{[h][a]}{K_{a2}} + \frac{[h]\ [a]}{K_{a1}\ K_{a2}} \qquad (9)$$

Expressions 10 and 11 may be written for the average number of ligands bound per metal atom in solution ($\bar{n}$).

$$\bar{n} = \frac{A - a\ [1 + h/K_{a2} + [h]^2/(K_{a1}\cdot K_{a2})]}{B} \qquad (10)$$

$$\bar{n} = \frac{\sum_{n=o}^{N} n\beta_n(a)^n}{\sum_{n=o}^{N} \beta_n(a)^n} \qquad (11)$$

Setting expression 10 equal to expression 11, one obtains equation 12.

$$\sum_{n=o}^{N} [A_i - a_i(1 + h_i/K_{a2} + (h_i)^2/(K_{a1}\cdot K_{a2})) - nB_i]\ \beta_n(a)^n = 0 \qquad (12)$$

Equation 12 can be solved exactly for any set of A, a, h, and B. However, a normal formation constant determination involved more than twenty data points. Since one could not obtain an exact fit of equation 12 for each data point by employing the same β_n values, the data were subjected to a least squares treatment in order to obtain

β_n values which best satisfied all of the data. The least squares treatment used is patterned after that of of Rydberg (11), and Sullivan, Rydgerg and Miller (12). The mathematical computations were written in a computer program by Stagg (13). Equation 12 is not in general equal to zero for each data point, but, rather, one obtains a residual U_i as indicated in equation 13.

$$U_i = \sum_{n=o}^{N} (A_i - a_i[1 + h_i/K_{a2} + (h_i)/(K_{a1} \cdot K_{a2})] - nB_i)\beta_n(a_i)^n \qquad (13)$$

The residuals are then squared and weighted according to the reliability of their preparation and, finally, summed to yield equation 14.

$$S = \sum_{i=o}^{I} W_i U_i^2$$

This sum is then minimized with respect to each β_n parameter. This yields N equations which are solved for the best β_n values.

The weighting factors themselves are based on the β_n values. Therefore, the values of the weighting factors are approximated initially. Having determined a set of β_n values, more accurate weighting factors can be calculated and a still better set of β_n values can be determined. This process was reiterated until

a recalculated set of β_n values differed by less than 0.01% from the previously calculated set.

Acid Dissociation Constants

The acid ionization constants were determined from pH_C measurements made upon a series of partially neutralized solutions of the organic acid. Material balance equations 15 and 16 were used in the ionization constant determinations.

$$H_T = h + HA + 2H_2A \tag{15}$$

$$A_T = a + HA + H_2A \tag{16}$$

These equations rearrange to give:

$$H - h = a[h/K_2 + 2h^2/K_1K_2] \tag{17}$$

$$A = a[1 + h/K_2 + h^2/K_1K_2] \ . \tag{18}$$

Dividing equation 17 by 18 we obtain:

$$\frac{H - h}{A} = \frac{[h/K_2 + 2h^2/K_1K_2]}{[1 + h/K_2 + h^2/K_1K_2]} \tag{19}$$

Where $\alpha_2 = \frac{1}{K_1K_2}$ and $\alpha_1 = \frac{1}{K_2}$,

$$\frac{H - h}{h\ [2A - H + h]} = \alpha_1 \frac{[A - H + h]}{h\ [2A - H + h]} + \alpha_2 \ . \tag{20}$$

This equation is in the form $y = mx + b$ which represents a straight line with slope α_1 and intercept α_2.

These ionization constants are not the thermodynamic dissociation constants, but are related to the thermodynamic constants as in equation 21.

$$T_{K_a} = \frac{\gamma H \cdot \gamma A}{\gamma HA} \cdot K_a \qquad (21)$$

Similarly, the step formation constants of the rare-earth malonate chelate species are not the thermodynamic constants but are related to them as in equation 22.

$$T_{K_1} = \frac{\gamma MA}{\gamma M \cdot \gamma A} \cdot K_1 \qquad (22)$$

EXPERIMENTAL PROCEDURE

Technique

Formation constants

The formation constant determinations reported in this work were based on the measurement of free hydrogen ion concentration and the acid dissociation constants of the ligand acid. All determinations were made at an ionic strength of 0.1 molar, using KNO_3 as the supporting electrolyte, at a temperature of 25.0 degrees centigrade. A set of twenty-five samples containing a constant amount of metal and varying amounts of the ligand buffer was prepared. The metal concentration was generally 0.004 molar, and the ligand concentration varied from 0.001 to 0.025 molar.

The prepared samples were placed in a constant temperature bath to equilibrate for a day. Upon equilibration some of the light rare earths formed sesquimalonate precipitates at the higher concentrations of ligand. In the cases of lanthanum, cerium, neodymium, and praseodymium the metal concentration was reduced to 0.002 molar to provide more data points in the concentration region where precipitation did not occur.

The hydrogen ion concentration was then determined by measuring the potential difference between a glass electrode and a saturated calomel electrode. A diagram of the

cell used in the determination of hydrogen ion concentration is given in figure 1. All hydrogen ion concentrations were determined with a Beckman Research pH meter model 1019. The instrument was standardized against a known concentration of hydrogen ion prepared by dilution of a standard HCl solution and was set to read the concentration of hydrogen ion rather than activity. The ionic strength of the standard HCl solution was adjusted to 0.1 molar by addition of KNO_3. The pH of the standard solution was near the middle of the pH range spanned in the formation constant determination.

In order to check for the possibility of polynuclear coordination, the step formation constants of dysprosium dimethylmalonate were determined at a dysprosium concentration of 0.01 molar as well as at 0.004 molar. In the calculation of the formation constants of polynuclear species the material balance expressions would contain several different powers of the free metal ion concentration, whereas the corresponding material balance equations for mononuclear chelate species only involve the metal concentration to the first power. The free metal ion concentration appears in the expression for $\bar{n}$ in the case of polynuclear coordination but not in the case of mononuclear coordination. Therefore, if the calculated formation constants are a function of metal ion concentration, one suspects that there are polynuclear species present in

Figure 1. Cross section of constant temperature cell and electrodes used for pH measurements

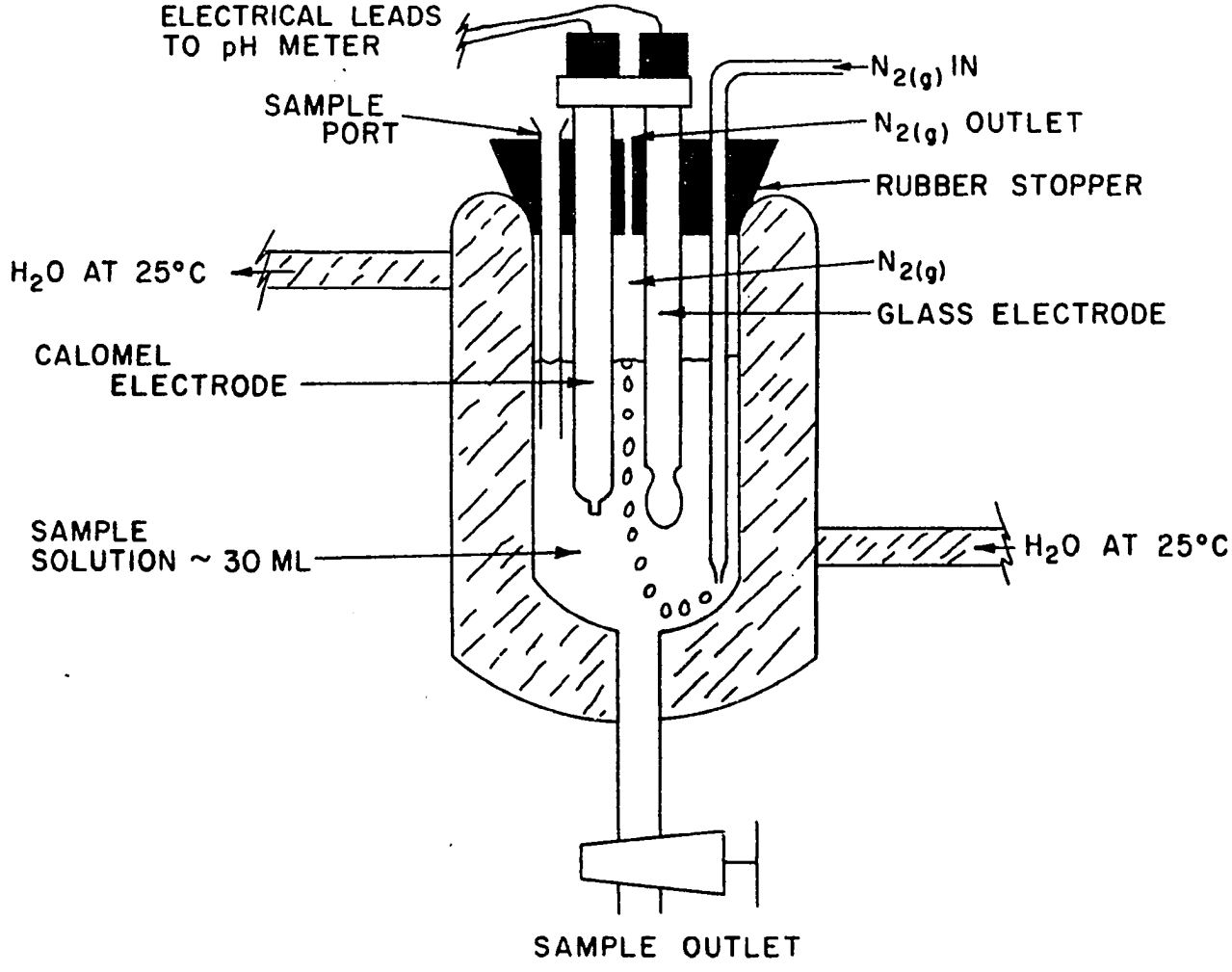
ELECTRICAL LEADS
TO pH METER
SAMPLE
PORT
$N_{2(g)}$ IN
$N_{2(g)}$ OUTLET
RUBBER STOPPER
H_2O AT 25°C
$N_{2(g)}$
GLASS ELECTRODE
CALOMEL
ELECTRODE
SAMPLE
SOLUTION ~ 30 ML
H_2O AT 25°C
SAMPLE OUTLET

solution. A similar check was made by Stagg in the case of a monobasic acid in which case no polynuclear coordination was observed (14). The dibasic acids used in this research were considered sufficiently different to warrant a separate evaluation.

Acid dissociation constants

The acid dissociation constants of all malonic acid derivatives used in this research were determined from the pH_c measurements on a series of partially neutralized solutions of the organic acid. The measurements were made at 25.0 degrees centigrade and 0.1 molar ionic strength, using KNO_3 as the supporting electrolyte. The total concentration of the organic acid anion was held constant at 0.01 molar. Varying amounts of standard base were added to each sample such that the degree of neutralization varied from 25% to 75%. This range in degree of neutralization was used in order that both constants might be determined from the same data. The data were collected in a pH range in which both HA and H_2A species were expected to be significant.

Preparation of Reagents

Rare-earth nitrate stock solutions

One tenth molar rare-earth nitrate stock solutions were prepared by dilution of 0.5 molar stock solutions prepared by Adolphson (3). The 0.5 molar stock solutions were

prepared by dissolution of the rare-earth oxides in nitric acid. Insufficient acid was supplied to convert the oxide completely to the stoichiometry of three nitrates to one lanthanide ion. After dissolution of the oxide was complete, the solutions were brought to the equivalence point (three nitrate to one lanthanide) by titrating with nitric acid.

Ligand buffer solutions

Dimethylmalonic acid and 1,1-cyclobutanedicarboxylic acid were purchased from Aldrich Chemical Co. Milwaukee, Wisconsin. The 1,1-cyclopentanedicarboxylic acid was synthesized via the malonic ester synthesis from the diethylester of malonic acid and 1,4-dibromobutane.

One tenth molar solutions of the dibasic malonic acid ligands were 75% neutralized with KOH. This provided a solution 0.05 molar in HA^- and 0.05 molar in $A^=$. A buffer is required to allow the metal to compete with hydrogen for the ligand.

The organic acids used as ligands were recrystallized from carbon tetrachloride containing 0.1% acetone. The purities of these acids were checked by titrating a known weight of each acid with standard base and comparing the equivalent weights determined with the theoretical equivalent weights. A further check was made by noting the sharpness of the melting points. In table 2 the melting

points and equivalent weights of the acids are given.

Table 2. Melting points and equivalent weights of acids

Acid	M. P. Range	Equivalent Weight	
		Actual	Theoretical
DMMA	196.0 - 196.5	131.7	132.1
CBDA	160.5 - 162.5	145.0	144.1
CPDA	185.0 - 185.5	158.1	158.1

The concentrations of stock buffer solutions were determined by titrating with standard KOH. The titrations were followed by a pH meter. The end point pH was determined from a plot of pH versus volume of titrant added. It was determined that the equivalence point was not identical with the inflection point on the titration curve. If the volume of the titrant at the first inflection point was doubled, it was found that this value was less than the volume of the titrant required to reach the inflection point at the second break in the titration curve. The first equivalence point occurred at 22.28 milliliters of base added, whereas the second equivalence point occurred at 46.42 milliliters.

Figures 2, 3, and 4 give a sample titration curve and plots of the first derivative of pH with respect to milliliters of titrant for both the first and second equivalence points. The actual end point should be neither the second equivalence point nor double the first equivalence point, but rather the average of both of

Figure 2. Titration curve of 1,1-cyclopentanedicarboxylic acid with an apparent equivalence point pH of 8.01

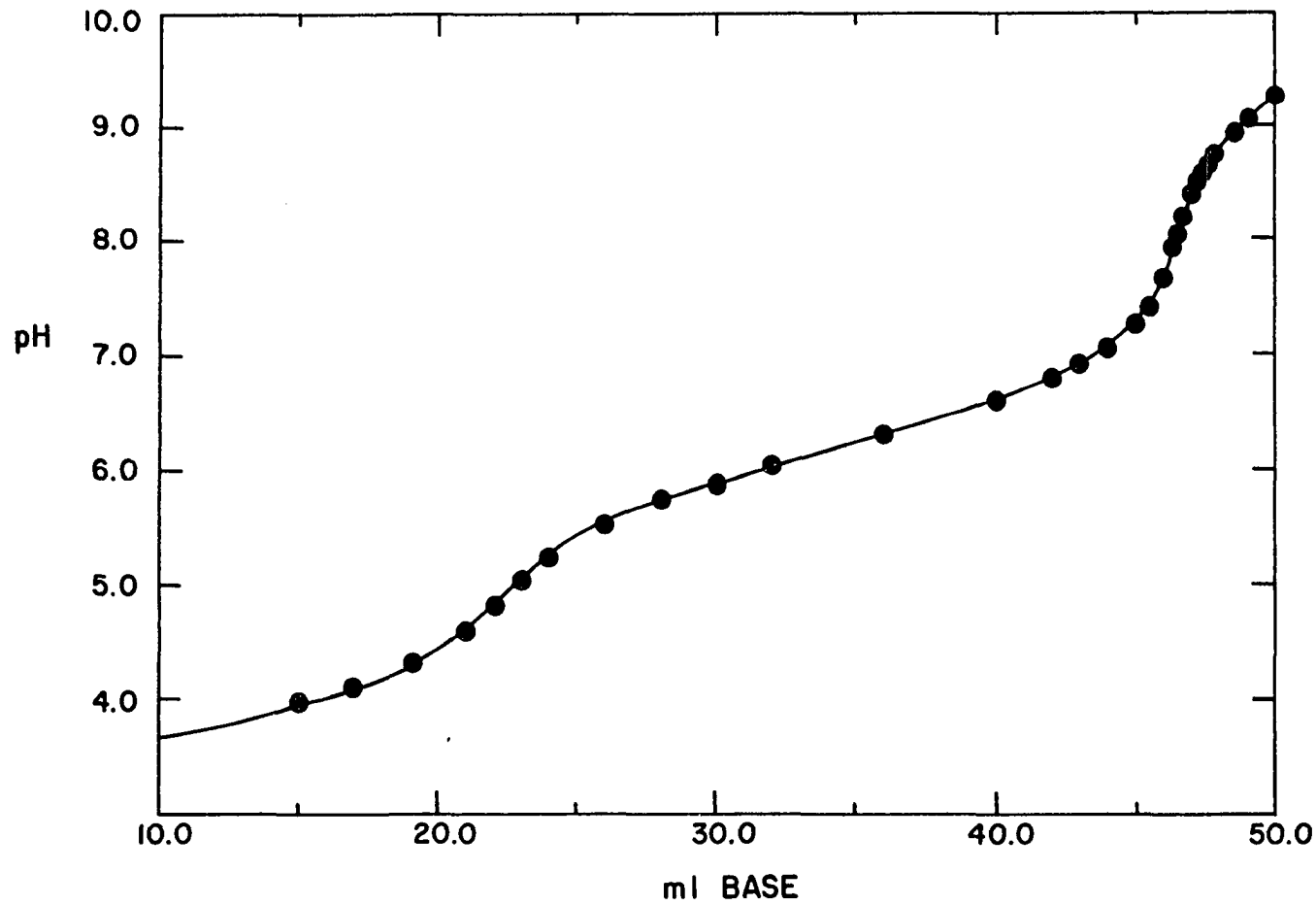
10.0
9.0
8.0
7.0
6.0
5.0
4.0
pH
10.0
20.0
30.0
40.0
50.0
ml BASE

Figure 3. First derivative plot of titration of 1,1-cyclopentanedicarboxylic acid in vicinity of first equivalence point

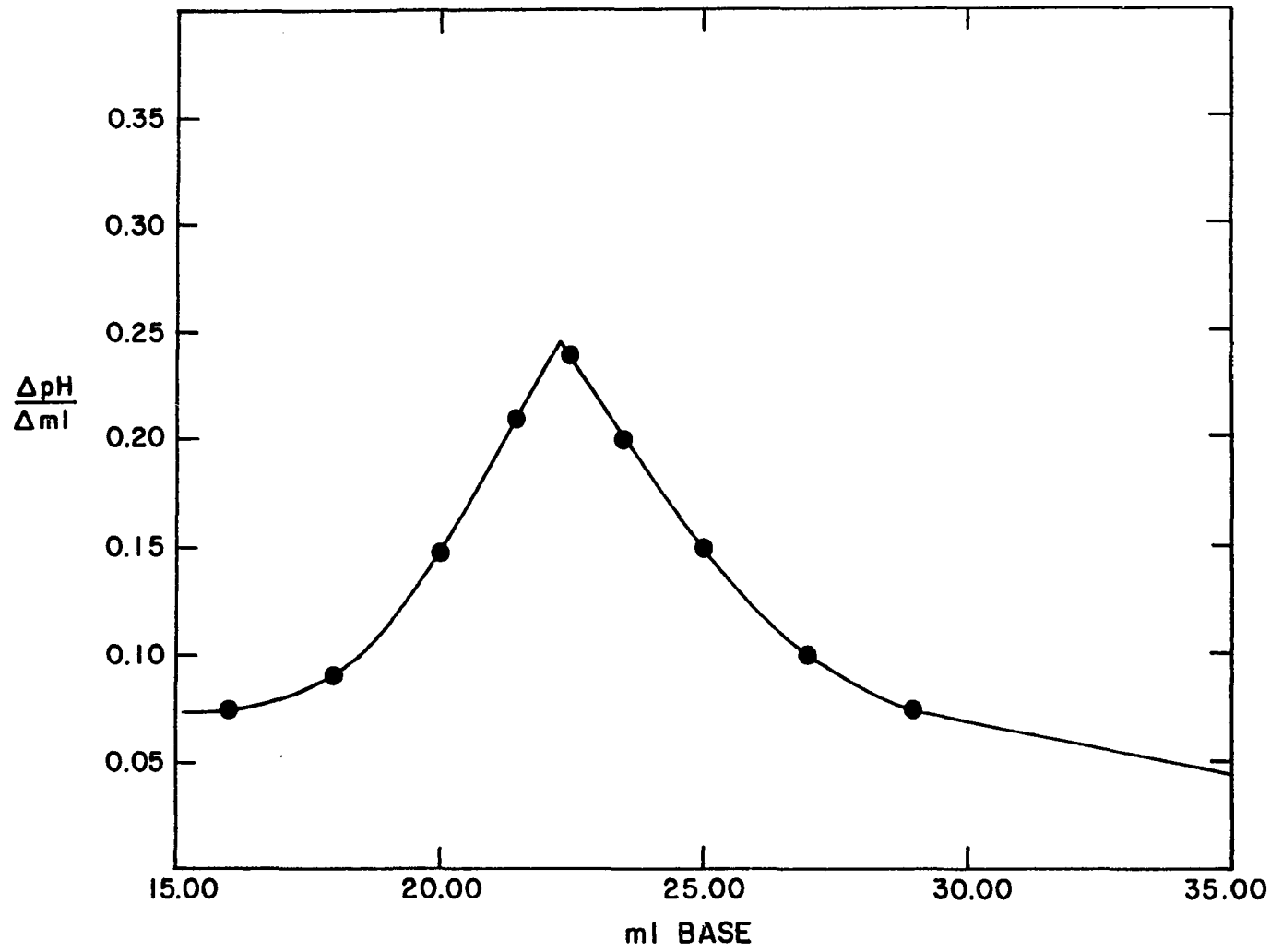
0.35
0.30
0.25
0.20
0.15
0.10
0.05
ΔpH / Δml
15.00
20.00
25.00
30.00
35.00
ml BASE

Figure 4. First derivative plot of titration of 1,1-cyclopentanedicarboxylic acid in vicinity of second equivalence point

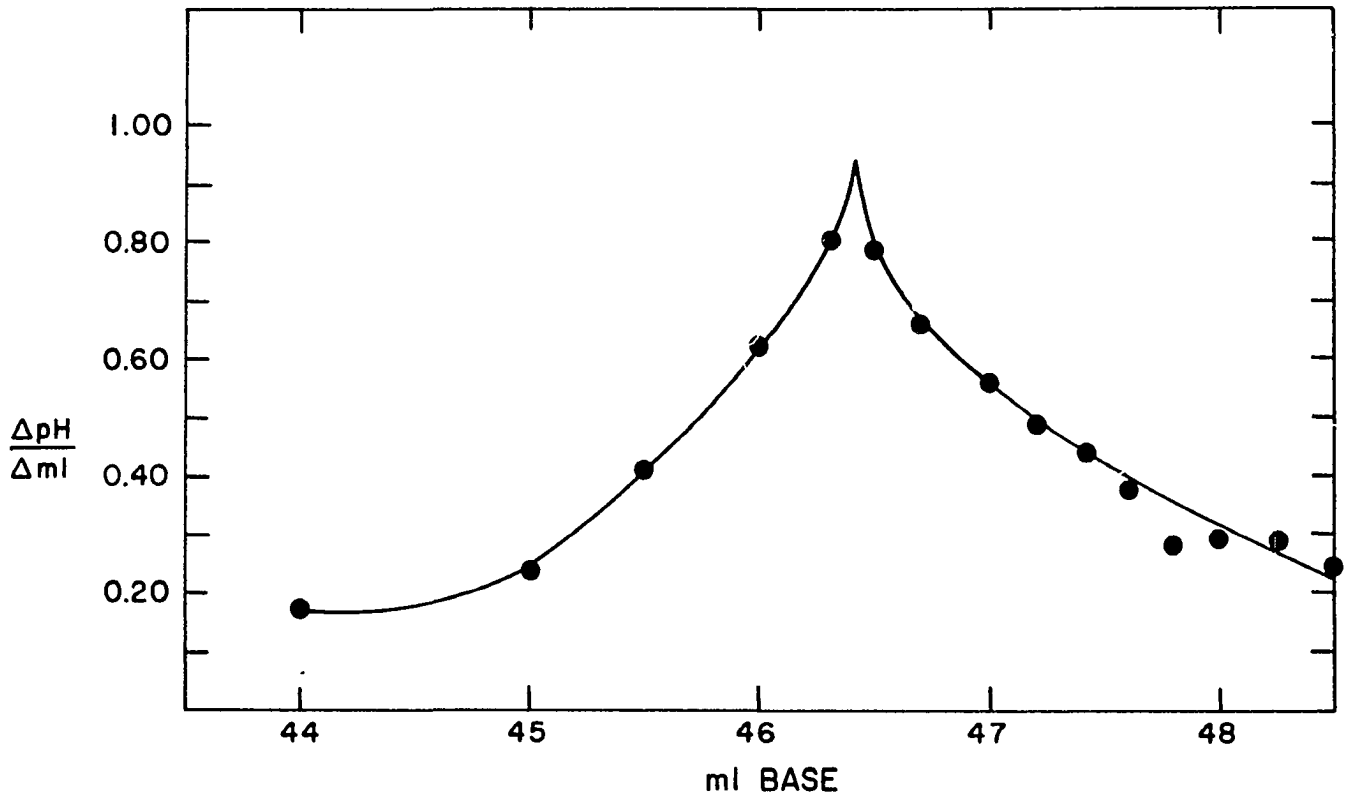
1.00
0.80
0.60
0.40
0.20
ΔpH / Δml
44
45
46
47
48
ml BASE

them, since the slope of the titration curve for each species is affected by the presence of the other species.

Preparation of standard base

Stock KOH solutions were prepared by adding commercially prepared aqueous solutions of $CO_3^=$ free KOH to distilled water which had previously been boiled to remove dissolved CO_2. This stock solution of KOH was then stored in a sealed container which had an inlet protected by Ascarite and $CaCl_2$ to absorb any moisture or CO_2 from the air entering the container. The base was standardized by titration of known weights of potassium acid phthalate.

Potassium nitrate preparation

Reagent grade KNO_3 was dissolved in distilled water to make a solution 1.5 molar in KNO_3. This stock solution was standardized by passing several aliquots through a cation exchange column and titrating the displaced hydrogen ion with standard base.

Analysis of precipitates

All of the α-substituted malonates used in this work precipitated the light members of the lanthanide series. A fresh CBDA precipitate of praseodymium was analyzed for metal, ligand and water content. The precipitate was air dried at room temperature and

weighted to three significant figures. It was then ignited to the oxide by heating at 900 degrees centigrade for one hour. The metal oxide was weighted again after ignition.

The weight of sample per mole of prasiodymium was determined from the weight of precipitate and the corresponding oxide weight, according to equation 23.

$$\frac{\text{gm sample}}{\text{mole Pr}} = \frac{\text{gm sample}}{\text{gm residue}} \times \frac{\text{gm } PrO_{1.5}}{\text{mole } PrO_{1.5}} \qquad (23)$$

Three independent measurements were made. Sample weights of 387, 373 and 389 grams per mole of praseodymium were obtained. The average value of 383 grams was taken as the empirical formula weight. If the atomic weight of praseodymium is subtracted from this value, one obtains 242 grams as the weight of CBDA and water associated with one m ole of praseodymium. The molecular weight of CBDA is 142. Two moles of water and 1.5 moles of CBDA would have a total weight of 249 grams. An empirical formula of $Pr(CBDA)_{1.5} \cdot 2H_2O$, therefore, appears to be a likely possibility for this precipitate, which is assumed to be a close representation of all lanthanide malonate precipitates.

EXPERIMENTAL RESULTS

The formation constants of the lanthanide chelate species of dimethylmalonate, 1,1-cyclobutanedicarboxylate and 1,1-cyclopentanedicarboxylate are given in tables 3, 4 and 5. The formation constants reported were determined using three β_n parameters. The number of iterations was never allowed to exceed ten. The number of iterations was generally four or five. However, ten iterations were performed in the case of one CPDA complex which had a slightly negative K_3 value. From the calculated β_n values a theoretical $\bar{n}$ was determined for each data point. If the experimental $\bar{n}$ and the theoretical $\bar{n}$ differed by more than 1%, the data point was assumed to be a poor value and was discarded. A new set of β_n values was calculated using the remainder of the data points. By comparing the final set of theoretical $\bar{n}$ values with the experimental $\bar{n}$ values, the general fit of the data with the calculated β_n parameters could be determined. The standard deviation in the calculated formation constants given in terms of each β_n is less than or equal to the following values: 1.0% for β_1, 5% for β_2, and 50% for β_3. The values of the individual step formation constants for each ligand are plotted as a function of atomic number in figures 5 and 6. The dissociation constants for each of the acids used in this research are given in table 6. A plot of X, Y values

Table 3. Stability constants for 1:1, 1:2 and 1:3 rare-earth 1,1-dimethylmalonate chelate species

rare-earth	$\bar{n}_{max}$	K_1	K_2	K_3	K_1/K_2	β_2	β_3
La	1.02	3,097	194	45.2	15.9	6.02×10^5	2.72×10^7
Ce	1.20	4,311	316	13.6	13.7	1.36×10^6	1.85
Pr	1.30	6,171	254	33.2	24.3	1.57	5.20
Nd	1.30	7,145	245	51.4	29.2	1.75	9.00
Sm	1.63	10,990	290	6.1	37.9	3.19	1.93
Eu	1.62	12,790	249	7.6	51.3	3.19	2.41
Gd	1.62	12,860	239	11.6	53.8	3.08	3.58
Tb	1.66	16,010	262	12.0	61.2	4.19	5.04
Dy	1.62	16,900	261	9.0	64.8	4.41	3.98
Dy[a]	(1.90)	(16,140)	(164)		(98.2)		
Ho	1.59	15,290	245	8.2	62.4	3.74	3.05
Er	1.60	15,260	262	6.8	58.1	4.00	2.71
Tm	1.65	15,280	286	8.1	53.3	4.38	3.55
Yb	1.65	16,250	321	6.3	50.6	5.22	3.27
Lu	1.70	14,660	338	7.3	43.3	4.96	3.63
Y	1.55	12,300	190	8.1	64.6	2.34	1.90

[a]Dysprosium concentration = 0.010 molar.

Table 4. Stability constants for 1:1, 1:2 and 1:3 rare-earth 1,1-cyclobutanedicarboxylate chelate species

rare-earth	$\bar{n}_{max}$	K_1	K_2	K_3	K_1/K_2	β_2	β_3
La	1.02	2600	129	——	20.2	——	——
Ce	1.03	3954	195	316	20.3	——	2.43×10^8
Pr	1.27	5768	282	29.3	20.4	1.622×10^7	4.23×10^7
Nd	1.44	6554	296	14.6	22.2	1.940	2.53
Sm	1.38	11500	292	21.6	39.4	3.352	6.52
Eu	1.60	13780	272	5.6	50.7	3.773	1.89
Gd	1.59	14170	249	10.5	57.0	3.515	3.31
Tb	1.60	17580	272	4.1	64.5	4.767	1.77
Dy	1.68	20120	304	21.1	66.2	6.108	1.24×10^8
Ho	1.68	18340	288	19.0	63.6	5.279	9.66×10^7
Er	1.65	18420	295	20.1	62.5	5.448	1.05×10^8
Tm	1.74	18950	344	23.3	55.1	6.506	1.46
Yb	1.73	19680	376	23.6	52.3	7.416	1.69
Lu	1.75	18020	412	21.2	43.8	7.432	1.69
Y	1.69	16230	201	39.4	80.0	3.24×10^6	1.28×10^8

Table 5. Stability constants for 1:1, 1:2 and 1:3 rare-earth 1,1-cyclopentanedicarboxylate chelate species

rare-earth	$\bar{n}_{max}$	K_1	K_2	K_3	K_1/K_2	β_2	β_3
Eu	1.59	15050	336	0.1	44.8	5.051×10^6	4.68×10^5
Gd	1.59	15160	309	3.1	49.1	4.681	1.47×10^7
Tb	1.60	18300	328	2.5	55.8	6.000	1.47
Dy	1.59	19570	330	-0.9	59.3	6.453	-5.93×10^6
Ho	1.58	17820	310	0.1	57.5	5.524	5.23×10^5
Er	1.60	17550	332	1.3	52.8	5.824	7.76×10^6
Tm	1.65	17640	376	2.3	46.9	6.617	1.51×10^7
Yb	1.66	18440	415	4.1	44.5	7.640	3.18
Lu	1.69	16510	441	4.4	37.5	7.289	3.24

Figure 5. First step formation constant as a function of ionic radius

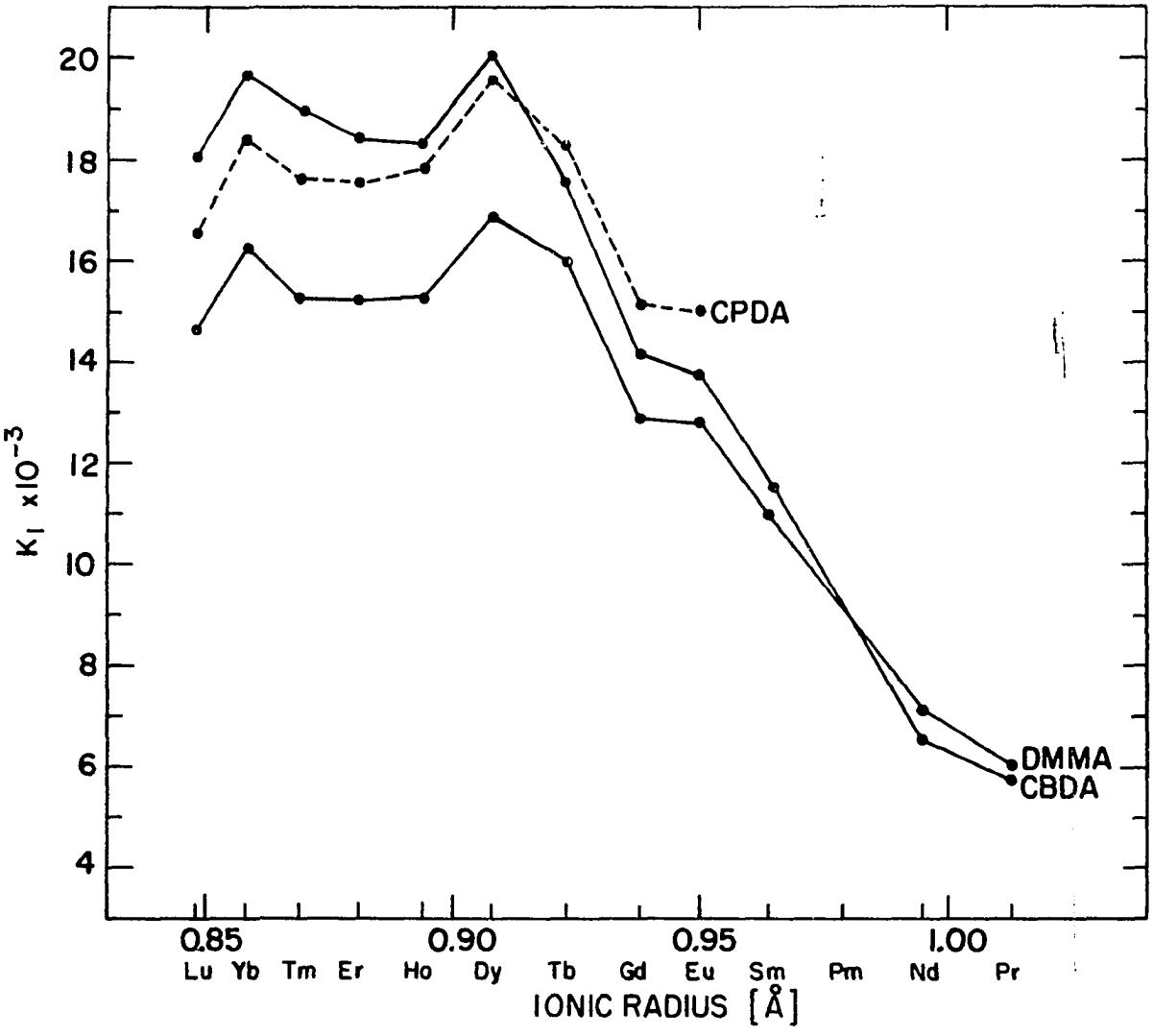
20
18
16
14
12
10
8
6
4
$K_1 \times 10^{-3}$
CPDA
DMMA
CBDA
0.85
0.90
0.95
1.00
Lu Yb Tm Er Ho Dy Tb Gd Eu Sm Pm Nd Pr
IONIC RADIUS [Å]

Figure 6. Second step formation constant as a function of ionic radius

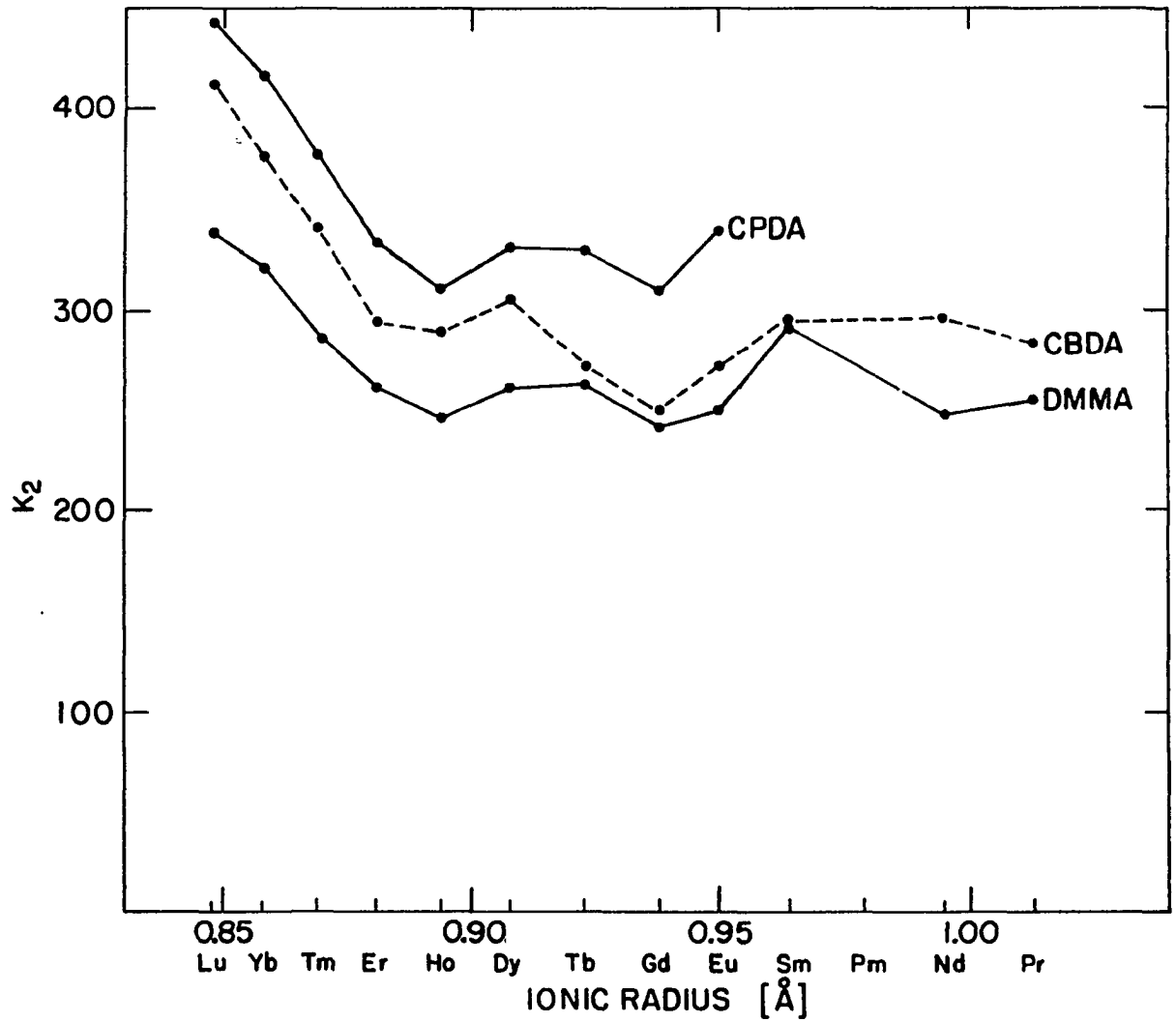
400
300
200
100
K_2
CPDA
CBDA
DMMA
0.85
0.90
0.95
1.00
Lu Yb Tm Er Ho Dy Tb Gd Eu Sm Pm Nd Pr
IONIC RADIUS [Å]

used in the determination of the ionization constants of cyclobutanedicarboxylic acid is given in figure 7. The X, Y values are calculated according to equation 20, which is in the form Y = mx + b.

Table 6. Acid dissociation constants

Acid	K_{a_1}	K_{a_2}
dimethylmalonic	1.09×10^{-3}	1.96×10^{-6}
1,1-cyclobutanedicarboxylic	1.72×10^{-3}	3.10×10^{-6}
1,1-cyclopentanedicarboxylic	9.02×10^{-4}	1.96×10^{-6}

Figure 7. Straight line data obtained for determining α_1 and α_2 for 1,1-cyclopentanedicarboxylic acid. This data is typical of data obtained for other acids investigated.

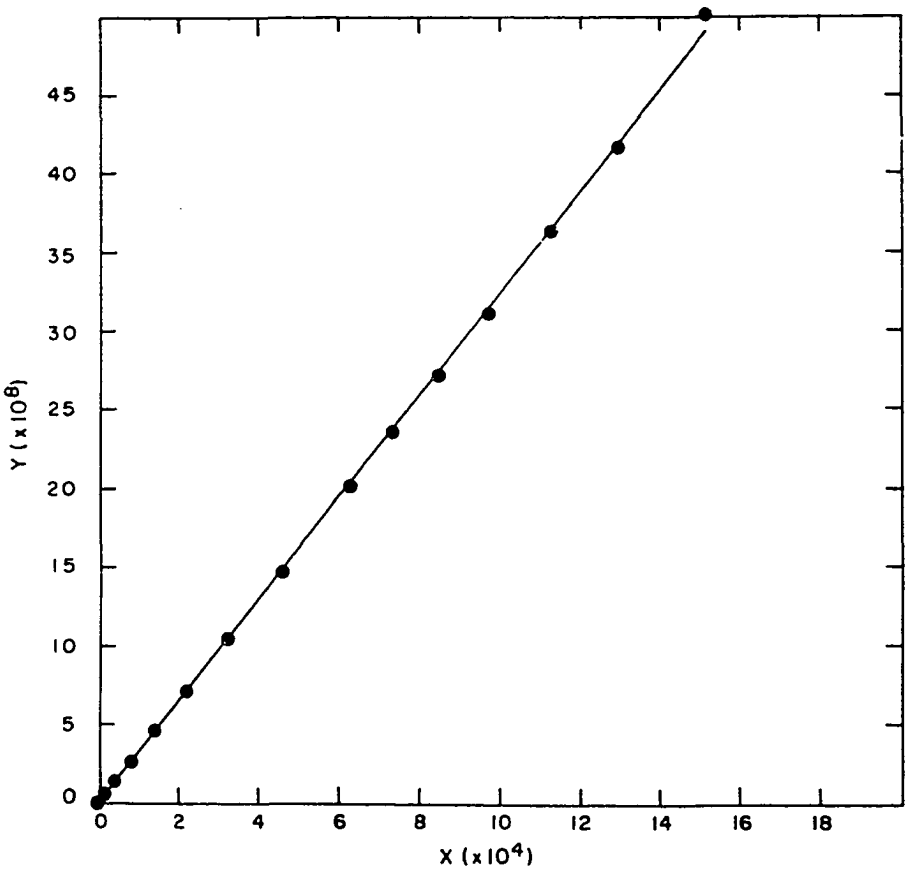
45
40
35
30
25
20
15
10
5
0
Y (x10^8)
0
2
4
6
8
10
12
14
16
18
X (x10^4)

PART II. ION PAIR CONSIDERATIONS IN METHYL ALCOHOL

The terbium-CBDA and terbium-α-HIBA systems were studied in methyl alcohol solution and are assumed to be representative of all of the lanthanide chelate species of these and similar ligands. The dielectric constant of methyl alcohol (31.5) is quite small compared to the dielectric constant of water (78.5) (15, p. 161). Due to this low dielectric constant all electrolytes have a high degree of ion pair formation in methanol. Therefore, some modifications of the method used to determine formation constants of lanthanide malonate chelate species in aqueous solution was necessary in order to employ it as a method for determining the same constants in methanol. Material balance equations 4, 5, 13 and 14 written for total metal, total acid anion, and total hydrogen ion in aqueous solution, are not strictly true in methyl alcohol solution. These equations were written assuming that ion pair species did not exist in aqueous solution. To be valid for a methanol solution of the same materials these equations must be rewritten to include all possible ion pair species.

In order to establish material balance equations in methyl alcohol, a knowledge of the dissociation constants and activity coefficients of the various electrolytes is necessary. Chloride ion was used as a common anion in the formation constant determination because of the convenient reversible reaction given in equation 24 (which was useful for activity coefficient

determinations). Due to its high solubility in methyl

$$Ag^0 + Cl^- \rightarrow AgCl - e^- \quad (24)$$

alcohol, LiCl was used as the supporting electrolyte. Hydrogen ion was liberated from the organic acid upon coordination with the lanthanide ion. Therefore, it was necessary to determine dissociation constants and activity coefficients of $TbCl_3$, LiCl and HCl.

DISSOCIATION CONSTANT DETERMINATION

Calculations

The equivalent conductance of an electrolyte is proportional to the concentration of that electrolyte in solution in the ionic form. The association constant for a uni-univalent electrolyte can be calculated from equivalent conductance data for dilute solutions of the electrolyte by employing Ostwald's dilution function (15, p. 286; 16, p. 289),

$$K = \frac{\Lambda^2 C}{\Lambda_o(\Lambda_o - \Lambda)} , \tag{25}$$

which can be written as follows:

$$\frac{1}{\Lambda} = \frac{1}{\Lambda_o} + \frac{C\Lambda}{K(\Lambda_o)^2} . \tag{26}$$

If $1/\Lambda$ is plotted versus ΛC one can determine the value of K from the slope $\frac{1}{K(\Lambda_o)^2}$ and the intercept $\frac{1}{\Lambda_o}$. Figures 8 and 9 show these functions plotted for HCl and LiCl. The plot of $1/\Lambda$ versus ΛC is a straight line only in the dilute region (less than 0.01 molar). Deviations from a straight line noted at higher concentration of electrolyte reflect a change in ionic mobilities and activity coefficients.

Ostwald's dilution function is based on the conductance ratio, α, which is a comparison of the equivalent conductance at some finite concentration of interest

to the equivalent conductance at infinite dilution, and represents the extent of dissociation (16 p. 96). The expression derived for α,

$$\alpha = \frac{\Lambda_c}{\Lambda_o} \tag{27}$$

$$\Lambda_o = (U + V)F \tag{28}$$

$$\Lambda_c = (U_c + V_c)F\alpha \tag{29}$$

has assumed that

$$U_c + V_c = U + V \ ,$$

which is a good approximation only when the electrolyte is extremely dilute.

The extent of ion pair formation in the 3:1 electrolyte, $TbCl_3$, was also determined from the conductance of the electrolyte in dilute solution. There is sufficient difference between the individual dissociation constants such that the plot of equivalent conductance versus concentration of electrolyte breaks into three straight line portions as shown in figures 10 and 11. The first dissociation constant can be determined by employing Ostwald's dilution function. The value of Λ_o is determined by extending the straight line portion of the Λ versus ΛC plot, given in figure 10, to infinite dilution. The data points composing this portion of the plot have been used in the construction of a new plot

of $1/\Lambda$ versus ΛC shown in figure 12. The value of K_1 has been determined from this plot in the manner previously described for a 1:1 electrolyte. The second and third dissociation constants were determined by extending the remaining two straight lines of the plot shown in figure 11, and taking Λ_{o2} and Λ_{o3} as the value at the intersection of those lines with the equivalent conductance axis. The equivalent conductances at infinite dilution can be set equal to the sum of the conductances of the individual ions which they represent, as in equations 31 and 32.

$$\Lambda_{o2} = \Lambda_{omx} + \Lambda_{ox_2} + \Lambda_{ox_1} \tag{31}$$

$$\Lambda_{o3} = \Lambda_{om} + \Lambda_{ox_3} + \Lambda_{ox_2} + \Lambda_{ox_1} \tag{32}$$

In order to use these equations with the given conductance data, the equivalent conductance of all ions present but not included in the equation must be subtracted from the total equivalent conductance Λ_c and Λ_o. The resulting Λ_c' and Λ_o' can be compared to yield a conductance ratio α, similar to the ratio used for a 1:1 electrolyte. An expression similar to Ostwald's dilution function (equation 25) can be written for the individual dissociation constants of $TbCl_3$. Ostwald's dilution function is derived from the mass action expression 33. The individual ion concentrations, are given by multiplying the conductance ratio by

$$K = \frac{(M)(X)}{(MX)} \tag{33}$$

the total concentration of the electrolyte as given in expression 34. This reduces to the Ostwald dilution function.

$$K = \frac{\left[\frac{\Lambda'_c}{\Lambda'_c}\right]c\left[\frac{\Lambda'_c}{\Lambda'_c}\right]c}{\left[1 - \frac{\Lambda'_c}{\Lambda'_o}\right]c} \qquad (34)$$

The species present during the second dissociation are: MX_2^+, MX^+, X_1^-, and X_2^- where X_1^- and X_2^- represent the first and second chloride ions to dissociate. The extrapolated value of the equivalent conductance at infinite dilution for any step of the dissociation is assumed to represent the theoretical conductances of the ions present when that dissociation step is complete, and before the next step has commenced. The value Λ_{o_2} would then represent the equivalent conductance of MX^{+2}, X_1^- and X_2^- at infinite dilution. To be used in expression 34, one must subtract the value of Λ_{ox_1} from Λ_{o_2} yielding a new Λ'_{o_2} A similar procedure was used to determine Λ'_{o_3}. The conductance ratio was determined from the expression for the ion concentration MX^{+2},

$$\frac{[\Lambda_c - \Lambda_{ox_1} - \Lambda_{omx_2}N_{mx_2}]}{\Lambda_{o2} - \Lambda_{ox_1}} \cdot M_T = [MX^{+2}] \qquad (35)$$

where N_{mx_2} represents the fraction of the total metal in the MX_2^+ form. Since the total metal concentration is

given by,

$$M_T = [MX^{+2}] + [MX_2^{+}] \quad , \tag{36}$$

the value of N_{mx_2} is simply

$$\frac{M_T - [MX]}{M_T} \quad .$$

If one then makes this substitution for N_{mx_2}, the following expression is obtained:

$$[MX^{+2}] = \frac{(\Lambda_C - \Lambda_{ox_1})M_T - \Lambda_{omx_2}(M_T - [MX])}{\Lambda_{o2} - \Lambda_{ox_1}} \quad . \tag{37}$$

Equation 37 reduces to equation 38,

$$[MX^{+2}] = \left[\frac{\Lambda_C - \Lambda_{ox_1} - \Lambda_{omx_2}}{\Lambda_o - \Lambda_{ox_1} - \Lambda_{omx_2}}\right] M_T \quad , \tag{38}$$

which is simply

$$[MX^{+2}] = \left[\frac{\Lambda_C - \Lambda_{o1}}{\Lambda_{o2} - \Lambda_{o1}}\right] M_T \tag{39}$$

$$\Lambda'_C = \Lambda_C - \Lambda_{o1} \tag{40}$$

$$\Lambda'_{o2} = \Lambda_{o2} - \Lambda_{o1} \tag{41}$$

where the conductance ratio α_2 is given by expression 42.

$$\alpha_2 = \frac{\Lambda_C - \Lambda_{o2}}{\Lambda_{o2} - \Lambda_{o1}} \tag{42}$$

Similarly, α_3 is given by expression 43.

$$\alpha_3 = \frac{\Lambda_C - \Lambda_{o2}}{\Lambda_{o3} - \Lambda_{o2}} \tag{43}$$

$$\Lambda'_C = \Lambda_C - \Lambda_{o2} \tag{44}$$

$$\Lambda'_{O3} = \Lambda_{O3} - \Lambda_{O2} \tag{45}$$

The dissociation constants are related to α_2 and α_3 as in equations 46 and 47.

$$K_2 = \frac{(\alpha_2)^2 c}{(1 - \alpha_2)} \tag{46}$$

$$K_3 = \frac{(\alpha_3)^2 c}{(1 - \alpha_3)} \quad . \tag{47}$$

Experimental Technique

The conductances of methanol solutions of the previously mentioned pure electrolytes were determined by measuring the resistance between two parallel platinum plates submerged in a solution of the electrolyte. The platinum plates were electrically attached to platinum leads sealed in Pyrex tubing which was affixed to the lid of a cylindrical Pyrex vessel. The lid was fitted to the vessel by means of a ground glass joint. The solution of which the conductance was to be determined was contained in this Pyrex tube, and the lid containing the electrode was placed in the tube during each measurement and removed for rinsing and refilling of the tube. Sixty-cycle alternating current was used in the measurements. The observed resistance was recorded. The cell constant was obtained by measuring the resistance of an aqueous solution 0.1000 normal in KCl. This solution has a specific conductance of 0.01289 cm^2/ohm. The cell constant

was calculated by multiplying the measured resistance of this solution by its specific conductance and was redetermined before each set of measurements.

A set of ten to twenty 100.0 millileter samples of each electrolyte were prepared in the concentration range of 10^{-2} to 10^{-5} molar by dilution from a common stock solution. The conductances were measured at 25 degrees centigrade. The methyl alcohol used had a specific conductance less than 5×10^{-7} cm^2/ohm.

In the determination of the conductance of HCl solutions, an abnormal trend in the equivalent conductance was observed. The equivalent conductance decreased as one approached infinite dilution. Upon checking the conductance bridge with an oscilloscope, it was discovered that there was a DC component in the AC signal. This DC current polarized the electrode slightly, allowing hydrogen ions to reduce to free hydrogen on the platinum electrodes. This coating of hydrogen on the electrodes lowered the apparent concentration of the solutions. This undesirable reaction was eliminated by placing a capacitor in series with the conductance cell.

The electrodes were electrolyzed in a solution of chloroplataninic acid before use. This deposited a layer of finely divided platinum on the electrode surface.

Results

Plots of $1/\Lambda$ versus ΛC are given for HCl and LiCl in figures 8 and 9 respectively. The equivalent conductance of $TbCl_3$ is given as a function of molar concentration in figure 10. figure 11 is a magnification of the dilute region of figure 10. A plot of $1/\Lambda$ versus ΛC corresponding to the plots given for the 1:1 electrolytes is given in figure 12 for the first step in the dissociation of $TbCl_3$. The values of the second and third dissociation constants determined by equations 46 and 47 are plotted in figures 13 and 14 respectively. The value of the dissociation constant varies with concentration. This is believed to be due to a change in ionic mobility over the concentration range in which the values were determined. The relation given in equation 30 would be invalid if this were the case. However, the thermodynamic values are determined by extrapolating the dissociation constant to infinite dilution.

Discussion of Results

Kraus and Bray (17) collected abundant data on the conductance of 1:1 electrolytes in a number of low dielectric solvents. They determined the ion pair dissociation constants between electrolyte concentrations of 10^{-4} to 10^{-3} molar from a plot of $1/\Lambda$ versus ΛC, which yielded a straight line. Deviation from this straight line occured

Figure 8. Inverse of the equivalent conductance versus the product of equivalent conductance and concentration for HCl

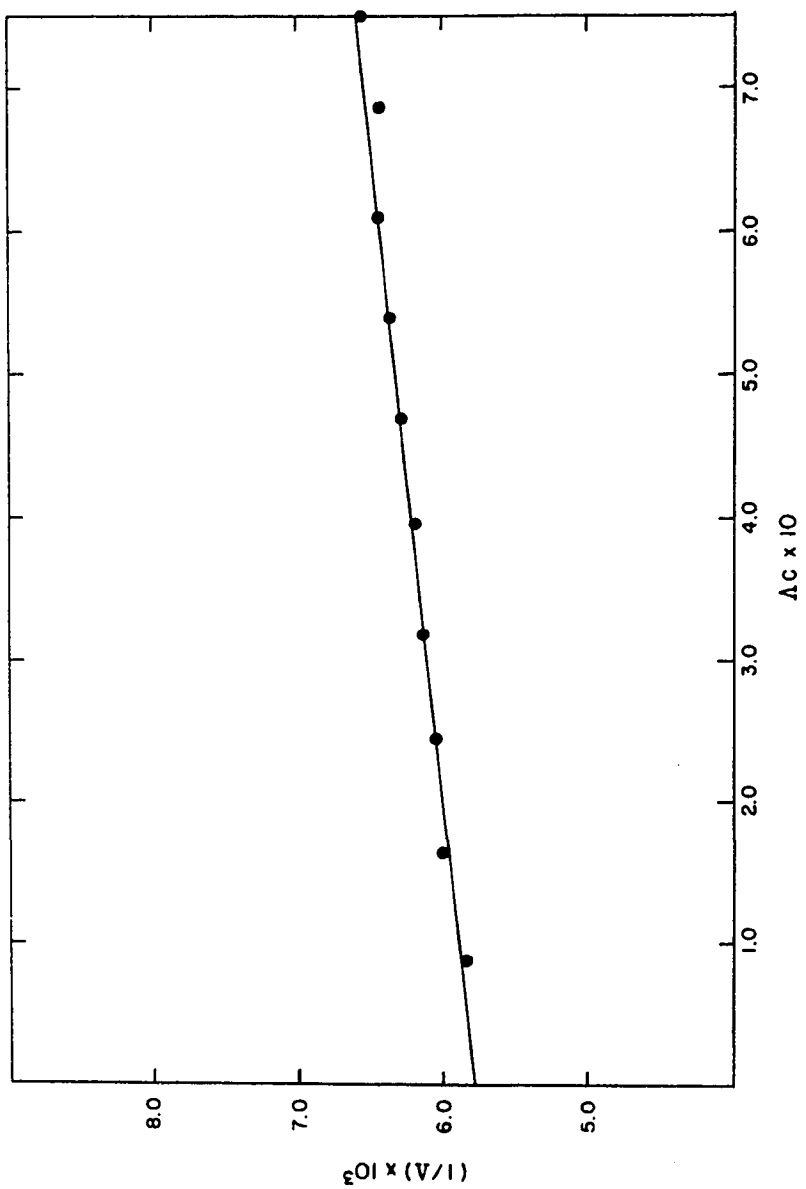
(1/Λ) x 10³
8.0
7.0
6.0
5.0
Δc x 10
1.0
2.0
3.0
4.0
5.0
6.0
7.0

Figure 9. Inverse of the equivalent conductance versus the product of equivalent conductance and equivalent concentration for LiCl

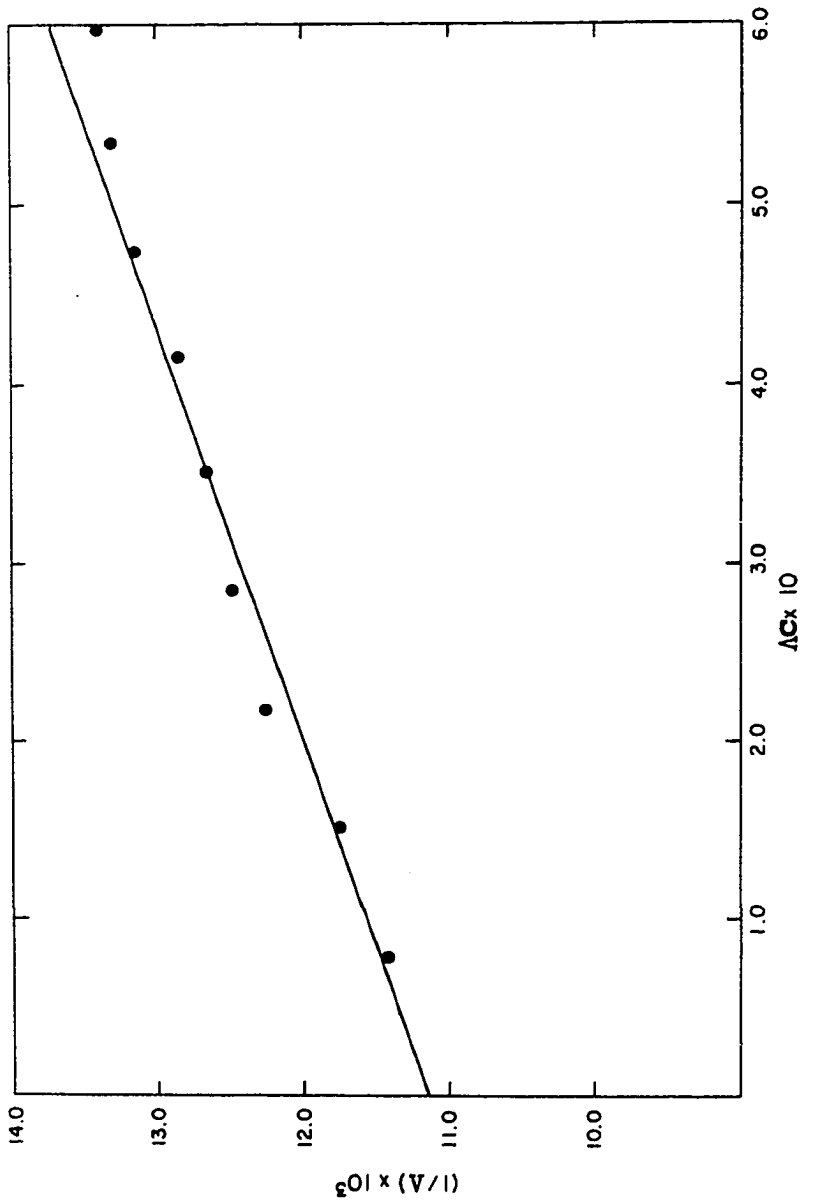
(1/A) x 10³
14.0
13.0
12.0
11.0
10.0
1.0
2.0
3.0
4.0
5.0
6.0
ΔCx 10

Figure 10. Equivalent conductance versus molar concentration of $TbCl_3$

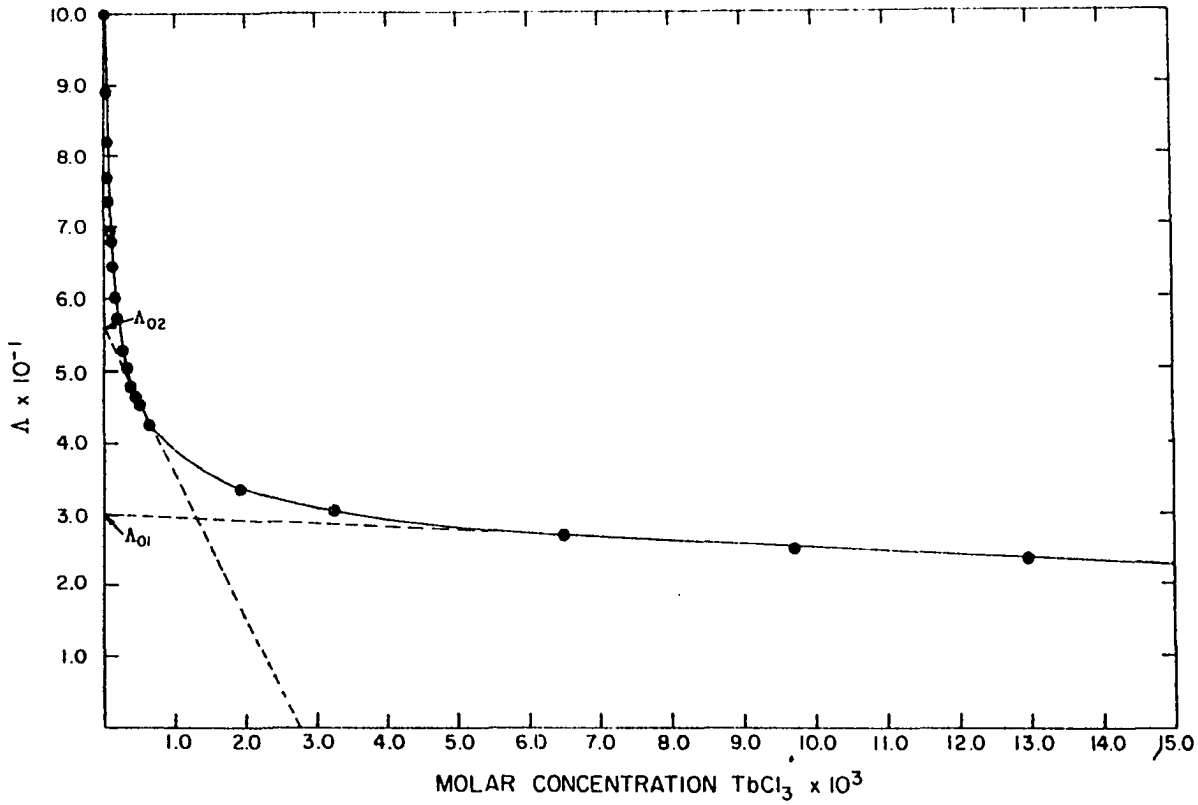
10.0
9.0
8.0
7.0
6.0
5.0
4.0
3.0
2.0
1.0
Λ x 10⁻¹
Λ02
Λ01
1.0
2.0
3.0
4.0
5.0
6.0
7.0
8.0
9.0
10.0
11.0
12.0
13.0
14.0
15.0
MOLAR CONCENTRATION TbCl3 x 10³

Figure 11. Equivalent conductance versus molar concentration of $TbCl_3$: magnification of dilute region in figure 10

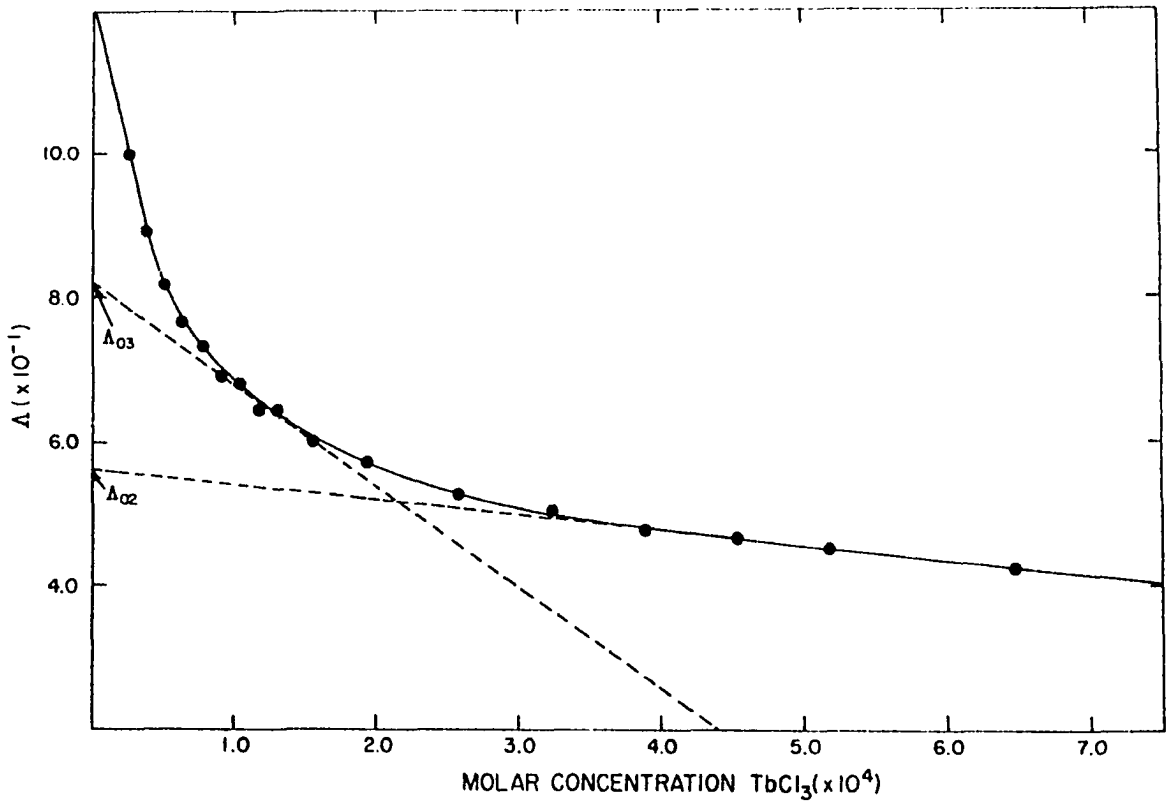
10.0
8.0
6.0
4.0
Λ (x 10⁻¹)
A03
A02
1.0
2.0
3.0
4.0
5.0
6.0
7.0
MOLAR CONCENTRATION TbCl3(x 10⁴)

Figure 12. Inverse of the equivalent conductance versus the product of equivalent conductance and equivalent concentration for the first step in the dissociation of $TbCl_3$

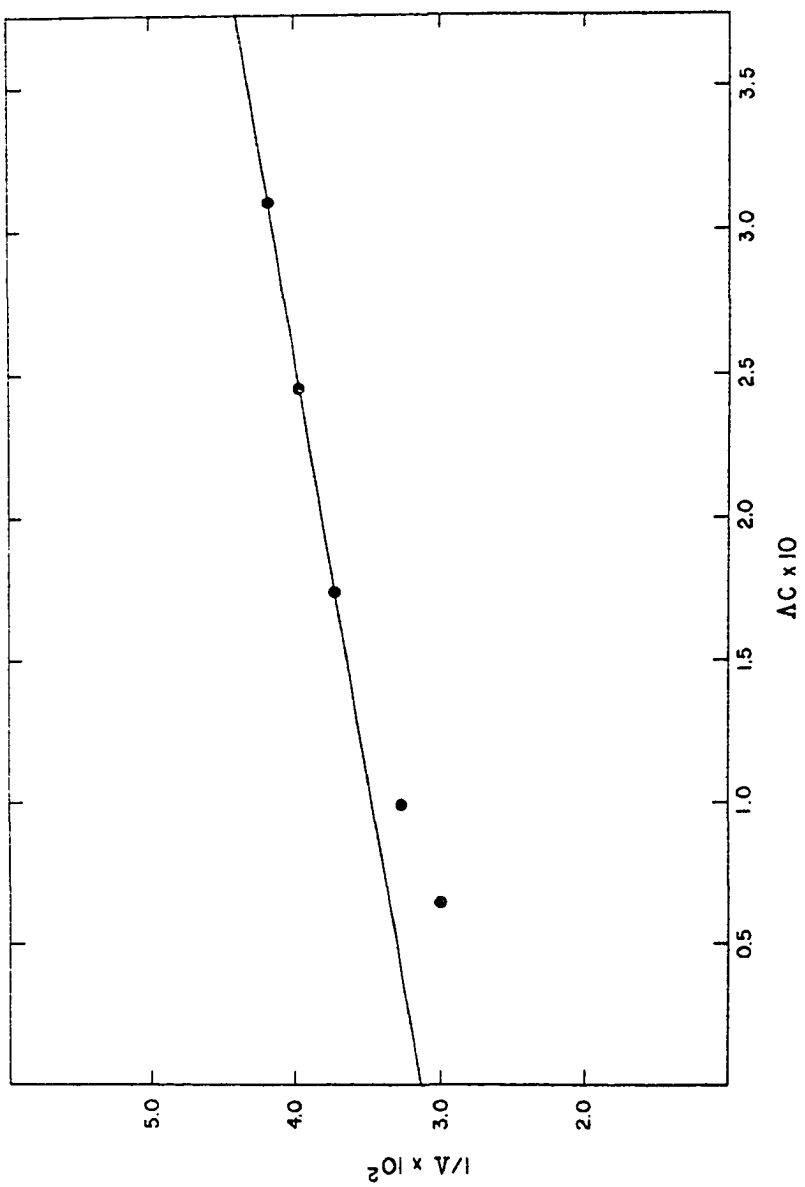
1/Λ x 10²
5.0
4.0
3.0
2.0
0.5
1.0
1.5
2.0
2.5
3.0
3.5
ΔC x 10

Figure 13. Calculated values of the second dissociation constant of $TbCl_3$ as a function of molar concentration of $TbCl_3$: T_{K2} obtained by extrapolation to infinite dilution = 1.95×10^{-3}

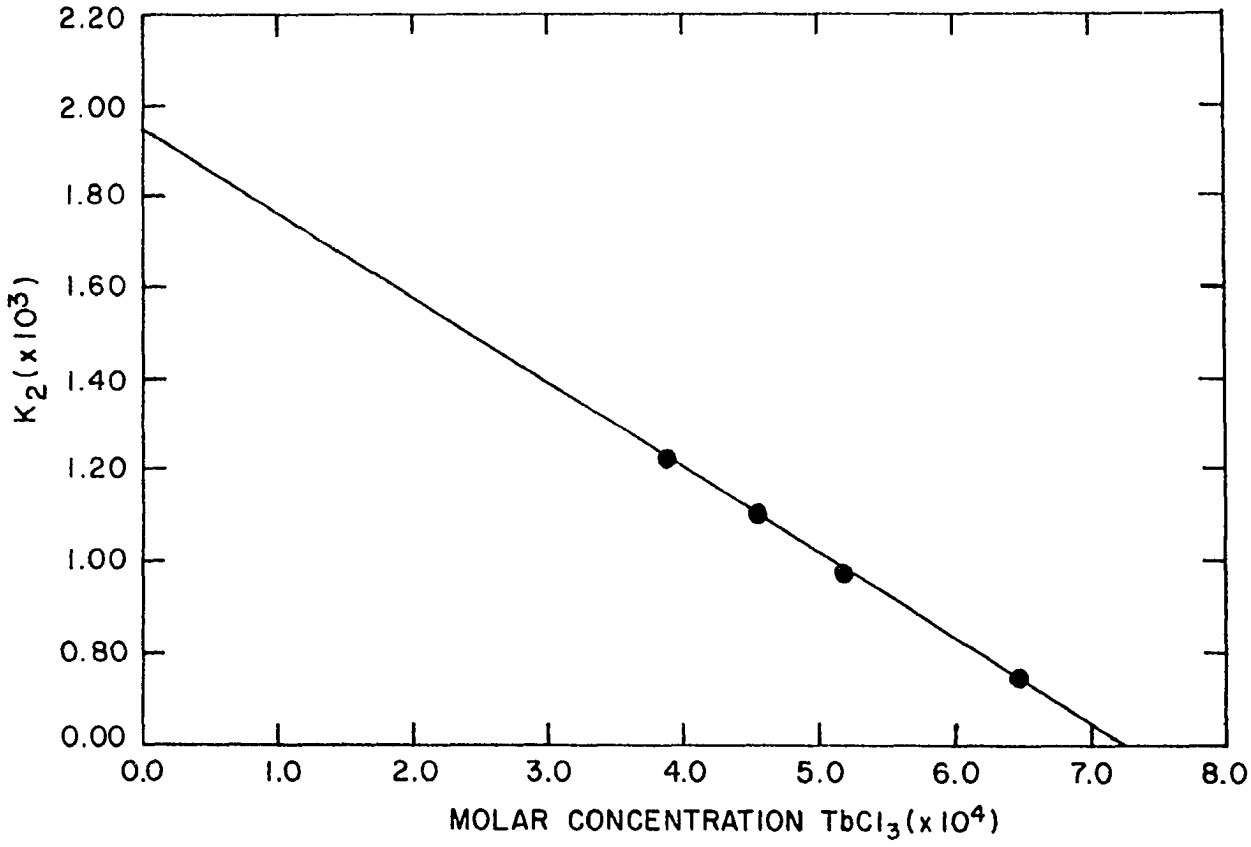
2.20
2.00
1.80
1.60
1.40
1.20
1.00
0.80
0.00
$K_2(x10^3)$
0.0
1.0
2.0
3.0
4.0
5.0
6.0
7.0
8.0
MOLAR CONCENTRATION $TbCl_3(x10^4)$

Figure 14. Calculated values of the third dissociation constant of $TbCl_3$ as a function of molar concentration of $TbCl_3$: T_{K_3} obtained by extrapolation to infinite dilution = 3.25×10^{-4}

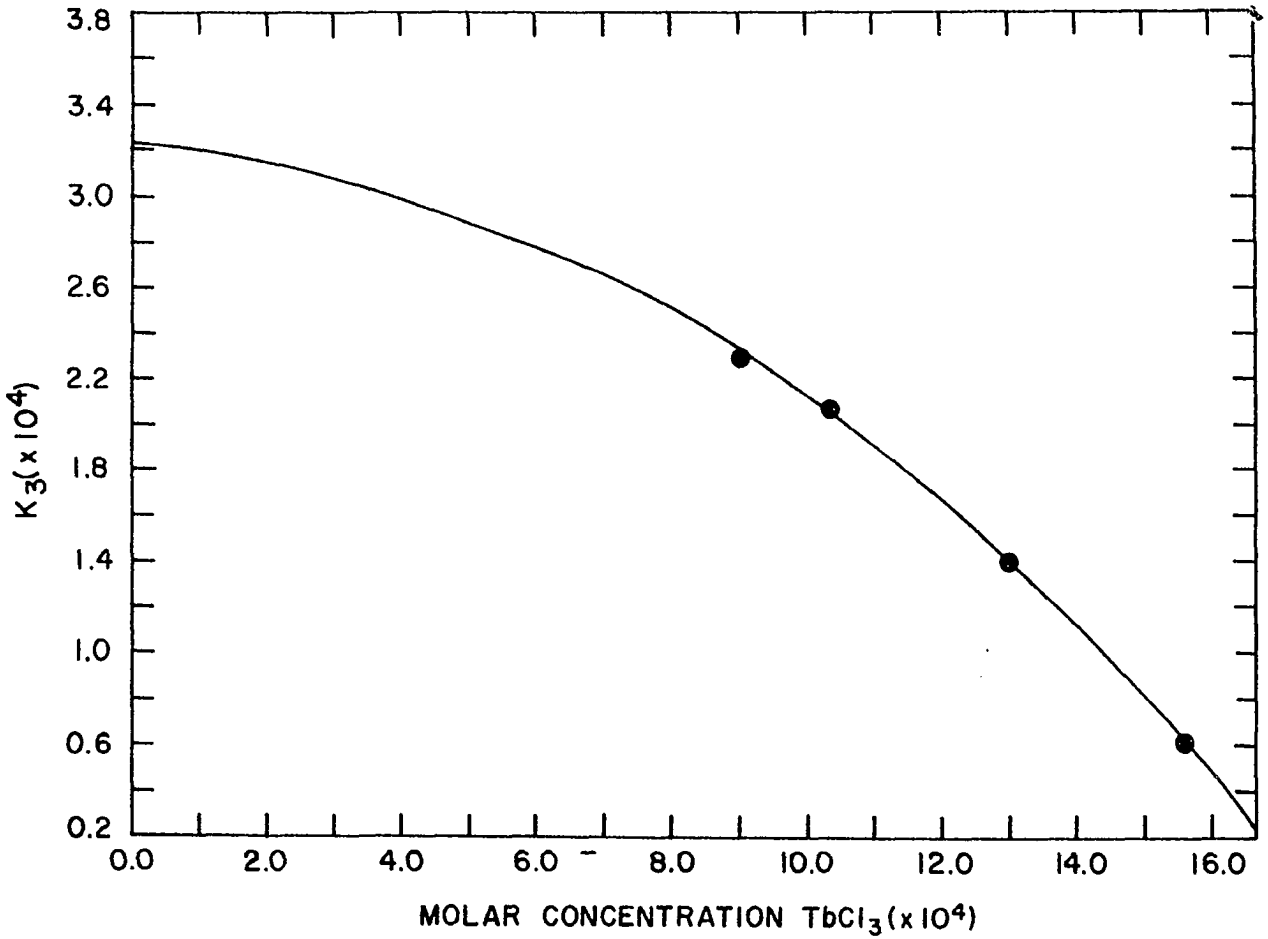
3.8
3.4
3.0
2.6
2.2
1.8
1.4
1.0
0.6
0.2
$K_3(\times 10^4)$
0.0
2.0
4.0
6.0
8.0
10.0
12.0
14.0
16.0
MOLAR CONCENTRATION $TbCl_3(\times 10^4)$

outside this 10^{-4} to 10^{-3} molar concentration range. At higher concentrations a change in ionic mobilities caused the points to fall below the straight line. A random scattering of points was obtained at the low end of the concentration range due to effects of the solvent on conduc tance. The conductance data collected in this work have trends similar to the data of Kraus and Bray (17). All ion pair dissociation constants calculated for the reaction $MX \rightarrow M^+ + X^-$, were within the range of 2.90×10^{-2} to 3.55×10^{-2}. The determinations appear to be self consistent, since one would expect the magnitude of the dissociation constants to depend only on the charge/size ratios of the metal and ligand. The ligand was always chloride ion and the cations were H^+, Li^+, and $TbCl_2^+$. The calculated ion pair dissociation constants do justify breaking the conductance curve for $TbCl_3$ into three portions, each part corresponding to a particular step in the dissociation. There is a factor of 15 between K_1 and K_2 and a factor of 7 between K_2 and K_3. This would indicate that the dissociation does occur in a stepwise fashion.

ACTIVITY COEFFICIENT DETERMINATION

Calculations

Activity coefficients of HCl, LiCl, and $TbCl_3$ were determined from the potential difference measured between two Ag/AgCl electrode, one dipping into either side of a concentration cell containing a reference and an unknown activity of chloride ion. A computer program was written to calculate the free chloride ion concentration and the mean activity coefficients at each ion concentration. These calculations were made using the following equations:

$$E = \frac{-2RT}{nF} \int_I^{II} \underline{T}^+ \, d \ln a \, . \tag{48}$$

Equation 48 rearranges to equation 49 and is given by Harned and Owen (15, p. 486).

$$-\Delta \log y = \frac{-E}{0.1183\, T_R} - \log\frac{c}{C_R} - \frac{1}{T_R} \int_{C_R}^{C} \Delta\underline{T}^+ \, d \log c - \frac{1}{T_R} \int_{Y_R}^{Y} \Delta\underline{T}^+ \, d \log y \tag{49}$$

$$K = \frac{(YC)^2}{X - C} \tag{50}$$

Equation 50 rearranges to equation 51 .

$$(YC)^2 + KC - KX = 0 \tag{51}$$

E = electrical potential

T = temperature

$\underline{T}$ = transference number

T_R = reference transference number @ infinite dilution

y = mean activity coefficient

K = dissociation constant of electrolyte

X = total electrolyte concentration

C = chloride ion concentration

Equation 48 is an expression for the total potential difference measured between the electrodes in a concentration cell with a liquid junction. The total potential arises from two sources. The ion involved in the reaction at each electrode has a different activity at each electrode, accounting for part of the measured potential difference. The remainder is accounted for by the liquid-liquid junction potential which develops at the interface between the two different concentrations of the electrolyte. The potential arises from the fact that ions are moving from the more concentrated to the more dilute region. Because the cations move at a different rate than the anions, an electric double layer is established at the boundary between the two solutions. The magnitude of this potential could be visualized as arising from nF coulombs of electricity flowing through the cell from the concentrated to the dilute solution (16, p. 202). During this flow of current, U/(U + V) gram atoms of cation are transferred from the concentrated to the dilute solution increasing the concentration of

cations from C_1 to C_2. The quantity of work expended at the interface is then given by:

$$A_1 = \frac{U}{U + V} RT \ln(c_2/c_1). \tag{52}$$

Simultaneously, V/(U + V) gram atoms of anion are transported from the dilute to the concentrated solution producing the quantity of work given by:

$$A_2 = \frac{V}{U + V} RT \ln(c_2/c_1). \tag{53}$$

The total work performed at the interface is, therefore, given by:

$$A = A_1 - A_2 = \frac{U - V}{U + V} RT \ln(c_2/c_1). \tag{54}$$

The overall cell potential is given by:

$$E_T = E_j + \frac{RT}{nF} \ln(c_2/c_1) \tag{55}$$

$$A = E_j nF \tag{56}$$

$$E_j = \frac{U - V}{U + V} \frac{RT}{nF} \ln(c_2/c_1) \tag{57}$$

$$E_T = \frac{2U}{U + V} \frac{RT}{nF} \ln(c_2/c_1) \tag{58}$$

$$E_T = 2T^+ \frac{RT}{nF} \ln(c_2/c_1). \tag{59}$$

At finite concentration c_1 and c_2 are replaced by the corresponding activities and $\underline{T}$ is a function of concentration. Thus, equation 59 reduces to equation 48.

An approximate value of the activity coefficient $\underline{y}$ is used in equation 51 to calculate the free ion concentration $\underline{c}$. This value of $\underline{c}$ is plugged into equation 49 and a better value of $\underline{y}$ is calculated. This process is reiterated until $\underline{y}$ changes by less than 0.01. The two integrals in equation 49 were omitted on the first calculation of $\underline{y}$. However, upon obtaining good approximate values of $\underline{y}$ and $\underline{c}$,,and a knowledge of the transference number as a function of $\underline{y}$ and $\underline{c}$, it was possible to express the change in transference number (ΔT) as a function of either the ion concentration or the activity coefficient by means of a second order polynomial equation in $\underline{c}$ or $\underline{y}$. This allowed the evaluation of the integrals in equation 49. The activity coefficients and ion concentrations were recalculated using the complete equation 49. This whole process was reiterated three times to obtain the final set of ion concentrations and activity coefficients.

In the case of $TbCl_3$, the determination of the free chloride ion concentration was more involved. From the known thermodynamic dissociation constants of $TbCl_3$, a chloride material balance equation can be written in terms of the dissociation constants, the mean activity coefficient and the chloride ion activity. This equation is fourth order in chloride ion activity. From the solution to this equation and an approximate value of the

activity coefficient, a value of the chloride concentration was obtained. This value of chloride ion concentration was plugged into equation 49 and a better value for the activity coefficient was obtained. The remainder of the process of solving for the mean ionic activity coefficient was identical to the process described for the 1:1 electrolytes.

Experimental Technique

A diagram of the concentration cell used in the activity coefficient determination is given in figure 15. The electrodes were silver chloride-coated silver wire sealed in 4 millimeter soft glass tubing. Electrical connection was made with the potentiometer leads through a mercury junction in the bottom of each glass tube. The point at which the solution from the two compartments made contact was a continuously flowing junction. This provided a continual renewal of the interface between the two solutions. Since there was a junction potential developed at this interface, it was important to maintain a sharp interface so that the junction potential remained constant and determinable.

Due to the high resistance of dilute solutions of the electrolytes in alcohol, it was difficult to obtain a stable, reproducible value for the most dilute solutions. However, the potentiometer that was used employed a vacuum

Figure 15. Diagram of concentration cell used in activity coefficient determinations

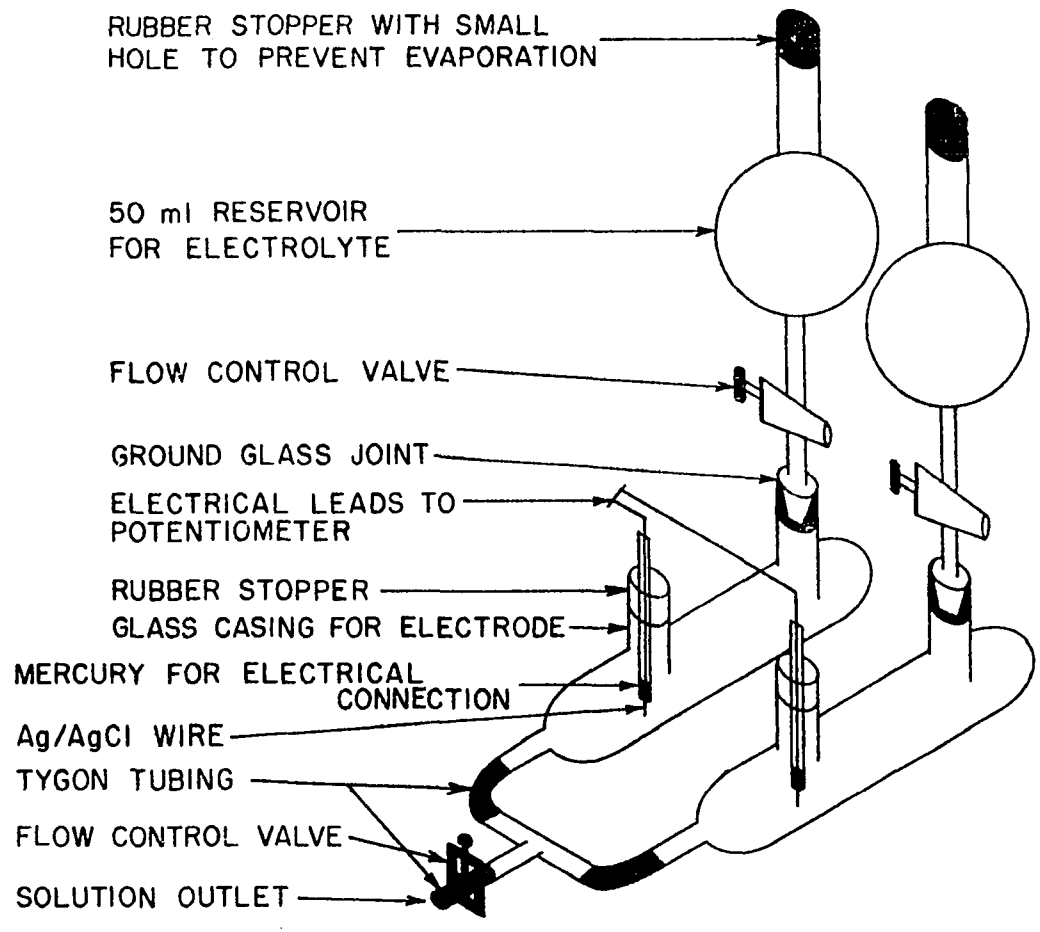
RUBBER STOPPER WITH SMALL HOLE TO PREVENT EVAPORATION
50 ml RESERVOIR FOR ELECTROLYTE
FLOW CONTROL VALVE
GROUND GLASS JOINT
ELECTRICAL LEADS TO POTENTIOMETER
RUBBER STOPPER
GLASS CASING FOR ELECTRODE
MERCURY FOR ELECTRICAL CONNECTION
Ag/AgCl WIRE
TYGON TUBING
FLOW CONTROL VALVE
SOLUTION OUTLET

tube voltmeter for measuring potential difference, which operates on currents as low as 10^{-12} amperes. Because of this instability in dilute solutions, the reference electrolyte was never more dilute than 3×10^{-4} molar. All activities of the electrolyte were measured against the same reference activity of the electrolyte. The activity of the reference electrolyte was determined by making a measurement against the same electrolyte at a concentration below 5×10^{-5} molar where the activity coefficient was taken as 1.00.

Results

The activity coefficients of HCl, LiCl and $TbCl_3$ in methyl alcohol are given as a function of ionic strength in figures 16, 17 and 18. The activity coefficients exhibit minima at ionic strengths near 0.05 molar. The activity coefficients of aqueous solutions of HCl (18), LiCl (15, p. 731), and $DyCl_3$ (19, p. 111) as a function of concentration are presented in table 7. The aqueous solutions of these electrolytes exhibit minima near an ionic strength of 0.5 molar. The shift in this minimum to lower ionic strengths in methyl alcohol is expected.

Discussion of Results

There are two opposing factors which determine the activity coefficient of an electrolyte as a function of ionic strength. One factor is the interionic

Figure 16. Activity coefficient of HCl as a function of ionic strength

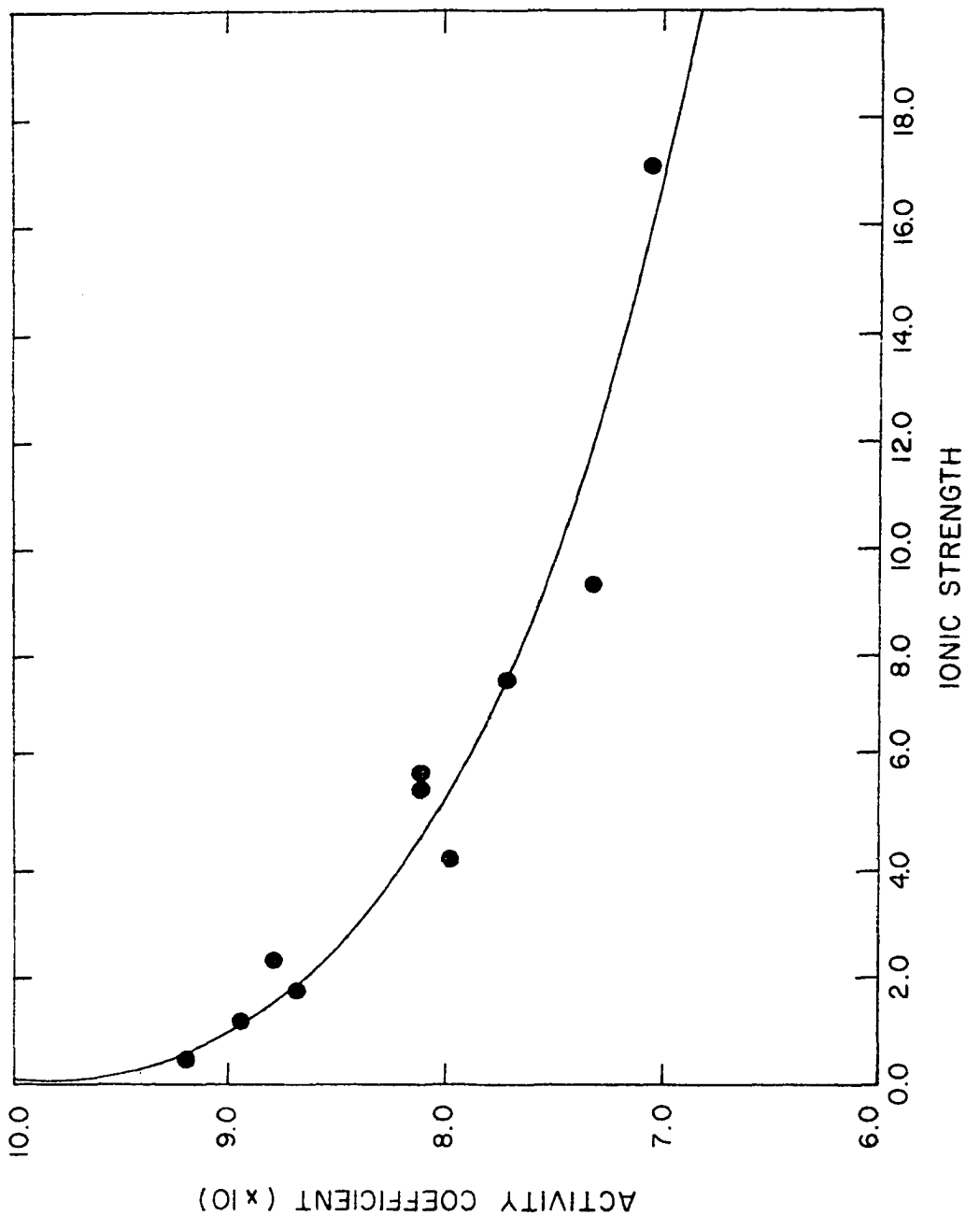
ACTIVITY COEFFICIENT (x 10)
10.0
9.0
8.0
7.0
6.0
0.0
2.0
4.0
6.0
8.0
10.0
12.0
14.0
16.0
18.0
IONIC STRENGTH

Figure 17. Activity coefficient of LiCl as a function of ionic strength

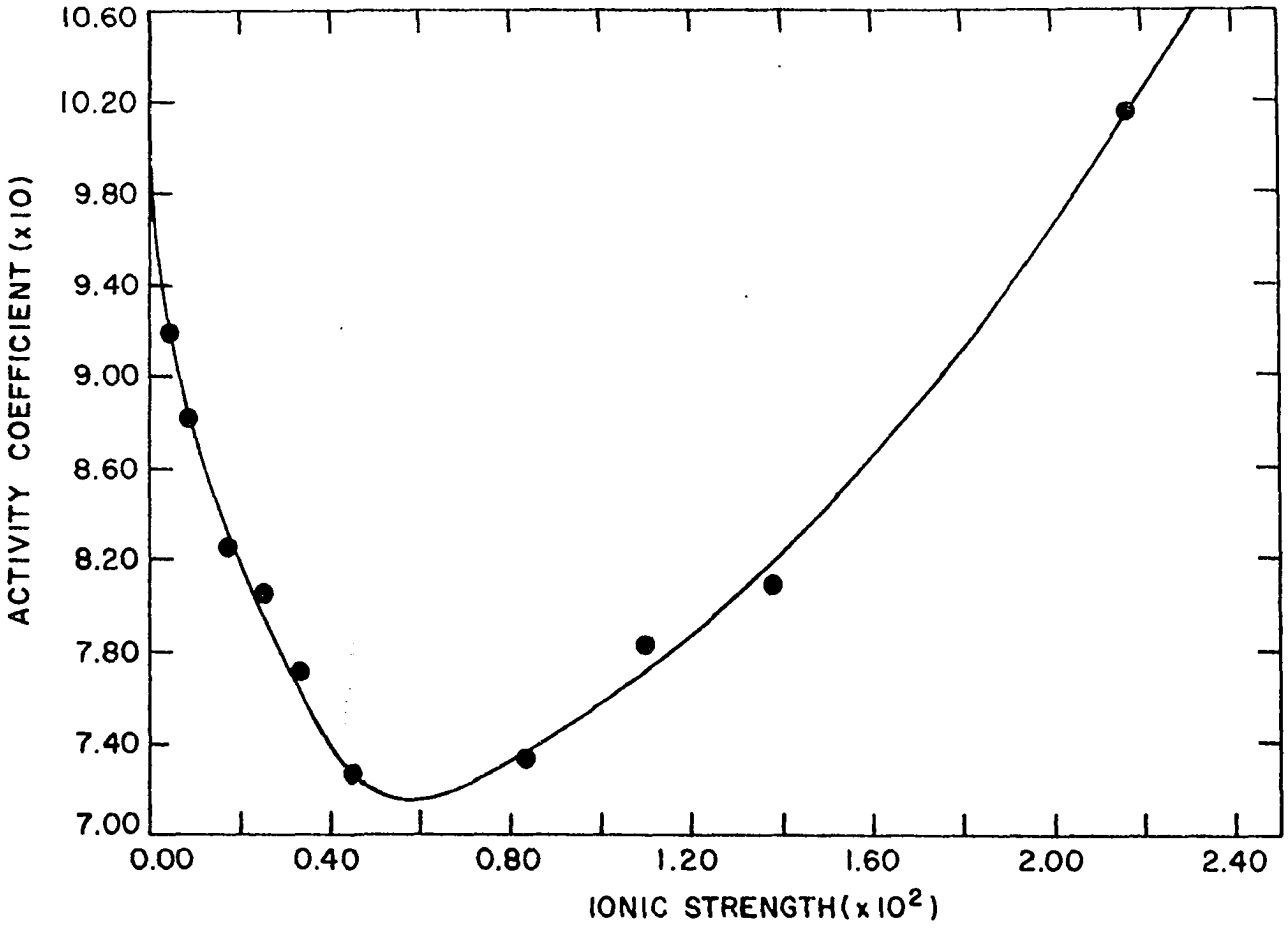
10.60
10.20
9.80
9.40
9.00
8.60
8.20
7.80
7.40
7.00
ACTIVITY COEFFICIENT (x10)
0.00
0.40
0.80
1.20
1.60
2.00
2.40
IONIC STRENGTH(x10^2)

Figure 18. Activity coefficient of $TbCl_3$ as a function of ionic strength

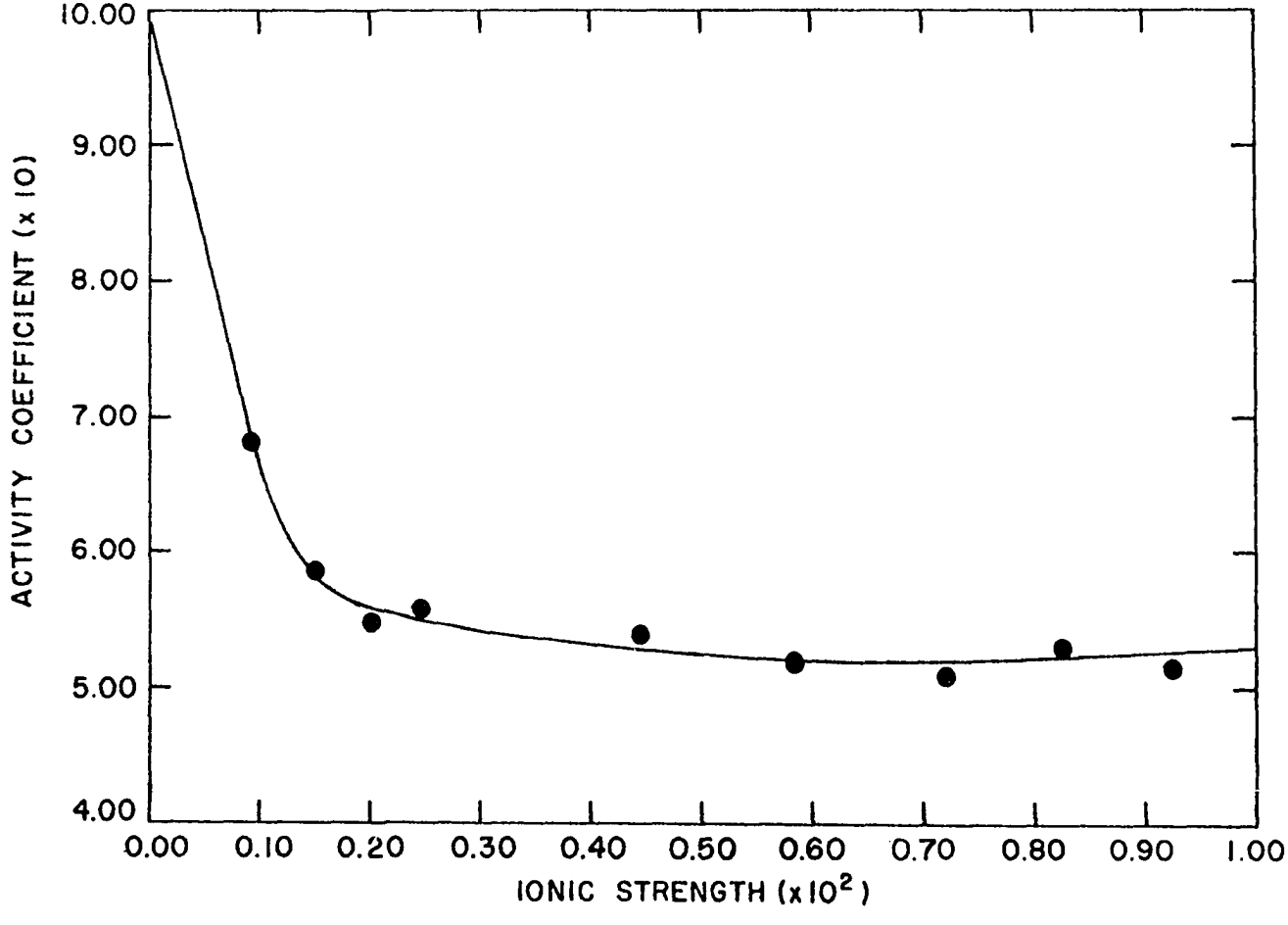
10.00
9.00
8.00
7.00
6.00
5.00
4.00
ACTIVITY COEFFICIENT (x 10)
0.00
0.10
0.20
0.30
0.40
0.50
0.60
0.70
0.80
0.90
1.00
IONIC STRENGTH (x10^2)

Table 7. Activities of HCl, LiCl and $DyCl_3$ at 25°C in aqueous solution

HCl		LiCl		$DyCl_3$	
molarity	$\gamma_\pm$	molality	$\gamma_\pm$	molarity	$\gamma_\pm$
0.0001	0.9891	0.1	0.792	0.000574	0.829
0.0002	0.9842	0.2	0.761	0.000976	0.789
0.0005	0.9752	0.3	0.748	0.00172	0.739
0.001	0.9656	0.5	0.742	0.00230	0.708
0.002	0.9521	1.0	0.781	0.00340	0.668
0.005	0.9285	1.5	0.841	0.00574	0.612
0.01	0.9048			0.00976	0.548
0.02	0.8755			0.0172	0.483
0.05	0.8304			0.0230	0.456
0.1	0.7964				

attraction which tends to reduce the activity coefficient of the electrolyte with an increase in ionic strength. The second factor is the reduction in free solvent molecules with an increase in ionic strength which increases the activity coefficient of the electrolyte according to the Gibbs-Duhem equation (20, p. 406).

$$X_1 \, d\mu_1 = -X_2 \, d\mu_2 \tag{60}$$

$$\mu = \mu_0 + RT \ln a \tag{61}$$

$$d\mu = RT \, d \ln a \tag{62}$$

$$X_1 \, d \ln a_1 = -X_2 \, d \ln a_2 \tag{63}$$

$$X_1 + X_2 = 1 \tag{64}$$

$$dX_1 = -dX_2 \tag{65}$$

$$X_1 \frac{dX_1}{X_1} = -X_2 \frac{dX_2}{X_2} \tag{66}$$

$$X_1 \, d \ln X_1 = -X_2 \, d \ln X_2 \tag{67}$$

$$X_1 \, d \ln \frac{a_1}{x_1} = -X_2 \, d \ln \frac{a_2}{x_2} \tag{68}$$

$$X_1 \, d \ln y_1 = -X_2 \, d \ln y_2 \tag{69}$$

The change in the activity coefficient of the solvent is opposite in sign to the change in the activity coefficient of the electrolyte. Therefore, as the solvent molecules become increasingly tied up due to addition of electrolyte, the first derivative of the activity coefficient changes from positive to negative for the solvent. This constrains the first derivative of the activity coefficient of the electrolyte to become positive. Since the

molarity of methyl alcohol (25 molar) is less than the molarity of water (55 molar), the free solvent molecules are depleted at a lower ionic strength in methanol as compared to water. Therefore, one would expect the first derivative of the activity coefficient for the solvent to become negative at a lower concentration of electrolyte in methanol solution than in water. It is observed that the minima in the activity coefficients occur at lower ionic strength in alcohol than the corresponding minima for aqueous solutions of the same electrolytes. The observed activity coefficients are at least in qualitative agreement with the above argument.

Stefan, Jastrzebska and Jadwiga determined the activity coefficient of LiCl in methyl alcohol as a function of ionic strength (21). The value of the coefficient at all ionic strengths was considerably lower than the corresponding value determined in this work. No minimum was observed in their work.

Each measurement was made with a liquid junction cell and a NaCl reference standard with the chloride ion activity of the LiCl solution being measured with Ag/AgCl electrodes. The junction between the two cell compartments was made with a salt bridge.

In calculating the mean activity coefficient of LiCl in each solution it was assumed that there was no junction potential arising at the salt bridge. Due to

the large difference between transference numbers of lithium ion and sodium ion in chloride solutions of similar concentration, one would expect the junction potential to be substantial according to equation 52. In addition, there was no account made for ion association, which was observed to be substantial in this work.

TRANSFERENCE NUMBER DETERMINATION

Calculations

The presence of the liquid junction in the concentration cell makes it necessary to determine the transference numbers of LiCl, HCl, and $TbCl_3$ over the concentration range in which the respecitve activity coefficients are desired. If a given number of coulombs is passed through a solution of an electrolyte, the transference number of an ion is defined as the fraction of the total number of coulombs passed that is carried by that particular ionic species. There are three methods for obtaining transference numbers. One method involves an E.M.F. measurement on a concentration cell without liquid junction (16, p. 214). A second method involves the observation of a moving boundary which indicates directly the relative mobility of the cation and anion and, therefore, the transference number of each if one knows the ion concentration and the number of coulombs passed per unit distance of travel of the boundary (15, p. 217). the third method is the Hittorf method, which is based on the measurement of the quantity of salt transferred from the anolyte to the catholyte for a known number of coulombs passed through the electrolyte (16, pp. 113-120).

The Hittorf method was used in this work. The quantity of salt transferred from the anode to the cathode compartment was determined from the initial and final concentration of electrolyte in the anode compartment, the total mass of

solution and the density of the solution.

$$C_{final} = \frac{\text{meq titrant}}{\text{ml titrant}} \times \frac{\text{ml titrant}}{\text{gm electrolyte}} \times \frac{\text{gm electrolyte}}{\text{ml electrolyte}} \quad (70)$$

$$\text{meq transferred} = (C_{initial} - C_{final}) \times \frac{\text{gm solution}}{\text{density}} \quad (71)$$

$$T^{+} = \text{meq transferred} \times F/(I \times T) \quad (72)$$

Experimental Procedure

Transference numbers were determined by the Hittorf method. A diagram of the cell is given in figure 19. The solution of which the transference numbers were to be determined was placed in the cell such that the level came above the ports connected to the middle portion of the cell. The solution was then electrolyzed until the concentration of the anolyte had changed by more than 5%. The anode and cathode were both Ag/AgCl electrodes. Thus, chloride ion was depleted from solution at the anode and added to the solution at the cathode. The net gain of electrolyte in equivalents per Faraday of current passed was equal to the transference number of the cation.

The following occurred at the cathode:

$$CH_3OH + e^{-} \rightarrow CH_3O^{-} + \tfrac{1}{2}H_2 \ ,$$

rendering the analysis of the catholyte worthless. This reaction was verified by noting the high pH of the aqueous solution resulting from mixing the catholyte with an equal volume of water.

Figure 19. Diagram of the Hittorf cell used in transference number determinations

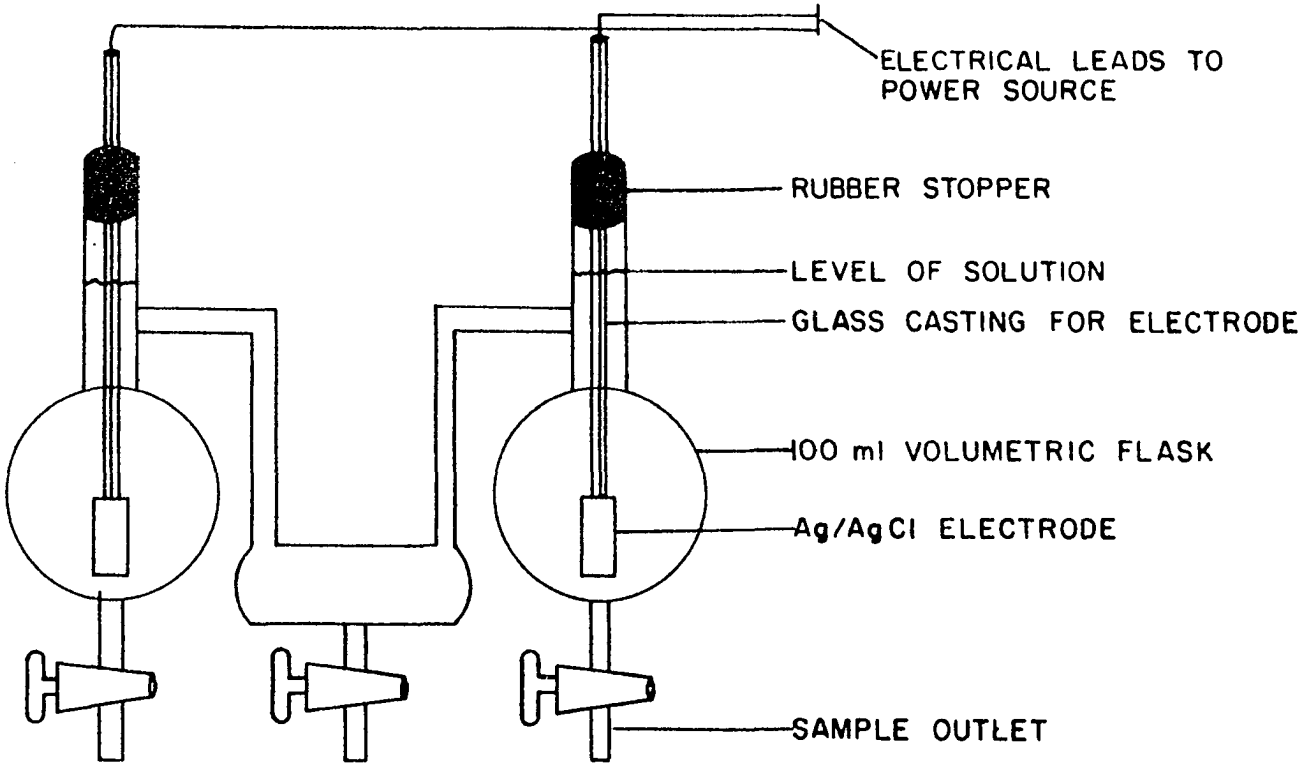
ELECTRICAL LEADS TO POWER SOURCE
RUBBER STOPPER
LEVEL OF SOLUTION
GLASS CASTING FOR ELECTRODE
100 ml VOLUMETRIC FLASK
Ag/AgCl ELECTRODE
SAMPLE OUTLET

The current was recorded by placing a resistor of known resistance in series with the cell. The potential drop across the resistor was determined by opposing a portion of this potential with a variable bucking potential and recording the remainder of the potential with a potentiometer. The potential supplied by the variable bucking potential source was accurately determined with a potentiometer. A circuit diagram is given in figure 20. From the sum of the recorded potential, the bucking potential and the known resistance the current could be determined from Ohm's law. Since the recording potentiometer recorded potential as a function of time, it was possible to integrate this plot of potential versus time and divide by the known resistance and obtain the total number of coulombs of electricity passed during the electrolysis.

The total mass of the anolyte was determined after electrolysis, and it was analyzed before and after electrolysis. The HCl solutions were mixed with an equal volume of water and titrated with standard KOH to a pH of 7.0. The LiCl solutions were titrated with standard $AgNO_3$ using dichlorofluorescein as an indicator. The $AgNO_3$ was standardized against accurately weighed quantities of dry NaCl. The $TbCl_3$ solutions were analyzed gravimetrically by precipitation as the oxalate and igniting to the oxide.

Figure 20. Diagram of circuit used in monitoring current in transference number determinations by the Hittorf method

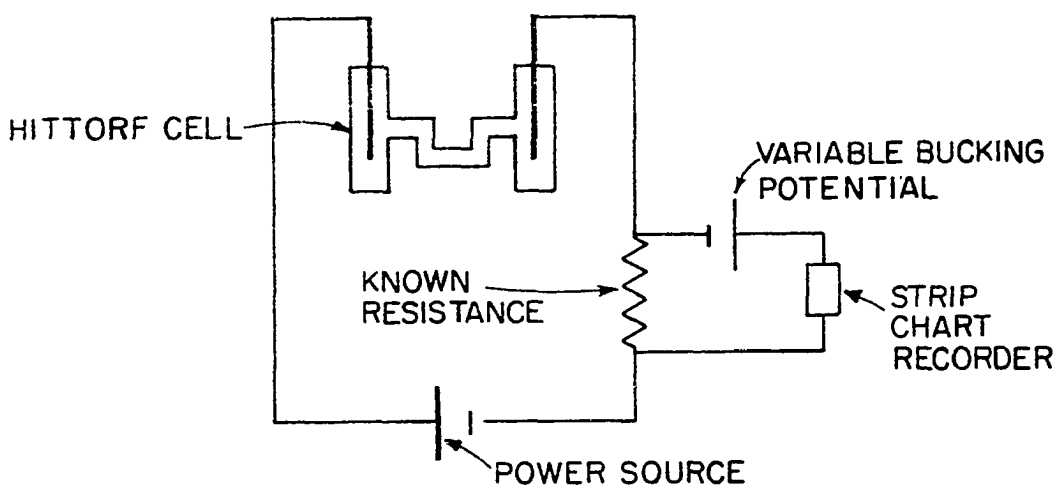
HITTORF CELL
VARIABLE BUCKING POTENTIAL
KNOWN RESISTANCE
STRIP CHART RECORDER
POWER SOURCE

The densities of the various electrolyte solutions used in the transference number determinations were obtained from a plot of density versus concentration for each electrolyte. The plots were prepared by weighing known volumes of each electrolyte at 0.01, 0.05 and 0.1 molar concentrations. Three determinations were made at each concentration and the average of the three values was used for each point in the construction of each plot. A volume of 10.00 ml of the electrolyte was delivered by pipet to a stoppered flask in each case.

Very accurate determinations of transference numbers of many electrolytes in aqueous solution have been made by the moving boundary method (22, 23). An attempt was made to apply this technique to the measurement of transference numbers of HCl, LiCl and $TbCl_3$ in methyl alcohol. The cell and techniques used for measuring transference numbers by the moving boundary technique were patterned after the cell and techniques described by Dye (19, p. 65). The cell consisted of a U-tube with graduated markings. The volume between markings was accurately determined. This U-tube was held in a vertical position and had an electrode compartment at either end.

The solution of the electrolyte of which the transference number was sought was placed in the U-tube and cathode compartment. A solution of an electrolyte

of similar concentration containing the same anion and a cation of lower mobility than the cation under investigation was used as an indicator to mark the movement of the cation of the electrolyte under investigation. The indication electrolyte was placed in the anode compartment. The electrolytes were separated by a one hole hollow bore stopcock. A sharp boundary between the electrolytes was initially formed by the shearing action of the stopcock as it was opened. The velocity of the boundary was directly related to the transference number of the cation. Cadmium metal served as the anode and an Ag/AgCl electrode served as the cathode.

Due to high resistance of the alcohol solution and the fact that an especially large portion of the total potential drop occurs immediately behind the boundary, the solution was found to have local heating in the region of the boundary. Even though the entire apparatus was submerged in a water bath, a large enough temperature gradient was present to disrupt the boundary.

The current had to be maintained at a level high enough to keep the boundary sharp. Since very dilute solutions require a lower current density to maintain a sharp boundary, the main work was done on dilute solutions. However, in dilute solutions the boundary detection becomes a problem. The common method of detection in aqueous solution is by refractive index difference. The refractive indexes of dilute solutions all approach

the refractive index of the solvent, and thus, become very similar, rendering this method of detection useless. Colored indicators which reacted with one of the cationic species were used to follow the boundary.

The boundary formed by the colored indicator was diffuse. The reaction between the indicator and cation at the boundary was believed to be causing local heating. Another explanation for the diffuse boundary and heating effect lies in the fact that the indicating electrolyte was a weak electrolyte in each case. Only the dissociated ions move under the influence of the electrical potential, and after a few ions have moved to a region previously unoccupied by that electrolyte a certain percentage of them reassociate with the anion. Thus, the total effect is to dilute the indicator electrolyte behind the boundary and, thereby, increase the potential drop in that region. This causes an increased heating problem as the boundary continues to move. The moving boundary method was discarded due to the above mentioned convection current problem.

Results

The transference numbers of HCl, LiCl and $TbCl_3$ obtained in this work are given as a function of molar concentration in figures 21, 22, and 23 respectively. The plot of transference number as a function of

Figure 21. Transference number versus molar concentration for HCl in methanol

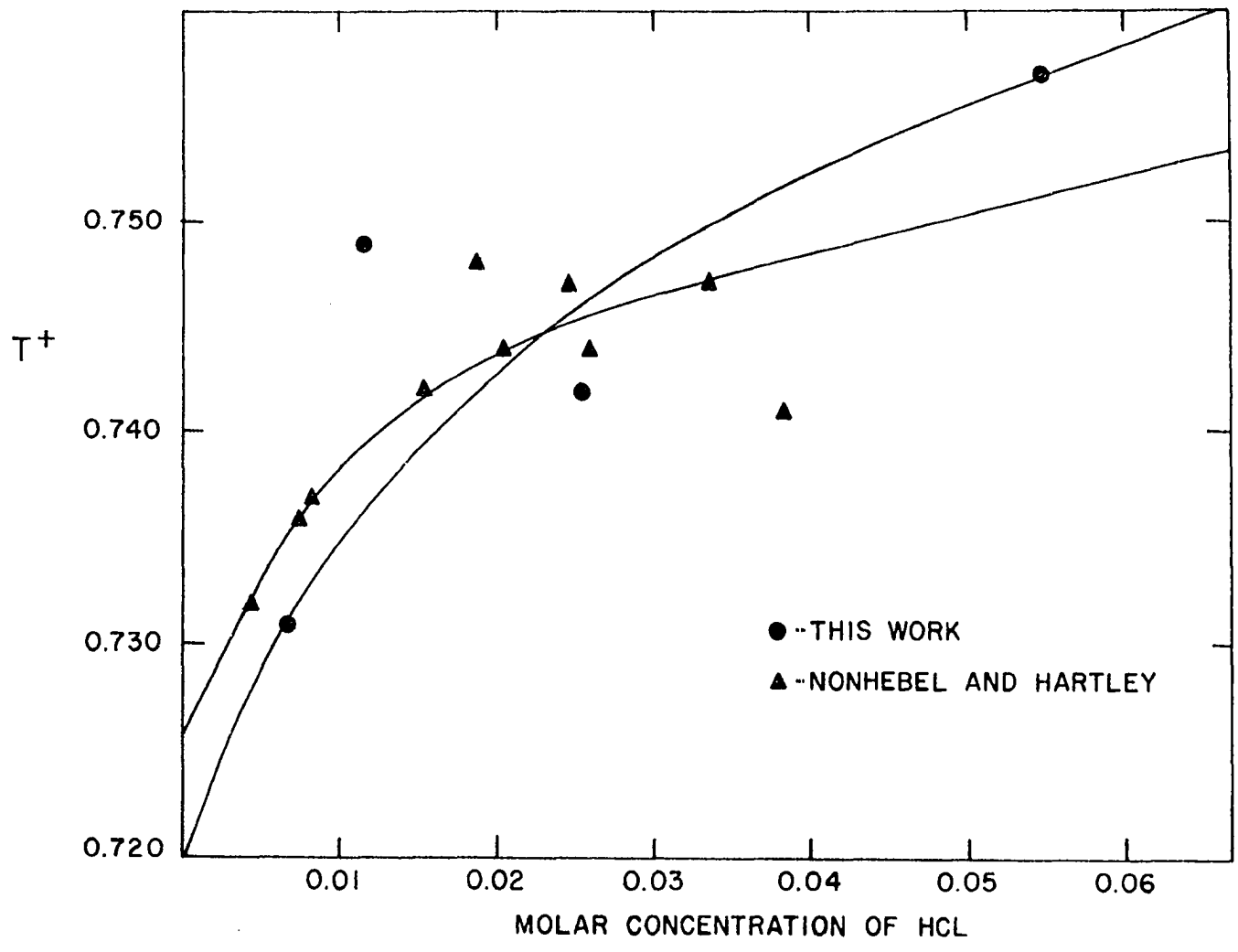
0.750
0.740
0.730
0.720
T+
0.01
0.02
0.03
0.04
0.05
0.06
MOLAR CONCENTRATION OF HCL
●-THIS WORK
▲-NONHEBEL AND HARTLEY

Figure 22. Transference number versus molar concentration for LiCl in methanol

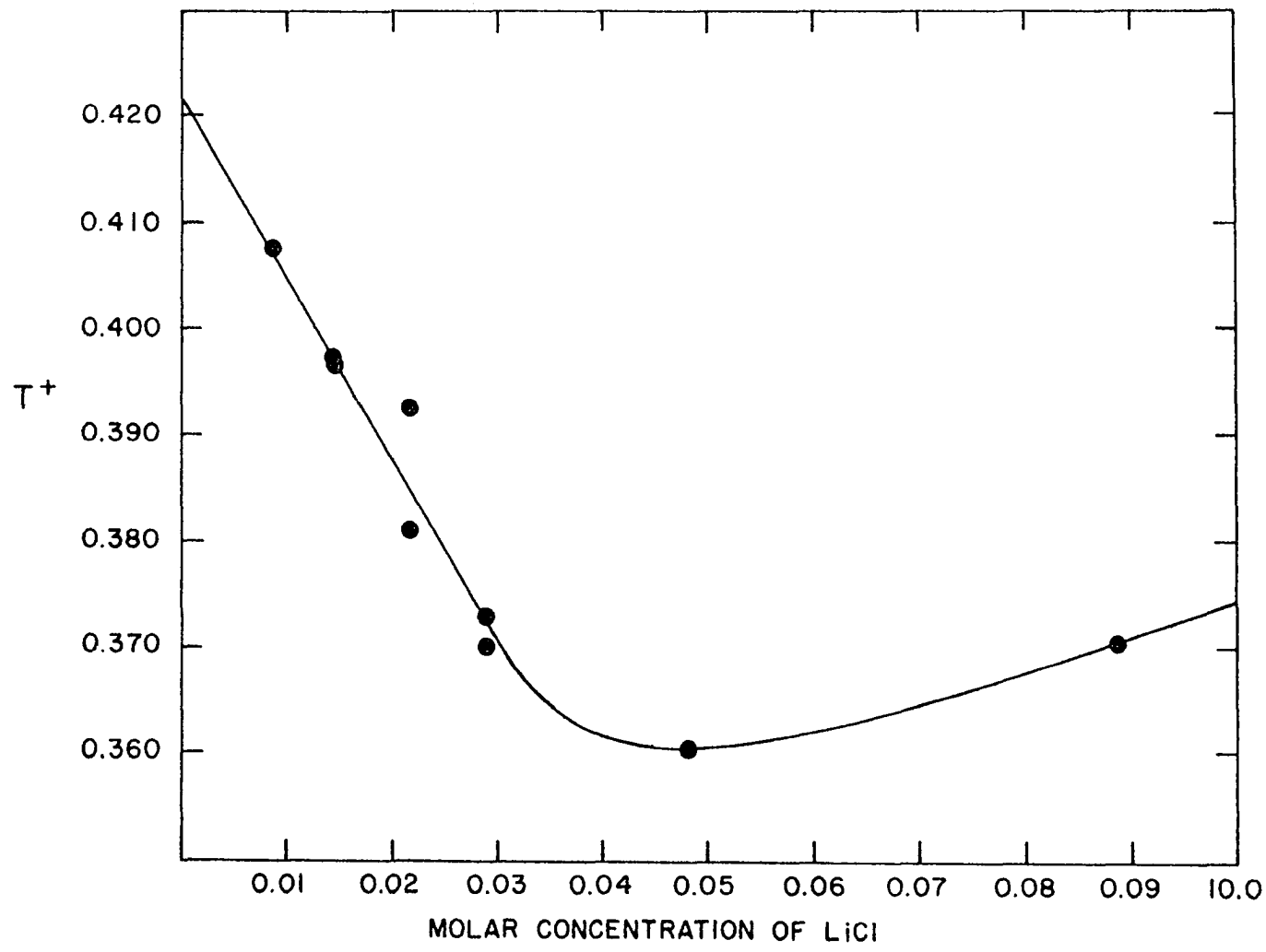
0.420
0.410
0.400
0.390
0.380
0.370
0.360
T+
0.01
0.02
0.03
0.04
0.05
0.06
0.07
0.08
0.09
10.0
MOLAR CONCENTRATION OF LiCl

Figure 23. Transference number versus molar concentration for $TbCl_3$ in methanol

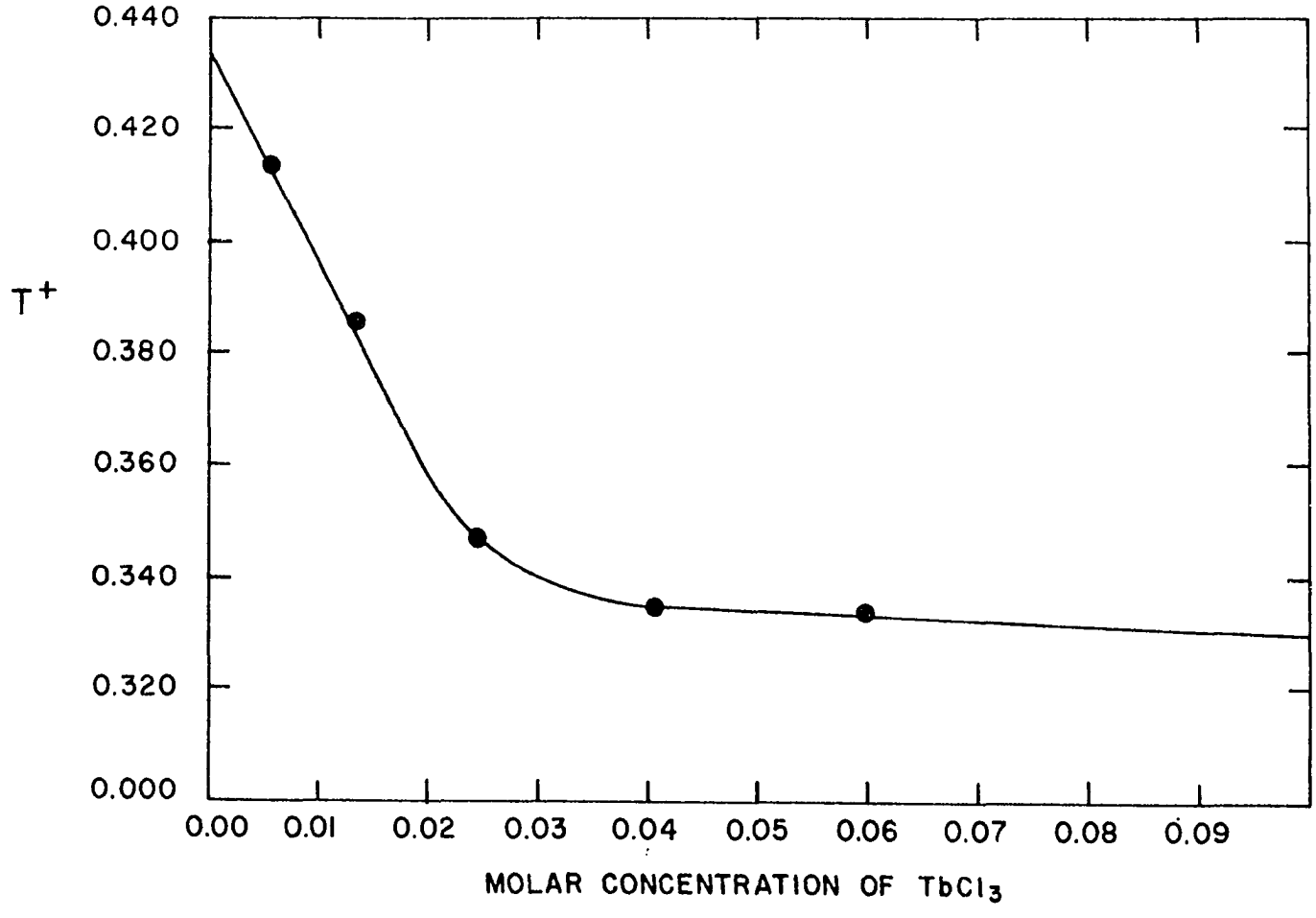
0.440
0.420
0.400
0.380
0.360
0.340
0.320
0.000
T+
0.00
0.01
0.02
0.03
0.04
0.05
0.06
0.07
0.08
0.09
MOLAR CONCENTRATION OF TbCl3

Figure 24. Transference number versus molar concentration for HCl in aqueous solution

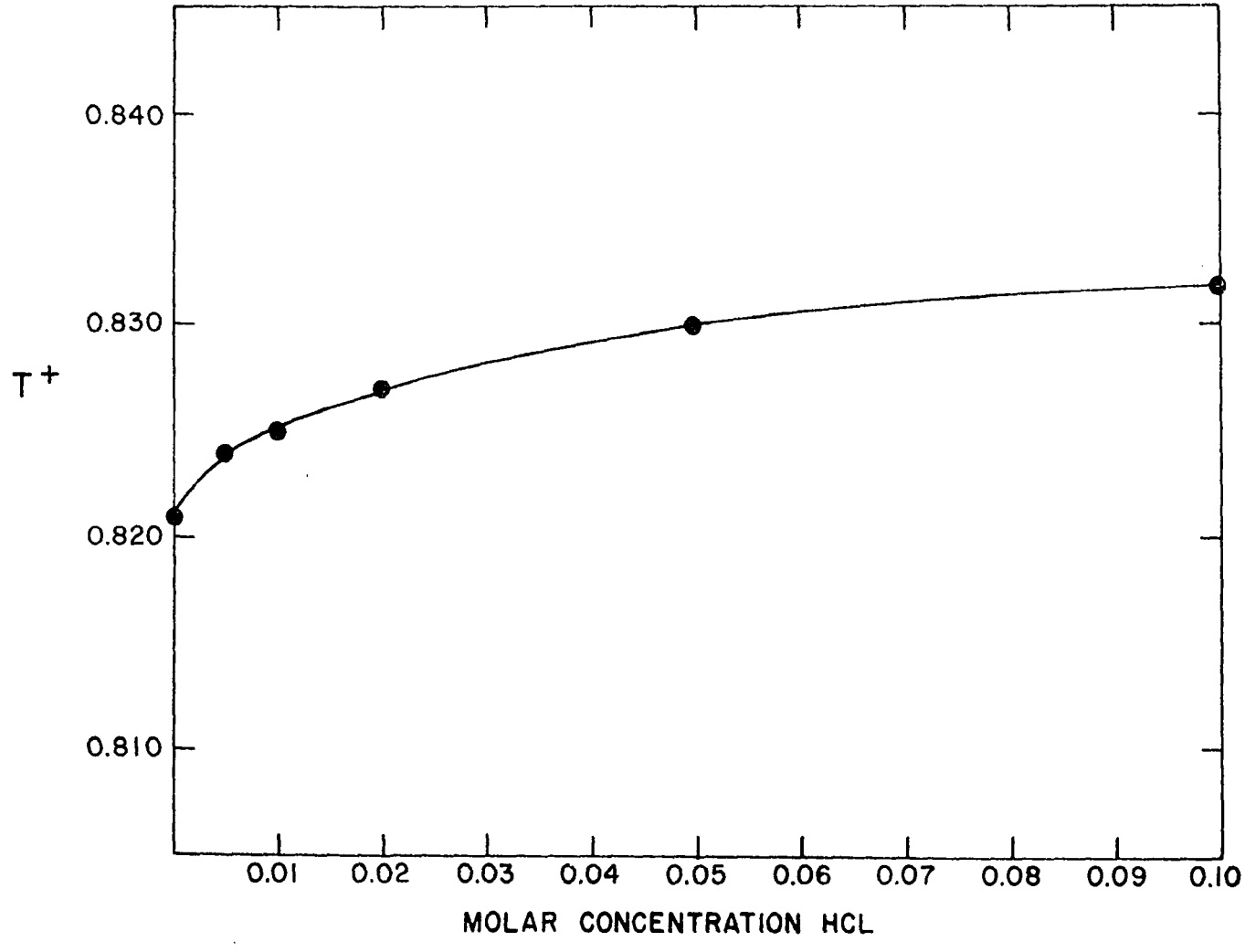
0.840
0.830
0.820
0.810
T+
0.01
0.02
0.03
0.04
0.05
0.06
0.07
0.08
0.09
0.10
MOLAR CONCENTRATION HCL

Figure 25. Transference number versus molar concentration for LiCl in aqueous solution

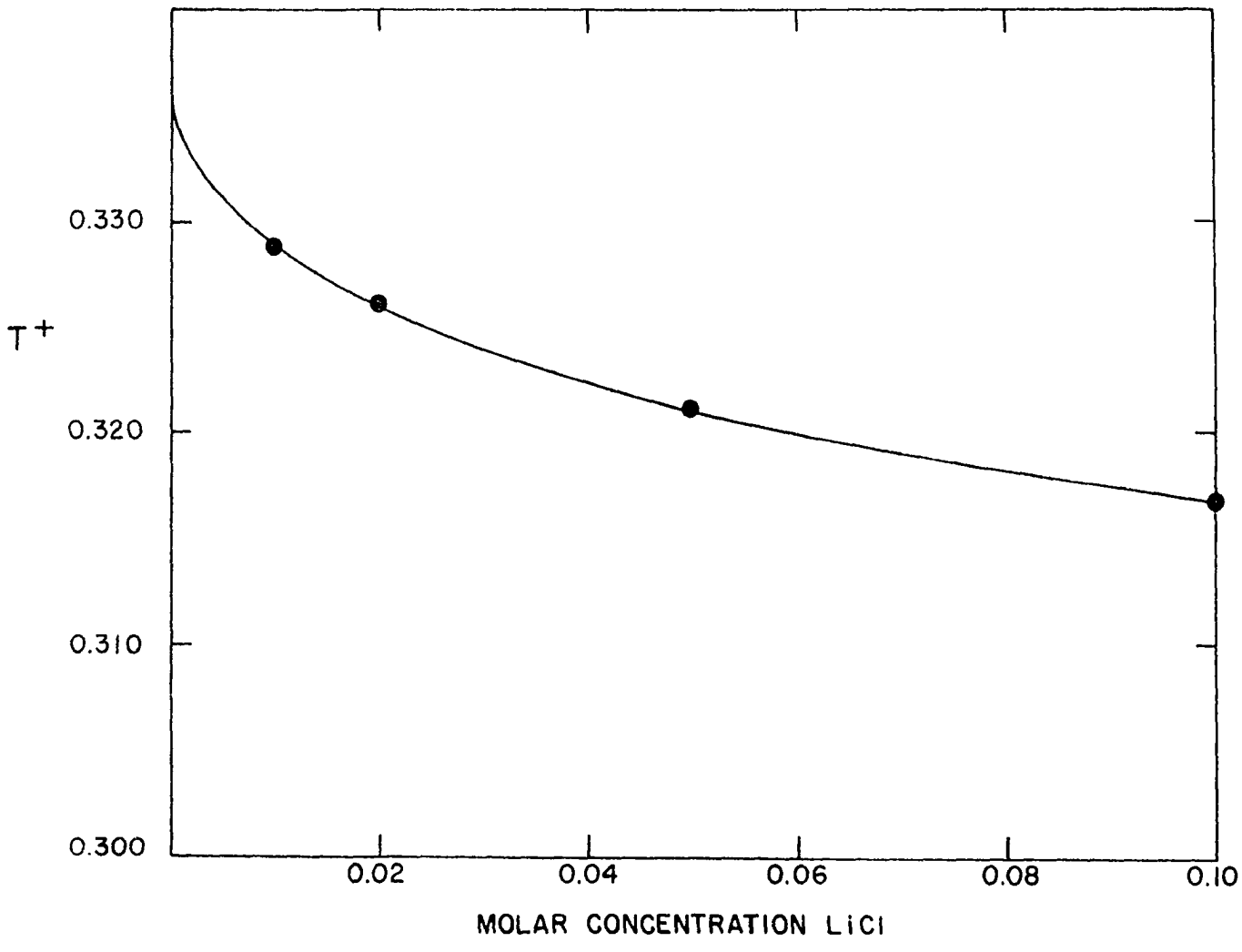
0.330
0.320
0.310
0.300
T+
0.02
0.04
0.06
0.08
0.10
MOLAR CONCENTRATION LiCl

Figure 26. Transference number versus molar concentration for $DyCl_3$ in aqueous solution

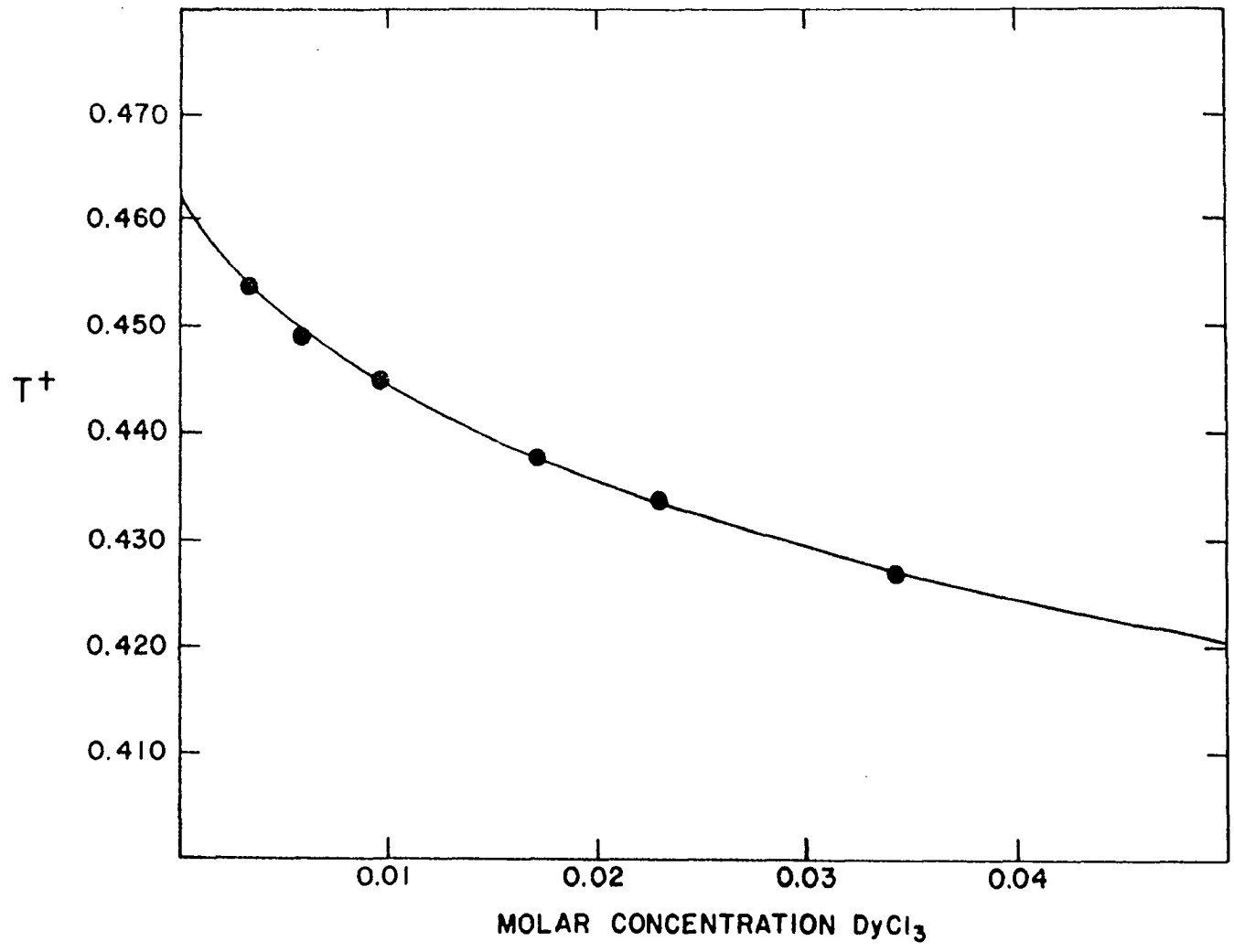
0.470
0.460
0.450
0.440
0.430
0.420
0.410
T+
0.01
0.02
0.03
0.04
MOLAR CONCENTRATION DyCl3

concentration for HCl given by Nonhebel and Hartley (24) is also provided in figure 21. Plots of transference number versus concentration for aqueous solutions of HCl (15, p. 699), LiCl (15, p. 699) and $DyCl_3$ (19, p. 84) are given for comparison in figures 24, 25 and 26 respectively.

Discussion of Results

The transference numbers of HCl, LiCl,and $TbCl_3$ in methanol are qualitatively similar to the corresponding transference numbers in aqueous solution. The cation transference number of HCl decreases as infinite dilution is approached as it does in aqueous solution. A few data points were taken for HCl in order to check agreement with the determinations made by Nonhebel and Hartley(24), and test the accuracy of the method by comparing with an alternate method.

No transference data for LiCl in methanol could be found in the literature. The data collected appears to be much more self consistent than the HCl data. The LiCl values in methyl alcohol compare well with LiCl transference numbers in water, both solvents showing an increase in cation transference numbers at infinite dil-tion and a constant transference number above 0.05 molar LiCl.

Terbium chloride cationic transference number versus concentration was compared to the dysprosium

chloride cationic transference number versus concentration in aqueous solution. The cation transference number of $TbCl_3$ in methanol is found to rapidly approach the corresponding value for $DyCl_3$ in aqueous solution at infinite dilution. The low transference number at higher concentrations can be explained by the greater tendency of $TbCl_3$ to exist as $TbCl^{+2}$ and $TbCl_2^{+}$ at higher concentrations as opposed to Tb^{+3} in aqueous solution.

PART III. CHELATE SPECIES IN METHYL ALCOHOL

The first step formation constants of terbium-α-hydroxyisobutyrate and 1,1-cyclobutanedicarboxylate chelate species were respectively three and five orders of magnitude greater than $1/K_3$ (the first formation constant) for $TbCl_3$ ion pair formation. Since the chloride ion concentration did not greatly exceed the total acid ligand concentration, it was assumed that the ion pair formation of the terbium ion could be disregarded in the calculations of the step formation constants of both terbium chelate species.

If it would be necessary to treat chloride ion as a competing ligand, the formation constants of the terbium acid anion chelate species could be determined as long as the step formation constants of $TbCl_3$ are known.

The effect of the ion pair on the formation of the metal chelate species is difficult to assess. The chelating ligand does not have to disrupt the ion pair in order to chelate to the metal ion since the ion pair is an outer sphere complex. Therefore, it would appear that the anion forming the ion pair has no real effect on the free metal ion concentration. However, the ion pair formation does reduce the charge on the metal and, thereby, reduces its attraction for the chelating ligand.

CALCULATIONS

Formation Constants

The formation constants were calculated by Fronaeus's method (10, p. 108). This required the measurement of hydrogen ion concentration and the predetermined dissociation constants of the corresponding acid. The large shift in hydrogen ion concentration upon addition of metal to the ligand buffer indicated that the step formation constants of the chelate species were large enough to justify the assumption that all of the anion neutralized by the addition of base to the organic acid was tied up by the metal. However, the inverse of the dissociation constants of the organic acids were greater than the step formation constants by at least two orders of magnitude. It was assumed, therefore, that $\bar{n}$ is given by equation 73 for a monobasic acid,

$$\bar{n} = \frac{[OH_T]}{B} , \tag{73}$$

($[OH_T]$ = total base added to the system; other terms used in this section have been identified on page 5)

and by equation 74 for a dibasic acid.

$$\bar{n} = \frac{[OH_T] - A}{B} \tag{74}$$

The value of a is given by equation 76 for a monobasic acid.

$$H = h + HA \tag{75}$$

$$a = \frac{K_{a1}(H - h)}{h} \tag{76}$$

In the case of a dibasic acid,

$$H = h + HA + H_2A \tag{77}$$

and the value of $\underline{a}$ is given by equation 78.

$$a = \frac{H - h}{\frac{h}{K_{a1}} + \frac{h^2}{K_{a1} \cdot K_{a2}}} \tag{78}$$

Fronaeus's method of determining formation constants involves plotting the function $F_n(a)$ versus the free ligand concentration for each formation constant.

$$F_n(a) = \beta_n a^{n-1} + \beta_{n+} a_n^n + \beta_{n+} a^{n+1} + \cdots \tag{79}$$

$$F_1(a) = \beta_1 + \beta_1 a + \beta_2 a^2 + \cdots \tag{80}$$

At low values of $\underline{a}$ the only species of significance are BA and BA_2. Thus, at low ligand concentrations the plot of $F_1(a)$ versus $\underline{a}$ approaches a straight line where β_1 is the intercept and β_2 is the slope. The value of $F_1(a)$ can be determined from α_c and $\bar{n}$ given in equations 81 and 82 respectively. A sketchy outline of this derivation is given by Rossotti and Rossotti (10, p. 41, 104). The complete derivation is given in appendix A. The expression derived for $F_1(a)$ is given in equation 83.

$$\alpha_c = \frac{[BA_c]}{B} = \frac{c a^c}{\sum_0^N \beta_n a^n} \tag{81}$$

$$\bar{n} = \frac{A - a}{B} = \frac{\sum_1^n n\beta_n a^n}{\sum_0^n \beta_n a^n} \tag{82}$$

$$F_1(a) = \frac{\exp \int_0^a \frac{\bar{n}}{a}\, da - 1}{a} \tag{83}$$

Higher β_n values can be determined by calculationg a new function, $F_n(a)$, and proceeding as in the β_1 calculation from $F_1(a)$. The function $F_n(a)$ is given by equation 84.

$$F_n(a) = \frac{F_{n-1}(a) - \beta_n}{a} \tag{84}$$

The value of

$$\exp \int_0^a \frac{\bar{n}}{a}\, da$$

was determined by graphical integration of the plot of $\bar{n}/a$ versus a.

Acid Dissociation Constants

The acid dissociation constants were determined for CBDA and α-HIBA in methyl alcohol from a potentiometric measurement of free hydrogen ion. The material balance equations for total anion concentration for α-HIBA and CBDA are given respectively in equations 85 and 86.

$$A = a + HA + LiA \tag{85}$$

$$A = a + HA + H_2A + LiA + Li_2A \tag{86}$$

The value of a is equal to the amount of acid neutralized. Equations 85 and 86 then yield equations 87 and 88 respectively.

$$A = a[1 + h/K_{a1} + Li/K_{Li1}] \tag{87}$$

$$A = a[1 + h/K_{a2} + h^2/K_{a1}K_{a2} + Li \cdot y^2/K_{Li2} + Li \cdot y^3/K_{Li1} \cdot K_{Li2}], \tag{88}$$

where Li_nA = lithium acid anion ion pair concentration,

Li = free lithium ion concentration,

y = mean activity coefficient for LiCl (used to replace mean activity coefficient of Li_nA which had not been determined), and

K_{Lin} = dissociation constant for Li_nA species.

The material balance equations for total hydrogen are given in equations 89 and 90 for the monobasic acid respectively.

$$H = h + HA \tag{89}$$

$$H = h + HA + 2H_2A \tag{90}$$

the free hydrogen ion is negligible compared to the undissociated acid species. Equations 89 and 90 can then be expressed in terms of the total hydroxide added.

$$A - [OH_T] = h \cdot a/K_{a_2} \tag{91}$$

$$2A - [OH_T] = a(h/K_{a2} + 2h^2/K_{a1} \cdot K_{a2}) \tag{92}$$

If equation 88 is divided by equation 92, one obtains the straight line equation 93 for the dibasic acid.

$$h\left[\frac{A}{2A - [OH_T]}\right]-1 = \frac{-h^2}{K_{a1}}\left[\frac{2A}{2A - [OH_T]}\right]-1 + K_{a2}(1 + c) \quad (93)$$

$$c = Li\cdot y^2/K_{Li2} + Li^2\cdot y^3/K_{Li1}\cdot K_{Li2} \quad (94)$$

Slope = $1/K_{a1}$ and intercept = $K_{a2}(1 + c)$.

If equation 87 is divided by equation 91, one obtains expression 95 for K_a of the monobasic acid in terms of free hydrogen ion concentration, total anion and total hydroxide added to the system.

$$K_{a1} = \left[\frac{[OH_T]}{A - [OH_T]}\right]\left[\frac{h}{1 + Li(y^2)/K_{Li1}}\right] \quad (95)$$

The dissociation constants were not determined for the LiA and Li_2A ion pairs formed with the organic acid anions. Since the attraction between Li^+ and A^- is only dependent on the concentration of charge on each species, it is assumed that the dissociation constant would be very close to the ion pair dissociation constant for LiCl. Very little difference was observed for the dissociation constants of LiCl, HCl, and K_1 for $TbCl_3$ as given in table 8. The value of K_2 for the dibasic acid was taken to be equal to K_2 for $TbCl_3$.

Table 8. First dissociation constants of some ion pairs

Ion Pairs	Dissociation Constant (K_1)
LiCl	3.08×10^{-2}
HCl	3.55×10^{-2}
$TbCl_3$	2.90×10^{-2}

EXPERIMENTAL PROCEDURE

Technique

Formation constants

The metal chelate step formation constants were determined from potentiometric measurements of free hydrogen ion concentration in a series of ten samples. In each sample there was a constant metal ion concentration of 0.0025 molar and a ligand buffer varying in concentration from 0.0005 to 0.005 molar. The measurements were made at 25.0 degrees centigrade and at a constant ionic strength of 0.02 molar. Lithium chloride was used as supporting electrolyte. In this constant ionic medium the activity coefficients of all ions were assumed to be invariant.

Acid dissociation constants

The dissociation constants of the organic acids were determined at 25.0 degrees centigrade from potentiometric measurements of free hydrogen ion concentration in a series of ten samples of partially neutralized solutions of the organic acids. The samples contained a constant amount of acid (0.01 molar) with the degree of neutralization varying from 25 to 75%. The acid was neutralized with standard $LiOCH_3$. All samples were held at an ionic strength of 0.02 molar by addition of LiCl as supporting electrolyte.

Measurement of hydrogen ion concentration

The glass electrode was employed in the measurement of hydrogen ion concentration in the methyl alcohol solutions mentioned above. The saturated calomel electrode was immersed in a saturated aqueous solution of LiCl. The two electrode compartments were connected by a salt bridge containing LiCl suspended in an agar gel.

A calibration curve of $\log[H^+]$ versus millivolt reading was prepared over a concentration range from 10^{-3} to 10^{-5} molar. A portion of this calibration curve is given in figure 27. The glass electrode yielded a nearly linear response to $\log[H^+]$ over this concentration range. The molar concentration of hydrogen ion in each sample was determined from the known millivolt reading and the calibration curve.

Marple and Fritz (25) obtained good reproducibility (2 millivolt deviation) of titration curves of organic acids with tetrabutylammonium hydroxide in methanol by employing a glass electrode. A saturated calomel electrode was used as a reference electrode. Initially, they modified the calomel electrode by replacing the aqueous KCl with a saturated methanol solution of KCl. Good titration curves were obtained but successive titrations differed by as much as 50 millivolts at the same point in the titration.

Figure 27. Calibration curve of log[H^+] versus potential difference between glass electrodes and calomel electrodes in methanol

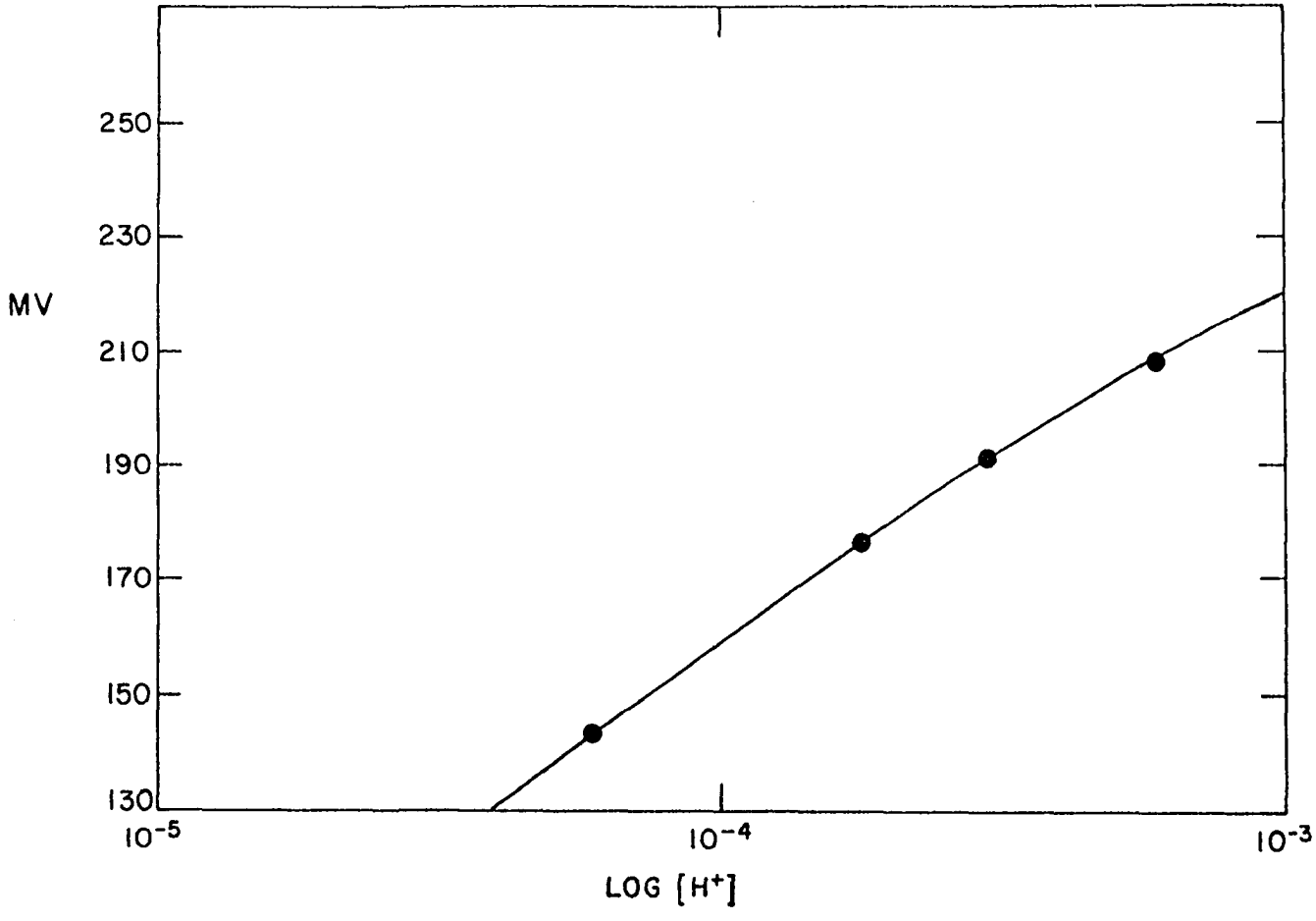
250
230
MV
210
190
170
150
130
10^{-5}
10^{-4}
10^{-3}
LOG [H^+]

This was believed to be due to the differences in the junction potential of the modified calomel electrode and the solution. A salt bridge of the following type:

SCE/aqueous phase/ methanol phase/MeOH/glass electrode,
MCl-H_2O-MeOH MCl-H_2O-MeOH

was prepared to eliminate this variation in junction potential. The usual saturated calomel electrode was used in this case. The reproducibility of titration curves was very good with this electrode system. The separate portions of the electrode system were separated by sintered glass frits.

Gelsema, deLigny and Blijleven (26) checked the response of the glass electrode versus a saturated calomel electrode in several methanol-water mixtures and concluded that the best accuracy was obtained when buffer standards were prepared in the same solvent in which the measurements were carried out.

Ionic strength adjustment

The calculations involved in determining the amount of LiCl required to adjust the ionic strength of each sample to 0.02 molar are given in appendix B for the determinations of the dissociation constants and terbium chelate formation constants of α-HIBA and CBDA.

Ionization of methyl alcohol

The ionization constant of methyl alcohol $CH_3OH \rightleftarrows CH_3O^- + H^+$ was required in order that the effects of its component species could be taken into consideration in the material balance equations for both K_a and formation constant determinations. Briere, Felici and Piot (27) measured the free energy of the self ionization of methanol as a function of dielectric constant. The function was given as:

$$\Delta G = A + B/\varepsilon \tag{96}$$

with A = 17,270 and B = 284,000. At 25 degrees centigrade in pure methanol the dielectric constant is 31.5. This makes ΔG = 26,300. One may then solve for the free H^+ concentration as follows:

$$\Delta G = 2.303\ RT\ \log[H^+][CH_3O^-] \tag{97}$$

$$[H^+] = [OCH_3^-] \tag{98}$$

$$-\log[H^+]^2 = \frac{26,300}{(2.303)(1.987)(298)} \tag{99}$$

$$-\log[H^+]^2 = 19.3 \tag{100}$$

$$\log[H^+] = -9.64 \tag{101}$$

$$[H^+] = 10^{-9.64} \tag{102}$$

$$[H^+] = 2.29 \times 10^{-10} \tag{103}$$

The ionization constant for methyl alcohol is then given by expression 104.

$$K_{ionization} = (2.29 \times 10^{-10})^2 = 5.25 \times 10^{-20} \tag{104}$$

One can conclude that, if the hydrogen ion concentration

is between 10^{-5} and 10^{-15} molar, neither OCH_3^- nor H^+ need to be considered in material balance equations.

Preparation of Reagents

Methyl alcohol preparation

It was found that the methyl alcohol obtained from Mallinckrodt contained approximately 0.1% water. This water was removed by reacting the alcohol with sodium metal and then distilling it using a spray trap above the boiling pot, and a 24-inch fractionating column above the trap. The first 1% of the distillate and the last 10% of the alcohol in the boiling pot was discarded. The distilled alcohol was stored in a glass vessel which had an air inlet protected by a $CaCl_2$ drying agent. The specific conductance of the distilled alcohol was less than 5×10^{-7} cm^2/ohm.

$TbCl_3$ preparation

Terbium chloride was prepared from Tb_4O_7 obtained from DR. J.E. Powell, A.E.C., I.S.U. by reaction with HCl in aqueous solution. The chloride prepared in this manner was recrystallized twice from water. After air drying the terbium ion was still quite heavily hydrated. All but two of these waters of hydration were easily removed upon heating to 120 degrees centigrade. The last two waters were very tightly bound and hydrolysis occurred when the compound was heated in air above 150 degrees C.

$TbCl_3\ 2H_2O \rightleftharpoons TbOCl + 2HCl + H_2O$

The anhydrous $TbCl_3$ was prepared by heating the hydrate in an HCl atmosphere in an electric tube furnace. The HCl was supplied from a cylinder and passed through a tube of $CaCl_2$ to remove water and acetylene. The partial pressure of HCl was maintained above atmospheric pressure by passing the HCl gas leaving the furnace through a column of concentrated sulfuric acid. This acid solution also attracted and removed water vapor from the atmosphere over the $TbCl_3$. A small amount of TbOCl was still formed but it was insoluble in methyl alcohol and could thus be separated from the solution. The hydrated $TbCl_3$ appeared to be much more soluble in methyl alcohol than the anhydrous form. This might suggest that there is a substantial difference in the activity coefficients of the two species.

HCl stock prepartion

Methanol solutions of HCl were prepared by passing dry HCl from a cylinder through glass wool and methyl alcohol in separate gas trap bottles and, subsequently, into purified methyl alcohol. Solutions approximately 0.5 molar in HCl were prepared and standardized by titrating aliquots with standard KOH. The concentration of HCl was observed to change slightly from day to day, continually becoming more dilute. This was due to a

reaction with the methyl alcohol. In order to inhibit this reaction, the stock solutions of HCl were stored in a refrigerator at 5 degrees centigrade. Solutions of HCl were frequently restandardized.

Lithium chloride stock preparation

Lithium chloride solutions were prepared by dissolving dry reagent grade LiCl obtained from J.T. Baker Co. in purified methyl alcohol. Solutions of LiCl used in this work were analyzed by titration with $AgNO_3$. The end point was determined with dichlorofluorescein indicator. A small amount of diextrin was used to hold AgCl particles in a colloidal suspension which was necessary to the functioning of the absorption indicator.

Lithium methoxide preparation

The lithium methoxide was prepared by reacting lithium metal of 99.9% purity with methyl alcohol. The lithium metal was obtained from Bernard Beaudry at A.E.C., I.S.U. The metal was handled in a dry box. An 0.15 molar stock solution was prepared and standardized against standard HCl.

EXPERIMENTAL RESULTS

The acid dissociation constant of α-HIBA varied with degree of neutralization. It is given as a function of the degree of neutralization (A_T - OH_T) in figure 28. Figure 29 is a plot of equation 93 for the dissociation constant determination of CBDA. The change in dissociation constant for α-HIBA and the deviation from linearity in the plot of equation for CBDA is believed to be due to a small amount of ammonia present in the methyl alcohol used to prepare the solutions.

It is suspected that the sodium metal used in the methyl alcohol purification contained a small amount of sodium nitride from reaction with nitrogen on being exposed to the air. Ammonia would be produced by the reaction of sodium nitride and methyl alcohol according to the following reaction:

$$Na_3N + 3\ CH_3OH \rightleftharpoons NH_3 + 3\ Na^+ + 3\ OCH_3^-$$

If ammonia were indeed formed, it would have been distilled along with the alcohol.

Due to the increase in concentration of OCH_3^- with an increase in degree of neutralization, the acid dissociation constants were determined from the data taken at high degrees of neutralization. The effect of any dissolved ammonia would be expected to be minimal at a high degree of neutralization. One observes that the

Figure 28. Dissociation constant of α-hydroxyisobutyric acid as a function of the degree of neutralization

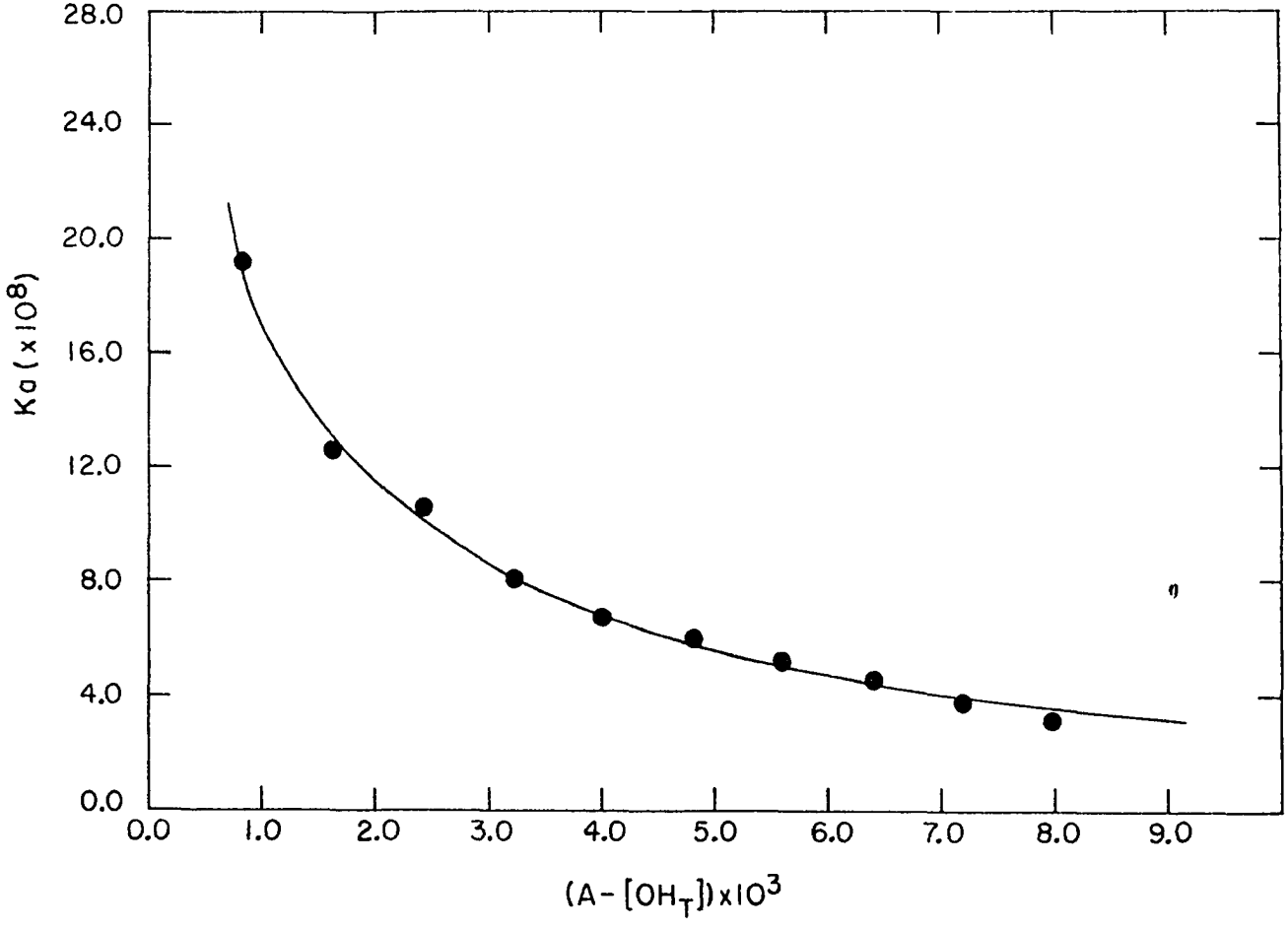
28.0
24.0
20.0
16.0
12.0
8.0
4.0
0.0
Ka (x10^8)
0.0
1.0
2.0
3.0
4.0
5.0
6.0
7.0
8.0
9.0
(A-[OH_T])x10^3

Figure 29. Plot of the variables X and Y for the determination of K_{a1} and K_{a2}; X and Y are functions of the degree of neutralization

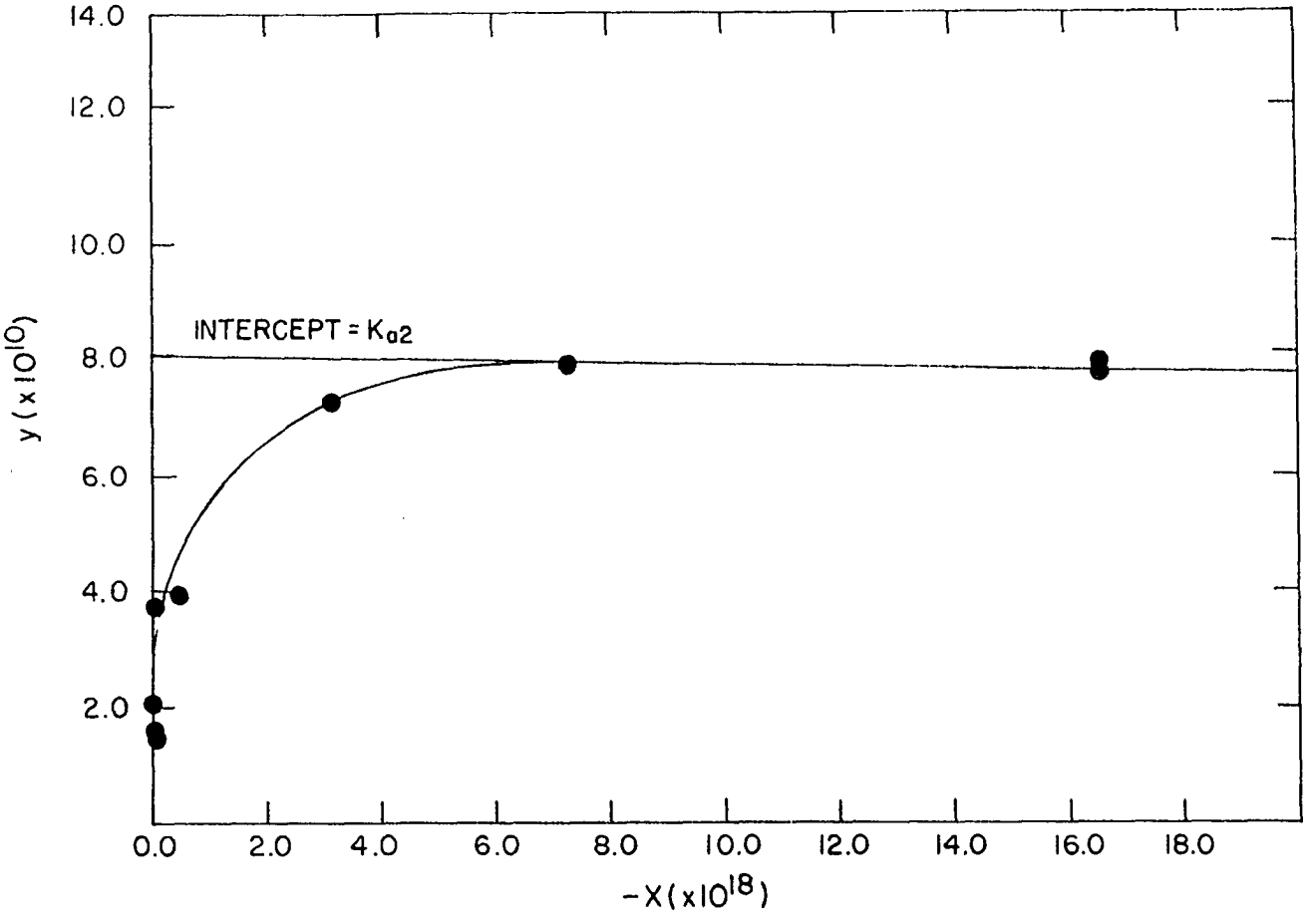
14.0
12.0
10.0
8.0
6.0
4.0
2.0
y (x 10^10)
INTERCEPT = Ka2
0.0
2.0
4.0
6.0
8.0
10.0
12.0
14.0
16.0
18.0
-X(x10^18)

acid dissociation constant for α-HIBA does, indeed, become nearly constant as the degree of neutralization increases. This would appear to justify the determination of the dissociation constants from the data taken at a high degree of neutralization. The dissociation constants used in this work are:

K_{a2} of CBDA = 4.57×10^{-11} , and

K_a of α-HIBA = 3.00×10^{-8} .

The graphical integrations of $\bar{n}/a$ versus $\underline{a}$ for α-HIBA and CBDA are given in figures 30 and 31 respectively. The plot of $F_1(a)$ versus $\underline{a}$ for α-HIBA CBDA are given in figures 32 and 33 respectively. The values of β_1 and β_2 are given respectively by the intercept and slope at low values of $\underline{a}$. The values of β_1, β_2, K_2 and K_1/K_2 are given in table 9.

Table 9. Formation constants of terbium chelate species of α-hydroxyisobutyrate and 1,1-cyclobutanedicarboxylate

Chelate Species	β_1	β_2	K_2	K_1/K_2
Tb-α-HIBA	2.95×10^{6}	2.17×10^{12}	7.35×10^{5}	4.01
Tb-CBDA	8.30×10^{7}	2.19×10^{18}	2.64×10^{10}	.00315

Figure 30. Graphical integration of $\bar{n}/a$ versus $\underline{a}$ for the terbium-α-hydroxyisobutyrate system

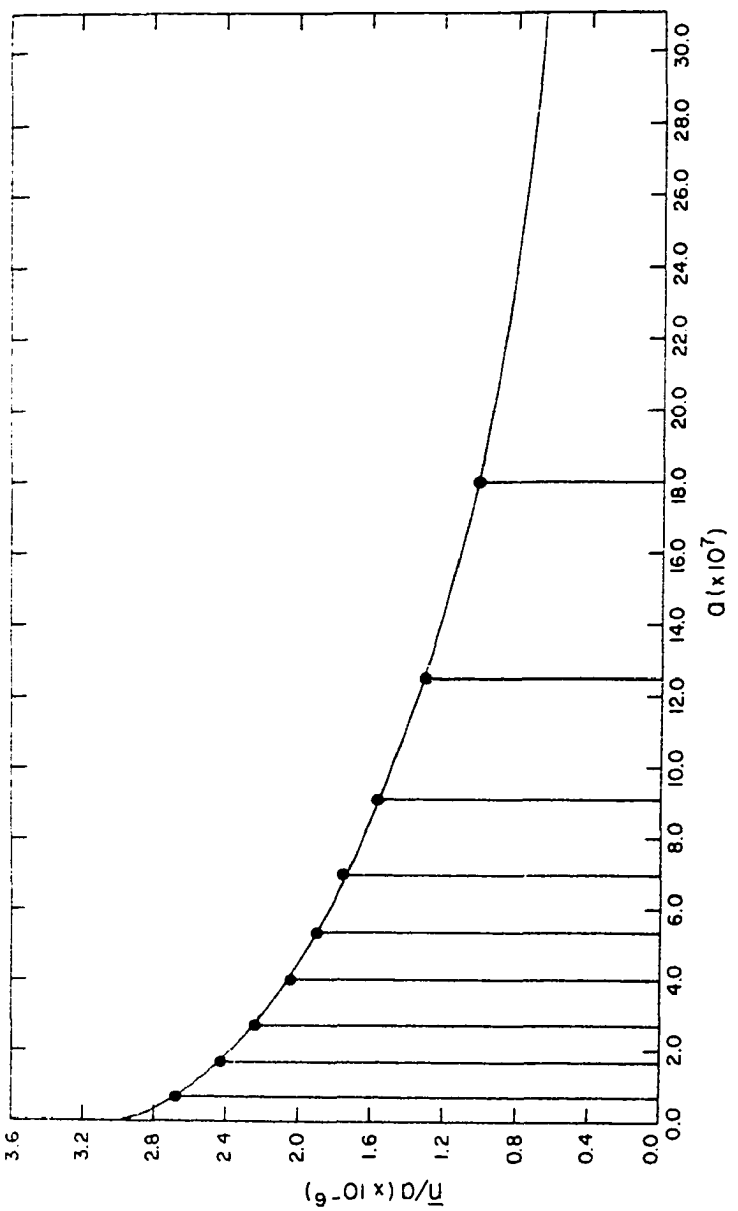
3.6
3.2
2.8
2.4
2.0
1.6
1.2
0.8
0.4
0.0
η/Q (x 10⁻⁸)
0.0
2.0
4.0
6.0
8.0
10.0
12.0
14.0
16.0
18.0
20.0
22.0
24.0
26.0
28.0
30.0
Q (x 10⁷)

Figure 30. Graphical integration of $\bar{n}/a$ versus $\underline{a}$ for the terbium-α-hydroxyisobutyrate system

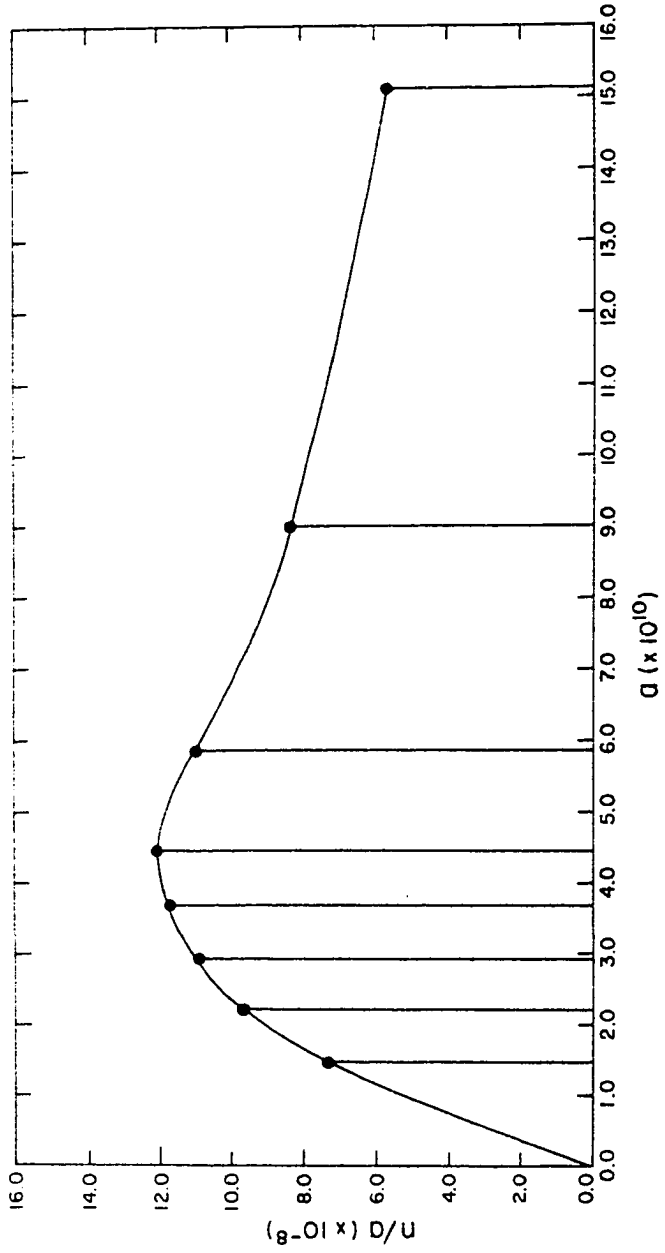
16.0
14.0
12.0
10.0
8.0
6.0
4.0
2.0
0.0
n/Q (x 10^-8)
0.0
1.0
2.0
3.0
4.0
5.0
6.0
7.0
8.0
9.0
10.0
11.0
12.0
13.0
14.0
15.0
16.0
Q (x 10^10)

Figure 32. $F_1(a)$ versus a for the terbium-α-hydroxyisobutyrate system

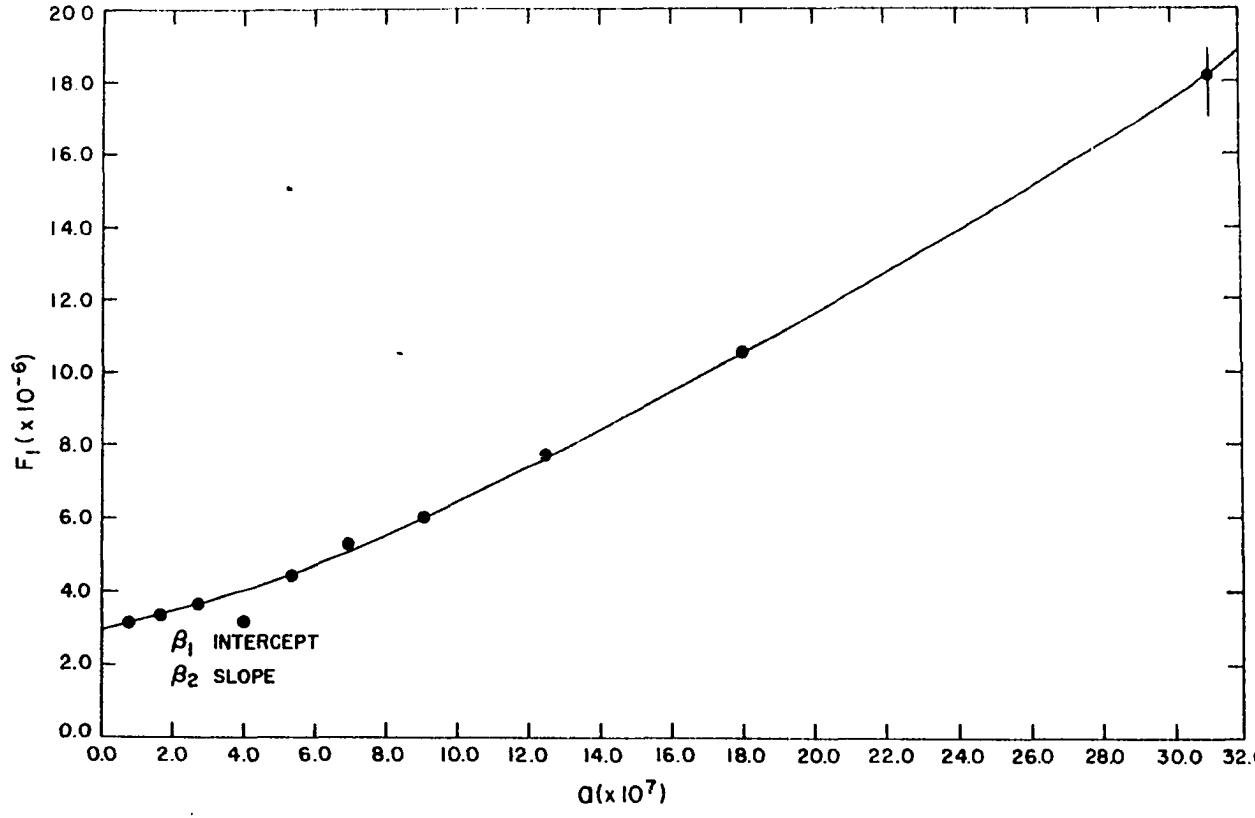
20.0
18.0
16.0
14.0
12.0
10.0
8.0
6.0
4.0
2.0
0.0
$F_1(\times 10^{-6})$
β_1 INTERCEPT
β_2 SLOPE
0.0
2.0
4.0
6.0
8.0
10.0
12.0
14.0
16.0
18.0
20.0
22.0
24.0
26.0
28.0
30.0
32.0
$Q(\times 10^7)$

Figure 33. $F_1(a)$ versus $\underline{a}$ for the terbium-1,1-cyclobutanedicarboxylate system

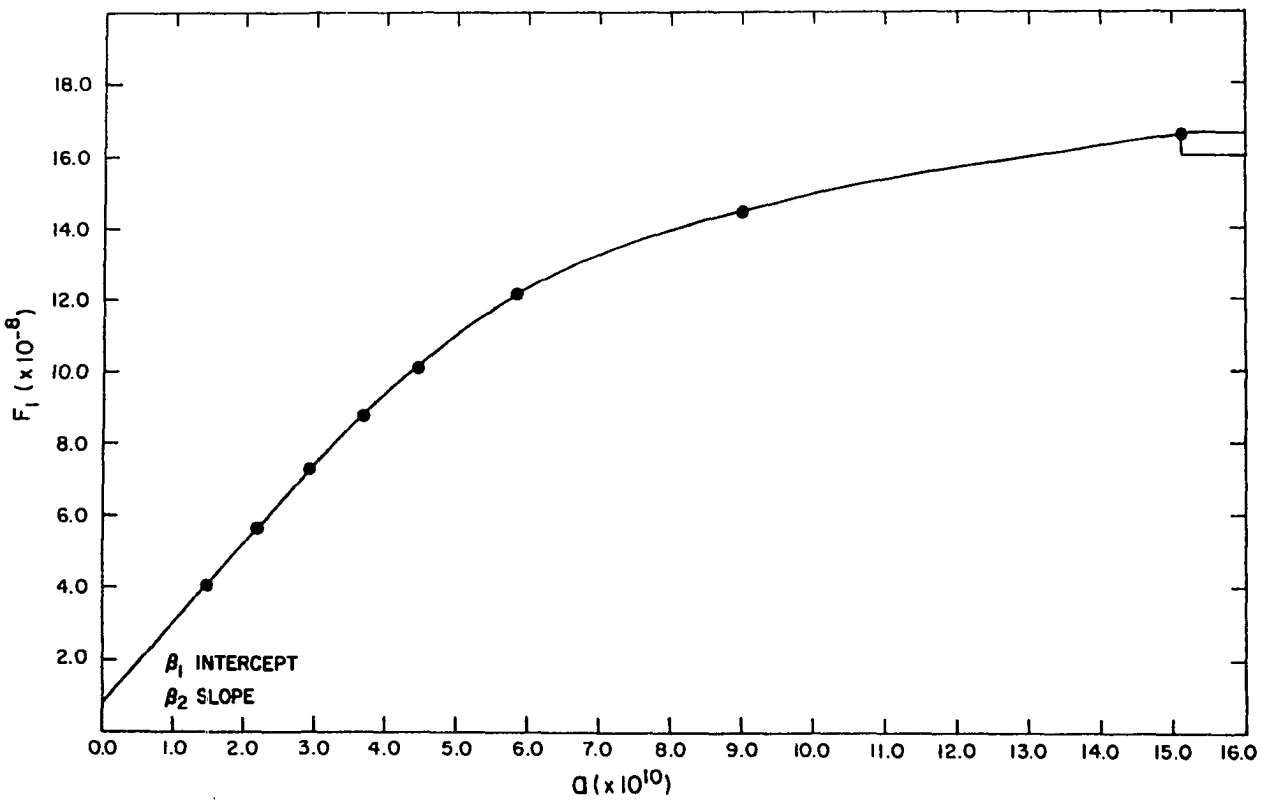
18.0
16.0
14.0
12.0
10.0
8.0
6.0
4.0
2.0
F_i ($\times 10^{-8}$)
β_1 INTERCEPT
β_2 SLOPE
0.0
1.0
2.0
3.0
4.0
5.0
6.0
7.0
8.0
9.0
10.0
11.0
12.0
13.0
14.0
15.0
16.0
Q ($\times 10^{10}$)

DISCUSSSION OF CHELATION

The actual coordination model for lanthanide chelate species is, in general, not immediately obvious from experimental data. It is common to propose several coordination models, examine them in the light of the experimental data, and select that model which best fits the data. In the case of lanthanide malonate chelate species the large number and similarity of possible coordination models prohibits the determination of an unambiguous coordination model. However, the available data does allow one to select a probable model.

It is believed that the lanthanide ions have a coordination number of at least nine. X-ray crystallographic data has shown solid $Nd(BrO_3)_3$ to have nine waters of hydration and, therefore, to be nine-coordinate (28). It has also been shown that the solid ethylsulfates of lanthanum, praseodymium, erbium and ytterbium have nine waters of hydration (29). Due to less rigid restrictions, the solvated ion might well be expected to have nine or more waters in its primary solvation sphere in aqueous solution. Activity coefficient and equivalent conductance data show a drop in coordination number as one traverses the lanthanide series from lanthanum to lutetium (30). Powell suggests that this change in coordination number is from ten (lanthanum to neodymium) to nine (gadolinium to lutetium) (4).

The coordination model assumed in this work is a trigonal prism with additional coordination sites above the center of each rectangular face. The same coordination model was used throughout since a coordination change from nine to ten would have little effect on the actual manner of coordination.

The dentate character of the malonate derivatives studied in this work is potentially as high as four since there are two available oxygens on each carboxyl group. If both oxygens of a carboxyl group were to bond directly to the lanthanide ion, however, one would obtain a highly strained four-membered ring. The bond angles in this ring would have to average 90 degrees. The normal bond angle of O-C-O in a carboxyl group is 120 degrees and the high charge density on the oxygen atoms would not allow this angle to be reduced significantly. Powell has suggested that each carboxyl group might function bidentately by hydrogen bonding one oxygen to a coordinated water molesule and bonding the second oxygen directly to the lanthanide ion (4). The actual scale representation of a carboxyl group coordinating bidentately to a samarium ion via hydrogen bonding to a coordinated water molecule is given in figure 34. Powell has shown that the K_1/K_2 ratios for several α-hydroxy carboxylic acids indeed indicate tridentate bonding for the light rare-earths. He has further supported this theory by pointing out that there

Figure 34. Scale diagram of a carboxyl group coordinating bidentately to a samarium ion via hydrogen bonding to a coordinated water molecule

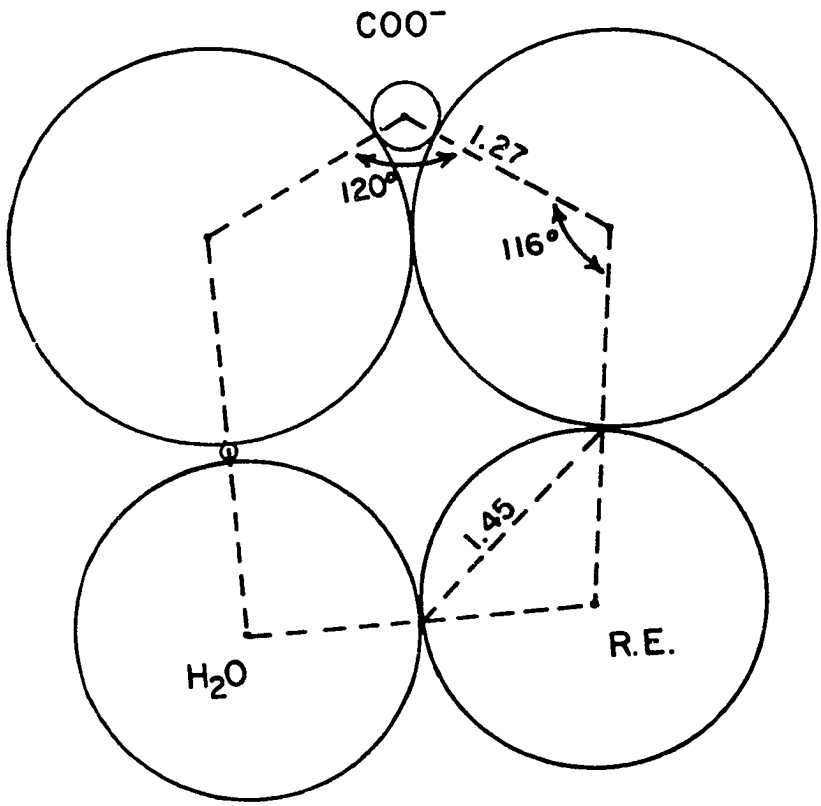
COO⁻
1.27
120°
116°
1.45
H2O
R.E.

is additional stability accompanying the proposed change to higher dentate character (4).

The K_1/K_2 ratio is commonly used as a tool in analyzing the manner in which a ligand coordinates to a metal ion. The ratio of the thermodynamic step formation constants, P', is equal to the product of S, T, and R (9):

$$P' = K_1'/K_2' = S \cdot T \cdot R, \qquad (105)$$

or p at some particular ionic strength is equal to the ratio of the formation constants at that ionic strength and is related to P' as in equation 106.

$$P' = P \cdot f(\gamma) = \frac{K_1}{K_2} f(\gamma) \qquad (106)$$

The function $f(\gamma)$ is the factor by which K_i/K_2 differs from K_1'/K_2'.

The S term is a statistical factor. It is proportional to the number of ways each species can form divided by the number of ways in which it can revert to its precursor. The S factor depends, therefore on the dentate character of the ligand and coordination number of the metal. The T term is an electrostatic factor and accounts for the change in affinity of a metal ion for a ligand with a change in charge. The R term is a rest factor including such things as steric hindrance and ligand field effects on the K_1/K_2 ratio and it is assumed to be approximately equal to one for small ligands. The T factor has been evaluated by Devine (31) and Manning

(32, 33, 34) as 1.5 for uninegative ligands. The value of $f(\gamma)$ is also approximately 1.5 at 0.1 molar ionic strength. Therefore, under these conditions the value of K_1/K_2 is simply equal to the statistical factor S.

The K_1/K_2 ratio is only useful if the manner of coordination is identical in both steps. It is suspected that this is not the case with the malonate ligands. It is also very difficult to estimate the T factor for a doubly charged species. For these reasons the K_1/K_2 ratio is discarded as a tool for analyzing the bonding in the lanthanide malonate chelate species.

The formation constants of the lanthanide chelate species of the malonate derivatives studied in this work show an apparent decrease in coordination number as the lanthanide radii decrease. The nearly linear increase in K_1 with a decrease in ionic radii from praseodymium to dysprosium indicates that the dentate character remained constant in this region. It is believed that, for the following reasons, the dentate character of the ligand in this region is four.

First of all, one observes two drops in K_1 at holmium and lutetium of equal magnitude for all ligands. This might very well be explained by the disappearance of two stabilizing hydrogen bonds to an oxygen of each carboxyl group. There would then be a change in dentate character from four to three at holmium, and from three to two at lutetium.

The drop in the formation constant between the pair: dysprosium-holmium and ytterbium-lutetium is approximately 0.1 of a log unit. This is similar to the drop in formation constant witnessed by Powell for the ethylglycolate ligand in proceeding from the light to the heavy lanthanides (4). Powell attributed this drop of stability to the loss of a hydrogen bond. Since

$\Delta G = \Delta H - T\Delta S$ and

$\Delta G = -RT \ln K$,

the same change in log K would be expected for the loss of a hydrogen bond in either system in spite of the value of the formation constants.

The slight decrease in K_2 from praseodymiun to holmium reflects the increased difficulty of bonding the second ligand as the cationic radius decreases. However, there is a sharp increase in K_2 beyond holmium corresponding to the reduction in dentate character of the first ligand at holmium. This change in dentate character allows the second ligand one more possible coordination site and should be accompanied by an increase in K_2 as is observed.

Data collected on the terbium-CBDA and terbium-α-HIBA systems in methyl alcohol support the bonding theories given above for the aqueous lanthanide malonate systems. The values of K_1 and K_2 for α-HIBA at 0.02 molar ionic strength are respectively 2.95×10^6 and 7.35×10^5

yielding a K_1/K_2 ratio of 4.01. Devine obtained a value of 3.40 for the same chelate species in aqueous solution at 0.1 molar ionic strength (31).

The K_1/K_2 ratios expected at 0.1 molar ionic strength are simply the statistical ratios of 4.92 for tridentate bonding, and 3.27 for bidentate bonding on a nine-coordinate metal ion. The K_1/K_2 ratio would be expected to increase slightly with a decrease in ionic strength. However, the Tb-α-HIBA chelate species in methyl alcohol would still appear to have a considerably higher percentage of tridentate bonding than the corresponding species in aqueous solution. There is no reason for the apparent preference of the tridentate bonding in alcohol as compared to water. Tridentate bonding would, in fact, seem less favorable in alcohol since a bulkier alcohol molecule is incorporated in the hydrogen bond with the carboxyl group instead of a water molecule. The anomaly may be explained by the steric hindrance encountered on bonding two ligands tridentately via hydrogen bonded methyl alcohol molecules. The methyl groups would be expected to cause much more steric hindrance than the corresponding hydrogen on bound water molecules and, thereby, increase the K_1/K_2 ratio. Powell has shown in the case of the diethylglycolate ligand that steric hindrance due to the ethyl substituents causes the K_1/K_2 ratios to be considerably greater than for a smaller or single substituent.

The formation constants for Tb-CBDA in methyl alcohol were:

$K_1 = 8.30 \times 10^7$ and

$K_2 = 2.64 \times 10^{10}$.

Since K_2 is larger than K_1, it is certain that the species BA_2^- is being removed from the system if it is indeed formed at all. This could be explained by hypothesizing a dinuclear species formed according to the reaction:

$$BA^+ + BA_2^- \rightarrow B_2A_3 \quad .$$

Praseodymium was precipitated from aqueous solution with the CBDA ligand. The solid was analyzed for metal ligand and water content. It was found that the simplest formula could be written $Pr_2(CBDA)_3 \cdot 2H_2O$. This lends support to the hypothesis of a sesquimalonate species in methanol. Further support is lent by the fact that a precipitate was obtained in the Tb-CBDA system when the ligand to metal ratio exceeded 0.9 in methanol solution.

To determine whether polynuclear coordination occurs with lanthanide chelates of malonate derivatives in aqueous solution the step formation constants for dysprosium dimethylmalonate were determined at metal concentrations of 0.004 and 0.010 molar. The mathematical expression used in calculating the formation constants of polynuclear chelate species is a function of the free metal ion concentration. A different set of formation

constants should be obtained if the metal ion concentration is changed significantly and polynuclear chelation does indeed occur.

In changing the metal concentration from 0.004 to 0.01 molar K_1 changed from 16,900 to 16,140, K_2 changed from 261 to 164 and K_1/K_2 changed from 64.8 to 98.2. The reliability of the step formation constants determined at 0.10 molar metal concentration is not as good as those determined at 0.004 molar metal concentration, however. The highest $\bar{n}$ obtained for the 0.010 molar metal concentration case was 0.90. Since K_1 is so large compared with K_2 there is actually very little of the doubly chelated (MA_2) species present at an $\bar{n}$ of 0.90. The error in K_2 would, therefore, be expected to be quite large. Due the large error in K_2 and the resultant large error in the K_1/K_2 ratio, one would look mainly at the change in K_1 to determine if there is any appreciable amount of polynuclear chelation occurring. If K_1 could be any value within the region ± three standard deviations from the calculated value, the ranges would be as given in table 10.

Table 10. First step formation constants for dysprosium dimethylmalonate at 0.01 and 0.004 molar with calculated range of ± three standard deviations

Concentration	K_1	low	high
0.004 M	16,900 ± 135	16,760	17,040
0.010 M	16,140 ± 366	15,770	16,510

There is nearly overlap between the two ranges. However, the data would indicate a slight tendency towards polynuclear chelation.

It is believed that the first malonate ligand bonds tetradentately to the lanthanide ion in methyl alcohol. The two methyl alcohol molecules incorporated in the first chelation would sterically hinder the second ligand. It is believed that this steric hindrance causes the second ligand to bridge between two lanthanides by bonding one carboxyl group to each metal center.

The hypothesis of bidentate behavior of carboxyl groups via hydrogen bonding to a coordinated solvent molecule is supported by the observed difference in behavior of the Tb-CBDA system in methanol and water. If there were no hydrogen bonded solvent molecules in either solvent, one would expect very little difference in the manner of chelation of the CBDA ligand between the two solvents, and one should, therefore, observe similar K_1/K_2 ratios in the two solvents. However, incorporation of solvent molecules in the chelation would cause a much greater steric hindrance in alcohol than in water. This appears to be the only explanation for the change in bonding with the change in solvent.

The three α-substituted malonate ligands studied in this work yield plots of K_1 versus ionic radius with nearly identical profiles. Furthermore, the plots of K_1

versus ionic radius given by Adolphson (3) and Powell (2) for the malonate ligands with the α-substituents, methyl, ethyl, propyl, n-butyl, n-pentyl, diethyl, di-n-propyl and di-n-butyl as well as the plain malonate ligand have appearances strikingly similar to those of ligands studied in this work. All ligands exhibit maxima at dysprosium and ytterbium with sharp drops of equal magnitude between the pairs: dysprosium-holmium and ytterbium-lutetium. An additional break in all K_1 curves occurs at gadolinium. The gadolinium break commonly occurs in coordination complexes of the lanthanides and is explained by the change in hydration of the lanthanides (35,p.114), or a change in bonding made in the vicinity of gadolinium. However, the other breaks mentioned indicate a change in dentate character.

The leveling of the K_1 plots between terbium and lutetium reflects the increased difficulty of fitting the lanthanides as the radius decreases. This leveling is most pronounced with the ligands having the smaller or more restricted α-substituents. If K_1 values are plotted for all of the α-substituted ligands mentioned above, one observes that the curves show a gradual separation with a decrease in cationic radius. Values of K_1 are very similar at lanthanum, but are widely separated at lutetium.

The following stability trend is observed for the α-substituted malonate ligand:

DMM < CPDA ≈ CBDA < M < MM < BM <EM < PrM < PnM < DEM < DPM < DBM .

The values of K_1 and K_2 for the lutetium and samarium complex of each ligand are given in table 11. There are several anomalies in the stability trends of ligands studied in this work. Dimethylmalonate formation constants appear to be abnormally low as does n-butylmalonate, as reported by Adolphson (3). The first formation constants of CPDA approach those of CBDA with decreasing ionic radius and drop below the corresponding CBDA values at dysprosium. The same trend is observed in the K_2 values for CPDA and CBDA. However, the values of K_2 never are less than the corresponding CBDA values.

The formation constants are directly related to $-\Delta H$ and ΔS for the reaction. Stability trends as a function of α-substituent on these malonate ligands may be conveniently analyzed by studying the effect of substituent on $-\Delta H$ and ΔS. Changing the substituent affects $-\Delta H$ and ΔS through at least three different mechanisms. From greatest to least importance these are: ligand bulk, bond angle between carboxyl groups and electronic inductive effect.

The stability of ligands with high dentate character has been attributed to the large favorable ΔS rather than the $-\Delta H$ contributed (35, p. 116). This is the chelate effect referred to by Schwarzenbach (36). The

Table 11. The first and second step formation constants of the samarium and lutetium complexes of various α-substituted malonate ligands

α Substituent	Sm		Lu	
	K_1	K_2	K_1	K_2
none	15,600	450	28,200	480
methyl	11,800	309	20,100	384
ethyl	13,100	427	22,800	965
n-propyl	15,400	692	26,600	128
n-butyl	14,200	617	23,000	106
n-pentyl	———	——	26,700	149
dimethyl	10,990	290	14,660	338
diethyl	21,300	390	48,700	520
di-n-propyl	28,300	780	60,800	560
di-n-butyl	27,100	——	60,800	950
cyclobutane	11,150	292	18,020	412
cyclopentane	———	——	16,510	441

entropy increase upon chelation is due to the release of water molecules bound both to the anion and cation. The bulkier ligands as well as those with higher dentate character would be expected to produce the larger favorable ΔS, i.e. more water molecules must be displaced to accommodate these ligands.

Large favorable changes in entropy might also be expected from those ligands having large bond angles between carboxyl groups. The ligands would be expected to be more heavily hydrated as the bond angle increased (due to additional room around carboxyl oxygens for waters of hydration) and would cover a larger solid angle on the cation. Both of these effects would produce a more favorable ΔS upon chelation.

The increase in charge on the carboxyl oxygens due to increasing substituent bulk would cause a slight increase in ΔS upon chelation. The change in entropy can be attributed to an increase in hydration of the ligand with an increase in charge on the carboxyl oxygens. The inductive effect is small for methylene groups, however. One would, therefore expect this effect to be less significant than the other two.

The enthalpy change occurring in chelation can be broken into three steps:

1) $B(H_2O)_x^{+3} \rightarrow B(H_2O)_{x-y}^{+3} + yH_2O$

2) $A(H_2O)_z^{-3} \rightarrow A^- + zH_2O$

3) $B(H_2O)^{+s}_{x-y} + A^- \rightarrow BA(H_2O)^{+}_{x-y}$

Steps 1 and 2 require energy, while step 3 releases energy. The bulky ligands and the ligands with the largest bond angles between carboxyl groups require the most energy in step 1 since a greater number of waters of hydration are displaced. An increase in bond angle between carboxyl groups as well as an increased inductive effect would cause the ligand to be hydrated to a greater extent, tending to decrease $-\Delta H$ in step 2. The value of $-\Delta H$ resulting from the third step depends on the fit of the ligand to the metal as well as the concentration of charge on the carboxyl oxygens. Due to the inductive effect, the value of $-\Delta H$ could be expected to increase with the addition of a few methylene units to the malonate ligand. However, $-\Delta H$ would begin to decrease with continued addition of methylene units due to the increased steric hindrance and decreased inductive effects of each additional methylene unit.

For any lanthanide ion there is a corresponding angle between the carboxyl groups of the ligand which yields the best possible fit. Therefore, $-\Delta H$ in the third step is going to be a function of the ligand for any particular lanthanide and a function of the lanthanide for any particular ligand. The value of $-\Delta H$ would be expected to decrease with either an increase or decrease in bond angle compared to that required for a perfect fit.

The observed stability trends appear to be in general conformity with the theory presented above. The increase in stability with decreased ionic radius for all ligands is due to increased lanthanide hydration and Lewis acidity. The increase in stability with increased ligand bulk is due to increased disruption of the cation hydration sphere and a correspondingly larger ΔS. The less important effects of bond angle between carboxyl groups and inductive effect become apparent in the low stabilities of DMMA, CBDA and CPDA. The two methyl groups in DMMA serve to decrease the bond angle without adding significant bulk to the ligand, thereby decreasing ΔS compared to the malonate ligand. The cyclic ligands would be expected to have an increased bond angle due to the small angles required in the four and five-membered rings. This would increase ΔS. The increased inductive effect would also increase ΔS. The only apparent explanation of the trend is a decrease in $-\Delta H$ due to a poorer fit of the ligands to the lanthanide ions.

The cross over in stability of the lanthanide chelate species of CPDA and CBDA as well as the increased separation in stabilities of other malonate chelate species with a decrease in ionic radius might be explained by the change in relative importance of ΔS and $-\Delta H$ for each ligand with a change in cationic radius. Powell (4) and Mackay, Powell, and Spedding (37) have shown that the

effect of ΔS on the stability of several lanthanide chelate species becomes more predominate with respect to the effect of $-\Delta H$ as the ionic radius decreases. The value of ΔS increases with a decrease in ionic radius while $-\Delta H$ has an overall decrease for these chelate species. However, the value of $-\Delta H$ changes much more slowly than the value of $T\Delta S$ with a change in ionic radius. The CBDA ligand, having a wider bond angle than CPDA, would be expected to have more difficulty in fitting the lanthanide ions, yielding a smaller $-\Delta H$. It is expected to have a larger ΔS, however, by virtue of its wider bond angle. If this is the case the stabilities of CBDA would approach, and finally exceed those of CPDA as the cationic radius decreases and ΔS becomes more important with respect to $-\Delta H$.

The success of the method used in this work to determine formation constants in methyl alcohol is heavily dependent on the ability of the glass electrode to measure hydrogen ion concentration accurately. The following evidence is cited as an indication that the glass electrode was reliable: the millivolt reading was a linear function of $\log[H^+]$; the formation curves were smooth; the values of K_1/K_2 for Tb-α-HIBA chelate species in methyl alcohol and aqueous solution were similar as expected if the type of bonding is similar; a trend to lower acid ionization constants and higher metal chelate

formation constants was found as expected in changing solvents from water to methyl alcohol. Alexa has determined the formation constants of Eu-α-HIBA in water methanol mixtures up to a methyl alcohol concentration of 83.3% by weight (7). He found that the log of the formation constant is a linear function of 1/(dielectric constant) in the region of his determination. A portion of his data is given in table 12. If one extended the table to pure methyl alcohol with a dielectric constant of 31.5, log β_2 would be 9.8. A value of 12.2 was obtained for β_2 in this work. Powell gives values of 3.05 and 3.15 for log K_1 of α-HIBA chelate species of europium and terbium respectively in aqueous solution at 0.1 molar ionic strength (4). He gives K_1/K_2 ratios of 4.6 and 3.4 for europium and terbium respectively. From log K_1 and K_1/K_2 ratios log β_2 is 5.5 for europium and 5.8 for terbium. If table 12 were extended to pure water, log β_2 would be near 4.4 for europium. This value of β_2 is 0.9 and 1.4 orders of magnitude less than β_2 given by Powell for the europium and terbium chelate species respectively.

Table 12. Formation constants of europium-α-hydroxyisobutyrate chelate species in aqueous-methanol mixtures as reported by Alexa (7)

Wt. Pecent methanol	1/D	log β_1	log β_2
16.67	0.014	2.78	5.04
83.33	0.026	3.45	8.34

By increasing the value of β_2 for the europium chelate species, calculated from Alexa's values, by 1.4 orders of magnitude one arrives at a value of 12.2 for log β_2 obtained in this work. The value of 12.2 for log β_2 is then in fair agreement with the values of formation constants of α-HIBA chelate species in aqueous solution cited above, considering the large effect on log β_2 due to a small change in slope of the plot of 1/D versus log β_2.

The accuracy of the activity coefficients and ion pair dissociation constants also have a bearing on the accuracy of the formation constant determinations. Ion activities were used in the ionic strength calculations and in preparing the calibration curve of log[H^+] versus millivolt reading. The reliability of the dissociation constants and mean activity coefficients for HCl, LiCl and $TbCl_3$ have been previously discussed. The dissociation constants and mean activity coefficients of lithium salts of the organic acids used in this work were no more than fair approximations. It would be expected, however, that small changes in these values would have little effect on the formation constants determined.

SUMMARY

The stability of the lanthanide malonato chelate species is dependent on the OOC-C-COO bond angle. There is a notable decrease in stability of these chelate species when the ligand has a cyclic α-substituent (four and five-membered ring). The available data indicate that the OOC-C-COO bond angle found in the ligands with cyclic α-substituents is too large to fit the heavy lanthanides well.

The carboxyl groups of malonate ligands are apparently able to function bidentately in lanthanide chelate species. This bidentate behavior is observed in both methanol and aqueous solutions of the chelate species. The carboxyl group is able to function bidentately by directly coordinating one oxygen atom to the metal center and forming a hydrogen bond between the second oxygen and a coordinated solvent molecule.

The glass-calomel electrode system gives a linear reproducible millivolt reading as a function of the hydrogen ion concentration in methanol. It appears to be feasible to measure formation constants of metal carboxylate chelate species in methanol from a measurement of free hydrogen ion concentration.

BIBLIOGRAPHY

1. Gelles, E. and G. H. Nancollas, Trans. Faraday Soc., 52, 680 (1956)

2. Powell, J. E., J. L. Farrell, W. F. S. Neillie, and R. Russell, J. Inorg. Nucl. Chem., 30, 2223 (1968).

3. Adolphson, M. L., Step formation constants of some malonate chelate species, unpublished Ph.D. thesis, Ames, Iowa, Library, Iowa State University of Science and Technology, 1969.

4. Powell, J. E., Proposed models for mono-, bi-, and tridentately bonded lanthanide complex species formed with homologues of acetate and glycolate ions, unpublished mimeographed paper, Ames, Iowa, Iowa State University of Science and Technology, Department of Chemistry, 1967.

5. Romanenko, E. D., N. A. Kostromina, Zh. Neorg. Khim., 13(7), 1840-7 (1968).

6. Vobecky, M., and M. Matalka, Collect. Czech. Chem. Commun., 28, 743-5 (1963).

7. Alexa, J., Collect. Czech. Chem. Commun., 33(1), 188-92 (1968).

8. Sonneson, A., Acta Chem. Scand., 12, 165 (1958).

9. Bjerrum, J., Metal Ammine formation in aqueous solution, Copenhagen, Denmark, P. Haase and Son, 1941.

10. Rossotti, F. J. C., and H. Rossotti, The determination of stability constants, New York, N. Y., McGraw-Hill Book Co., Inc., 1961.

11. Rydberg, J., Acta Chem. Scand., 14, 157 (1960).

12. Sullivan, J. C., J. Rydberg, and W. F. Miller, Acta Chem. Scand., 13, 2023 (1959).

13. Stagg, W. R., and J. E. Powell, Inorg. Chem., 3, 242, (1964).

14. Stagg, W. R., Formation constants of some rare-earth complexes, unpublished Ph.D. thesis, Ames, Iowa, Library, Iowa State University of Science and Technology, 1963.

15. Harned, H. S., and B. B. Owen, The Physical Chemistry of Electrolytic Solutions, New York, N. Y., Reinhold Pub. Corp., 1958.

16. Creighton, H. J., Electrochemistry vol I, 4th ed., New York, N. Y., John Wiley and Sons, 1943.

17. Kraus, G. A., and W. C. Bray, J. Am. Chem. Soc., 35, 1315 (1913).

18. Harned, H. S., and R.W. Ehlers, J. Am. Chem. Soc., 55, 2179 (1933).

19. Dye, J. L., Some thermodynamic properiies of rare-earth chloride solutions, unpublished Ph.D. thesis, Ames, Iowa, Library, Iowa State University of Science and Technology, 1958.

20. Everdell, M. H., Introduction to Chemical Thermodynamics, New York N. Y., W. W. Norton and Co., Inc., 1965.

21. Stefan, M., Jastrzebska, and Jadwiga, Rocz. Chem., 42(4), 719-24 (1968).

22. MacInnes, D. A., and L. G. Longsworth, Chem. Rev., 11, 171 (1932).

23. Wright, J., Conductances, transference numbers and activity coefficients of chlorides of some high atomic number rare-earths in aqueous solution, Ph.D. thesis, Ames, Iowa, Library, Iowa State University of Science and Technology, 1951.

24. Nonhebel, G., and H. Hartley, Phil. Mag., (6)50, 298, 729 (1962).

25. Marple, L. W., and J. S. Fritz, Anal. Chem., 34, 796 (1962).

26. Gelsema, W. J., C. L. deLigny, and H. A. Blijleven, Rec. Trav. Chim. Pays-Bas, 86(9), 852-64 (1967.

27. Briere, G., N. Felici, and E. Piot, Compt. Rend., 255, 107 (1962).

28. Helmholtz, L. J., J. Am. Chem. Soc., 61, 1544 (1939).

29. Fitzwater, D. R. , and R. E. Rundle, Z. Kristallogr. 112, 362 (1959).

30. Spedding, F. H., and G. Atkinson, Properties of rare-earth salts in electrolytic solutions, in W. J. Harner, ed., The structure of electrolytic solutions, New York, N. Y., John Wiley and Sons, Inc., 1959.

31. Devine, C. D., The stability constants of some carboxylate complexes of the trivalent lanthanons, unpublished Ph.D. thesis, Ames, Iowa, Library, Iowa State University of Science and Technology, 1969.

32. Manning, P. G., Can. J. Chem., 41, 2557 (1963).

33. Manning, P. G., Can. J. Chem., 43, 2911, 3258, 3476 (1965).

34. Manning, P. G., Can. J. Chem., 44, 1471, 1975, 3057 (1966).

35. Phillips, C. S. G. and R. J. P. Williams, Inorganic Chemistry, vol. II, Oxford, Oxford University Press, 1966.

36. Schwarzenbach, G., Helv. Chim. Acta, 35, 2344 (1952).

37. Mackay J. L., J. E. Powell and F. H. Spedding, J. Am. Chem. Soc., 84, 2047 (1962).

ACKNOWLEDGEMENTS

The author wishes to express his appreciation to Dr. J. E. Powell for his counsel and endless patience.

The author also wishes to thank Harvey Burkholder, Marvin Adolphson, Donald Johnson and Roy Whetstone for their cheerful assistance.

Finally, the author wishes to thank his wife Charlene for her loving support and aid in preparation of this manuscript.

APPENDIX A

Derivation of Function $F_1(a)$

Initial conditions

$$\alpha_c = \frac{[BA_c]}{B} = \frac{B_c a^c}{\sum_{n=0}^{N} \beta_n a^n}$$

$$\bar{n} = \frac{A - a}{B} = \frac{\sum_{1}^{N} \beta_n a^n}{\sum_{0}^{N} \beta_n a^n}$$

Derivation

$$\log \alpha_c = \log b + \log \beta_c + c \log a - \log B$$

$$d \log \alpha_c = d \log b + cd \log a$$

$$\frac{d \log \alpha_c}{d \log a} = \frac{d \log b}{d \log a} + c$$

$$B = b[\beta_1 a + \beta_2 a^2]$$

$$\frac{dB}{da} = \frac{db}{da}[\beta_1 a + \beta_2 a^2] = b[\beta_1 + 2\beta_2 a]$$

$$\frac{dB}{da} = 0$$

$$\frac{db}{da} = \frac{-b[\beta_1 + 2\beta_2 a]}{\beta_1 a + \beta_2 a^2}$$

$$\frac{d \log b}{d \log a} = \frac{adb}{bda}$$

$$\frac{d \log b}{d \log a} = \frac{-[\beta_1 a + 2\beta_2 a^2]}{\beta_1 a + \beta_2 a^2}$$

$$\frac{d \log b}{d \log a} = -\bar{n}$$

$$\frac{d \log \alpha_c}{d \log a} = c - \bar{n}$$

$$\log \alpha_c = \int (c - \bar{n})\, d \log a + \text{const.}$$

In the special case where $c = 0$, $BA_c = b$, and $\alpha_c = \log \frac{b}{B}$ the above equation becomes:

$$\log \frac{B}{b} = \int_0^a \frac{\bar{n}}{a}\, da$$

$$B = b \sum_{n=0}^{N} \beta_n a^n$$

$$\sum_{n=0}^{N} \beta_n a^n = \exp \int_0^a \frac{\bar{n}}{a}\, da$$

$$\beta_0 = 1$$

$$F_1(a) = \frac{\exp \int_0^a \frac{\bar{n}}{a}\, da}{a} .$$

APPENDIX B

Ionic Strength Adjustment

Acid dissociation constant of α-HIBA at 0.02 M ionic strength

Species of importance

A^-, HA, LiA, Cl^-. Li^+

Calculations

$$OH_T = A^- + LiA$$

$$A^- = OH_T / 1 + Li \cdot y^2/K_{Li1}$$

$$LiCl = (0.02 - A^-)\ Li^+\ y^2/K_{Li1}$$

$$LiCl_T = LiCl + Li^+ + LiA - OH_T$$

Acid dissociation constant of CBDA at 0.02 M ionic strength

Species of importance

LI^+, Cl^-, H_2A, HA^-, $A^=$, LiHA, LiA^-, Li_2A

Calculations

$$OH_T - A_T = A^= (1 + Li\ A + LiA^-)$$

$$A^- = (OH_T - A_T)/(1 + (Li^+)^2\ y^3/K_{Li2} \cdot K_{Li1} + Li^+ \cdot y/K_{Li2}$$

$$LiA = A^=\ Li^+ \cdot y/K_{Li2}$$

$$HA^- = 2A_T - OH_T$$

$$LiHA = HA^-\ Li^+ \cdot y/K_{Li2}$$

$$HA^- = 2A_T - OH_T$$

$$LiHA = HA^-\ Li^+ \cdot y^2/K_{Li1}$$

$$Li_2A = LiA^-\ Li^+ \cdot y^2/K_{Li1}$$

$$LiCl = (0.02 - (HA^- + LiA^- + 3A^=))\ Li \cdot y^2/K_{Li1}$$

$$LiCl_T = LiCl + Li + 2Li_2A + LiA^- + LiHA - OH_T$$

Formation constant of Tb-α-HIBA at 0.02 M ionic strength

Species of importance

M^{+3}, MCl^{+2}, MCl_2^{+}, MCl_3, MA^{+2}, $MACl^{+}$, $MACl_2$, MA_2^{+}, MA_2Cl, HA, Li^{+}, Cl^{-}

Calculations

If $< OH_T < M_T$

Then $M = M_T - OH_T$

If $M_T < OH_T < 2M_T$

Then $M = 0$

$MA = 2M_T - OH_T$

$MA = OH_T - M_T$

If $2M_T < OH_T < 3M_T$

Then $M = 0$

$MA = 0$

$MA = 3M_T - OH_T$

$$M = (M^{+3})1 + \beta_1(Cl^-)Y_1 + \beta_2(Cl^-)^2Y_1^2 + \beta_3(Cl^-)^3Y_1^4$$

$$M^{+3} = M/(1 + \beta_1(Cl^-)Y_1 + \beta_2(Cl^-)^2Y_1^2 + \beta_3(Cl^-)^3Y_1^4)$$

$$MCl^{+2} = (M^{+3})\,\beta_1(Cl^-)Y_1$$

$$MCl_2^{+} = (M^{+3})\,\beta_2(Cl^-)^2Y_1^2$$

$$MCl_3 = (M^{+3})\,\beta_3(Cl^-)^3Y_1^4$$

$$MA_T = MA^{+2} + MACl^{+} + MACl_2$$

$$MACl^{+} = (MA^{+2})(Cl^-)\,Y/K_{Li_2}$$

$$MACl_2 = (MA_2^{+})(Cl^-)^2Y^3/K_{Li_1}\cdot K_{Li_2}$$

$$MA_{2T} = MA_2^{+} + MA_2Cl$$

$MA_2Cl = (MA_2^+)(Cl^-)Y^2/K_1$

$HA = A_T - OH_T$

$Li^+ = 0.02 - (6(M^{+3}) + 3(MCl^{+2} + MA^{+2}) + MACl^+ + MA_2^+ + MCl_2^+)$

$LiCl = (Li^+)(Cl^-)Y^2$

$LiCl_T = LiCl + Li^+ - OH_T$

Formation constants of Tb-CBDA at 0.02 M ionic strength

Species of importance

M^{+3}, MCl^{+2}, MCl_2^+, MCl_3, MA^+, $MACl$, HA^-, H_2A, Li^+, Cl^-

Calculations

$MA_T = OH_T/2$

$MA_T = MA^+ + MACl$

$MA^+ = MA_T/(1 + (Cl^-)Y^2/K_{Li1}$

$Li^+ = 0.02 - (6(M^{+3}) + 3(MCl^{+2}) + MCl_2^+ + MA^+$

$LiCl_T = Li^+ + LiCl + LiHA - OH_T$

$LiCl = (Li^+)(Cl^-)Y^2/K_{Li1}$